中国石油大学（北京）
2026 年申报博士研究生指导教师支撑材料目录

申报人姓名：陈朝伟

申报学科或专业学位领域代码及名称：石油与天然气工程（082000）

序号	支撑材料名称
1	天然气工业编委会委员聘书
2	石油科学通报执行编委聘书
3	石油钻采工艺编委会委员聘书
4	中国岩石力学与工程学会理事会理事聘书
5	中国岩石力学与工程学会低碳能源岩石力学与工程专业委员会第一届委员会副主任委员聘书
6	斯坦福访问学者
7	论文检索证明
8	论文 1：Experimental investigation on fracture growth for integrated hydraulic fracturing in multiple gas bearing formations（SCI 二区）
9	论文2：预防页岩气套变的橡胶组合套管研制及其抗剪切性能评价（EI）
10	论文3：四川长宁页岩气套管变形井微地震特征分析 （EI）
11	论文 4：解决工程问题的通用方法和哲学思考——以四川页岩气开发套管变形问题为例 （中文核心）
12	论文5：四川盆地页岩气开发套管变形一体化防控技术 （中文核心）

序号	支撑材料名称
13	专著教材：Casing Deformation Induced by Fault Slip During Shale Hydraulic Fracturing
14	专著教材：四川页岩气套管变形机理和防控技术
15	专利 1：一种页岩油气套管变形预警方法和装置.
16	专利2：一种断层激活控制方法和装置
17	中国石油天然气集团有限公司基础研究奖二等奖（排名 1）
18	中国石油和化工自动化协会科技进步奖一等奖（排名 6）
19	中国石油天然气集团有限公司科技项目：复杂油气钻完井基础理论与新技术新方法研究
20	国家科技重大专项课题：油气田地质力学与储层改造新技术

聘　书

陈朝伟 先生

鉴于您在石油天然气及新能源相关专业领域突出的学术成就和不凡的影响力，特聘请您担任《天然气工业》第九届编委会委员，任期为2021—2025年。

天然气工业杂志社

2021年7月31日

聘 书

陈朝伟老师：

基于您的学术成就和影响力，我很荣幸地聘请您担任《石油科学通报》执行编委，让我和您一起努力，持续提高我刊水平和质量。

《石油科学通报》是教育部主管，中国石油大学（北京）和清华大学出版社有限公司主办，清华大学出版社有限公司出版的学术期刊。发表石油自然科学与社会科学多学科交叉基础研究最新进展，为石油科学研究者提供高水平的学术交流平台，推动石油科学创新发展。

主编：陈勉

《石油科学通报》

2022年4月

石油科学通报编辑部

石油钻采工艺

OIL DRILLING & PRODUCTION TECHNOLOGY

Letter of Appointment

Scholar Chen Chaowei,

In view of your outstanding achievements and academic contributions in the field of oil and gas industry, it is hereby granted to you for your appointment as the member of the Editorial Board of Oil Drilling & Production Technology subject to review and decision by the Editorial Board. The appointment is from August 2024 to July 2027.

Oil Drilling & Production Technology

July 2024

编委会聘书

陈朝伟 教授/专家：

鉴于您在石油天然气工业领域的卓越成就和学术贡献，经期刊编委会审核决定，兹聘请您为《石油钻采工艺》编委会委员。

聘期 3 年

自2024年8月至2027年7月

《石油钻采工艺》杂志社

二〇二四年七月

CSRME

聘 书

尊敬的 陈朝伟 同志：

经第十届理事会第一次全体会议选举通过，聘请您为中国岩石力学与工程学会第十届理事会理事，聘期五年，自2025年9月6日至2030年9月5日。

特发此证！

中国岩石力学与工程学会

2025年9月6日

证书编号：CSRME-LSH-2025-068

聘　书

陈朝伟 同志：

兹聘任您为中国岩石力学与工程学会低碳能源岩石力学与工程专业委员会第一届委员会副主任委员。

聘期：2022年12月~2026年12月

特发此证！

中国岩石力学与工程学会
低碳能源岩石力学与工程专业委员会
2022年12月

Stanford University

Chen, Zhaowei

050005498

Visitor

Valid:

05/12/2017 – 10/01/2017

806092553767242

报告编号：2026-1413

论文收录引用

检索证明报告

中华人民共和国教育部科技查新站（SH01）

论文作者：　陈朝伟

委托单位：　中国石油大学（北京）

论文发表年限：　2021-2025 年

检索数据库：

SCI-EXPANDED	2001- present	网络版
EI- Compendex	1967- present	网络版
CNKI	1994- present	网络版

检索结果：（作者提供文章）

1）　SCI-E 收录：有 1 篇被收录

2）　EI 收录：有 2 篇被收录

3）　CNKI 收录：有 2 篇被收录

（详细结果见附件）

特此证明！

（盖章）

检索报告人：　　**2026 年 07 月 14 日**

附件：

一、 SCI-E 收录情况

第 1 条，共 1 条

标题: Experimental investigation on fracture growth for integrated hydraulic fracturing in multiple gas bearing formations

作者: Tan, P (Tan, Peng); Chen, ZW (Chen, Zhaowei); Fu, SH (Fu, Shihao); Zhao, Q (Zhao, Qing)

来源出版物: GEOENERGY SCIENCE AND ENGINEERING 卷: 231 文献号: 212316 DOI: 10.1016/j.geoen.2023.212316 Early Access Date: SEP 2023 Published Date: 2023 DEC 子辑: A

Web of Science 核心合集中的 "被引频次": 76

被引频次合计: 79

入藏号: WOS:001081723300001

文献类型: Article

地址: [Tan, Peng; Chen, Zhaowei; Zhao, Qing] CNPC Engn Technol R&D Co Ltd, Beijing 102206, Peoples R China.

[Tan, Peng; Chen, Zhaowei; Zhao, Qing] Natl Engn Res Ctr Oil & Gas Drilling & Complet Tec, Qingdao 266580, Peoples R China.

[Fu, Shihao] China Univ Petr, Beijing 102249, Peoples R China.

通讯作者地址: Chen, ZW (通讯作者)，CNPC Engn Technol R&D Co Ltd, Beijing 102206, Peoples R China.

电子邮件地址: tanpeng09jy@163.com; chenzwdri@cnpc.com.cn

ISSN: 2949-8929

eISSN: 2949-8910

2025 年期刊的影响因子：4.4

2025 年期刊的中科院分区（升级版）：大类 工程技术 2 TOP 期刊

二、 EI 收录情况

1. Development of rubber composite casing for preventing shale gas casing deformation and its shear resistance evaluation (预防页岩气套变的橡胶组合套管研制及其抗剪切性能评价)

Chen, Zhaowei (CNPC Engineering Technology R & D Co., Ltd., Beijing; 102206, China); Zhou, Wengao; Xiang, Degui; Tan, Peng; Song, Jian; Chen, Xiaojun; Ren, Lejia; Huang, Hao Source: Natural Gas Industry, v 43, n 11, p 131-136, November 2023 Language: Chinese

Database: Compendex

2. Microseismic characteristics of shale gas wells with casing deformation in Changning, Sichuan (四川长宁页岩气套管变形井微地震特征分析)

Chen, Zhaowei (CNPC Engineering Technology R & D Company Limited, Beijing; 102206, China); Zhang, Haozhe; Zhou, Xiaojin; Cao, Hu Source: Shiyou Diqiu Wuli Kantan/Oil Geophysical Prospecting, v 56, n 6, p 1286-1292, December 15, 2021 Language: Chinese

Database: Compendex

三、 CNKI 收录情况

[1]陈朝伟. 解决工程问题的通用方法和哲学思考——以四川页岩气开发套管变形问题为例 [J].

工程研究——跨学科视野中的工程, 2025, 17 (3) 387-396.（中文核心）

[2]陈朝伟,项德贵. 四川盆地页岩气开发套管变形一体化防控技术 [J]. 中国石油勘探, 2022, 27 (1) 135-141.（中文核心）

（End）

经委托人确认签字:

231 (2023) 212316

Contents lists available at ScienceDirect

Geoenergy Science and Engineering

journal homepage: www.sciencedirect.com/journal/geoenergy-science-and-engineering

Experimental investigation on fracture growth for integrated hydraulic fracturing in multiple gas bearing formations

Peng Tan [a,b], Zhaowei Chen [a,b,*], Shihao Fu [c], Qing Zhao [a,b]

[a] CNPC Engineering Technology R&D Company Limited, Beijing, 102206, China
[b] National Engineering Research Center for Oil & Gas Drilling and Completion Technology, 102206, China
[c] China University of Petroleum, Beijing, 102249, China

ARTICLE INFO

Keywords:
Coal measure strata
Integrated hydraulic fracturing
Fracture propagation
Natural fractures

ABSTRACT

The key to extracting multiple natural gases from coalbed methane, shale and other tight gases through integrated hydraulic fracturing in coal measure strata (CMS) is determining whether hydraulic fracture can connect different gas-bearing zones. In this paper, several groups of combination samples comprised of artificial rocks were prepared. True triaxial hydraulic fracturing experiments were conducted to stimulate the hydraulic fracture propagation and penetration behavior. The effects of in-situ stress, injection rate, natural fracture and well type on fracture growth were studied. The main results were as follows: (1) Fracture geometries in CMS exhibited strong asymmetric, nonplanar extension and unilateral expansion features in the vertical plane. (2) Higher values of the vertical stress difference coefficient and injection rate led to larger vertical fracture extension and an increased likelihood of fracture connection to adjacent gas-bearing layers. (3) The behavior of the hydraulic fracture varied significantly between vertical and horizontal wells. In vertical wells, the main fracture presented a "+" shape and fully communicated natural coal cleats system, while in horizontal wells, fracture height growth was limited, resulting in fracture patterns that presented vertically as “H” or “T” shape due to the hydraulic fracture’s tendency to turn direction when propagating to natural weak planes. The study found that the fracture vertical extension ability increased with rising vertical stress difference coefficient. (4) Natural fractures could induce fracture turning and branching, which improved fracture network complexity but also caused fracturing fluid loss and hydraulic energy dissipation. Therefore, choosing shale or coal layer with developed natural fractures as fracturing layer was unhelpful for integrated fracturing operation. Finally, higher fracturing fluid viscosity, injection rate and gradient sanding could enhance fracturing operation efficiency. These results could provide theoretical guidance for integrated fracturing operation in CMS.

1. Introduction

The Ordos Basin in China contains a suite of gas-bearing strata known as coal measure strata (CMS), which consist of large amounts of coalbed, shale and bits of tight stone that were deposited and preserved alternately within a few tens of meters in the vertical profile (see Fig. 1). However, the thick cumulative rock layers and ample thin single rock sheet with uneven thickness present challenges for packer setting and upper workover in slim hole during multi-layered fracturing. To address these problems, integrative cross-layer hydraulic fracturing may be a viable solution, allowing for the successful co-exploitation of multiple types of gases such as coalbed methane, shale and tight gases. Field tests of integrative fracturing technology have been performed in some areas and have achieved great progress, such as Surat Basin in Australia (Shen et al., 2017) and Xuanhua Basin in China (Li et al., 2014).

For the successful implement of integrated fracturing technology in CMS, it is crucial that different gas-bearing zones are effectively connected by hydraulic fractures in the vertical profile. This requires effective interface penetration, large extension distance and high complexity degree during hydraulic fracture vertical propagation. Previous studies have extensively investigated the problem of fracture height growth in layered media. In the aspect of analytic model, Oyedokun and Schubert (2017) established a mathematical mode for anisotropic layered media based on energy conservation method and proposed the concept of effective fracture toughness. Huang and Liu (2018) obtained the 3D criterion of hydraulic fracture penetration

* Corresponding author. CNPC Engineering Technology R&D Company Limited, Beijing, 102206, China.
E-mail addresses: tanpeng09jy@163.com (P. Tan), chenzwdri@cnpc.com.cn (Z. Chen).

https://doi.org/10.1016/j.geoen.2023.212316
Received 22 April 2022; Received in revised form 27 April 2023; Accepted 5 September 2023
Available online 11 September 2023

Fig. 1. Multiple gas bearing outcrops for CMS.

through beddings. Zhao and Chen (2010) and Liu and Valkó (2015) came up with the mechanical and mathematical model for hydraulic fracture vertical propagation based on fracture mechanics theory. Considering the inference of plastic region at fracture tip, Li et al. (2020) built a hydraulic fracture height mathematical model. Dontsov (2022) analyzed a constant height hydraulic fracture driven by a power-law fluid. These studies provide valuable insights for understanding and optimizing hydraulic fracture propagation in layered media, which is critical for successful integrated fracturing operations in CMS.

In the aspect of physical experiments, Warpinski et al. (1982) and Teufel and Clark (1984) found that the interface shear strength and the minimum stress difference between layers determined the fracture height growth for sand-mudstone formations. Liu et al. (2016) conducted the tri-axial fracturing experiment and analyzed the hydraulic fracture non-planar extension behavior for layered formation inclined well. Thiercelin and Lemanczyk (1986), Jeffrey and Bunger (2007) and Xing et al. (2018a) studied the hydraulic fracture height growth under different testing parameters through triaxial experiment with PMMA transparent material. For layered shale formation, Zhang et al. (2019), Guo et al. (2014) and Zou et al. (2016a) found that bedding planes had a significant effect on fracture height geometries. Through statistics and analysis of a large number of the shale experimental results, Tan et al. (2017, 2020) summarized fracture morphology types in vertical profile for shadow and deep shale formation. For shadow shales, fracture geometries were characterized by simple fracture, fishbone-like fracture, fishbone-like fracture with fissure opening, multilateral fishbone-like fracture network (Tan et al., 2017). For deep shales, fracture geometries were characterized by horizontal hydraulic fracture, transverse fracture, step-shaped hydraulic fracture with fissure opening and multilateral step-shaped hydraulic fracture network (Tan et al., 2020). In addition, the hydraulic fracture vertical propagation behavior of transversely isotropic shale by considering the lithological transition zone is studied based on XFEM-based CZM method (Tan et al., 2021). For CMS, Li et al. (2014), Wan et al. (2019), Zhao et al. (2019), Tan et al. (2019) performed a large number of physical experiments to study the non-planar fracture vertical propagation behavior. They found that the natural fractures in tight rocks could affect the interface penetration effect and that in coal would determine the finial complexity degree of hydraulic fracture network. These studies have provided valuable insights into the behavior of hydraulic fractures in layered media and can guide the successful implementation of integrative fracturing technology in CMS.

In the aspect of numerical experiments, Zhang and Jeffrey (2007) and Tang et al. (2018) studied the fracture height growth behavior in layered media based on displacement discontinuity method. Wang et al. (2017), Wang et al. (2021), Zhang et al. (2017, 2019), Huang et al. (2019, 2023), Li et al. (2023), and Abdelaziz et al. (2023) studied the hydraulic fracture initiation and propagation behavior based on discrete element modeling method. Zhu et al. (2014), Li et al. (2017) and Guo et al. (2017) investigated the effects of geological and engineering factors on porous layered formation based on cohesive damage method. Chen et al. (2015) built a fracture intersection model that hydraulic fracture was orthogonal to the bedding plane and studied the formation mechanism of T-Shape and Z-Shape fracture. Feng et al. (2017) used the similar method to quantify the fluid-driven interface debonding of an injector well. Haddad et al. (2018) took the dip angle of bedding plane into account in the numerical model. Zou et al. (2016b) studied the effects of multiple factors on 3D fracture propagation based on coupled finite element and discrete element method. Ouchi et al. (2017) studied the vertical propagation behavior of hydraulic fractures quantitatively and obtained three types of fracture propagation patterns, including crossing, turning, branching, which was proved by the experimental results (AITammar and Sharma, 2017). Settgast et al. (2017) carried out full coupling 3D hydraulic fracturing numerical simulation for laminated shale reservoirs though a fully coupled finite element and finite volume approach based on massively parallel computing platforms. Xing et al. (2018b) used a lattice method to simulate the fracture vertical propagation behavior and established a control chart of multiple parameters, including interlayer stress difference, vertical stress difference, fracture toughness and interface property. In addition, some machine learning methods were used in the studies of geomechanical behavior of shale (Tang et al., 2021; Zhao et al., 2022).

The afore-mentioned studies mainly focused on the single lithology or homogeneous layered media, ignoring the effects of developed complex natural fractures in each layer. Previous studies showed that affected by distinctive rock mechanical and fracture characteristics, hydraulic fracture geometries in coal and shale differed extremely and showed greater complexity than those in tight limestone (Hou et al., 2018). Therefore, when natural coals, shale and homogeneous tight stone are fractured jointly in CMS, hydraulic fracture geometries might be more complicated and the mechanism of fracture height growth was unclear. To understand the hydraulic fracture extension behavior of CMS, this paper carried out several groups of true triaxial hydraulic fracturing experiments on layered combination samples comprised of artificial rocks. Two typical tri-layered combination samples of "coal--shale-coal" and "coal-shale-limestone" were made. Beddings planes and coal cleats system were simulated. The effects of different factors, including in-situ stress, injection rate and well type on hydraulic fracture geometries and vertical propagation were studied.

2. Geological characteristics

In the Ordos Basin's X formation, the rock is primarily composed of horizontal shale and coal, with some limestone present. The individual layers are relatively thin, ranging from 0.5 to 3 m, but they accumulate to form a significant thickness of 20–80 m, with the coal-shale-limestone combination being the typical production layer. The reservoir is buried at a depth of approximately 3 km. The in-situ stresses vary for the vertical, horizontal maximum and minimum stresses, ranging from 39.65 to 44.8 MPa, 31.35–42.74 MPa and 28.11–37.93 MPa, respectively.

It has been observed that the total organic content (TOC) in the reservoir is greater than 2%. The highest TOC values were found in coal and shale with an average of 27.29% and 8.02%, respectively. The porosity of the reservoir varied from 1.13% to 10.67%, while the permeability was below 0.1 mD with an average value of 0.015 mD. Table 1 showed the mineral composition of coal, shale and limestone in X formation based on the X-ray diffraction (XRD) microanalysis. The rock mechanics parameters were measured trough GCTS equipment (Ge et al., 2011) and the testing results were displayed in Table 2 and Table 3. Based on the above analyses, CMS exhibited complex lithological combinations, rock mechanical properties and geological conditions. Thus, connecting more pay layers for the CMS integrated hydraulic fracturing faced many challenges.

Table 1
Mineral content.

Rock type	Quartz	Analcite	Calcite	Barite	Dolomite	Hematite	Plagioclase	Clay minerals
Coal	15.2	25.8	30.3	28.7	15.2	/	/	/
Shale	20.8		18.7	3.9	/	26.1	3.7	26.8
Limestone	10.8		/	/	83.9	4.1	/	1.2

Table 2
Mechanical parameters of real rocks.

Rock type	Real cores			
	Elastic Modulus / GPa	Poisson's ratio	Tensile strength / MPa	Compressive strength / MPa
Coal	5.29	0.35	0.74	15.00
Shale	11.29	0.24	2.58	16.64
Limestone	33.31	0.17	6.04	49.06

Table 3
Mechanical parameters of artificial rocks.

Rock type	Artificial rocks		
	Mass ratio of cement, sand, water	Tensile strength / MPa	Compressive strength / MPa
Coal	0.92:5:1	0.63	12
Shale	1.03:5:1	1.87	18
Limestone	1.52:5:1	5.96	36

3. Experimental methods

3.1. Experimental equipment

A true triaxial hydraulic fracturing testing system (see Fig. 2) was utilized to conduct all sets of experiments. This system had been successfully used to simulate the initiation and propagation behavior of hydraulic fractures in a variety of materials (Fan and Zhang, 2014; Zhang et al., 2018, 2020, 2021). This apparatus mainly consisted of true tri-axial assembly, a servo-controlled supercharge of Mechanical Testing and Simulation (MTS) 816, data acquisition system, hydraulically voltage stabilizer, isolating assembly of hydraulic fluid and hydraulic power oil and other auxiliary devices. During the hydraulic fracturing process, confining stresses put on the specimen were applied by the hydraulic voltage stabilizer and the fluid injection pressure was supplied utilizing the servo-controlled supercharge MTS 816. The peak confining stress and injection pressure for this equipment were up to 28 MPa and 140 MPa. The maximum fluid volume of 800 ml could be injected to the sample continuously. Experimental control and data acquisition were conducted using a customized software running on a desktop computer. Some significant information could be output in real time, such as pressure-time curve and displacement-time curve and pressure-displacement curve.

3.2. Specimen preparation

The analogy method was used to study the rock mechanical behavior, since the obtainment of real borehole cores was difficult (Tien et al., 2006; Andra et al., 2008). Precisely, the preparation of artificial specimens was able to simulate the natural structure and rock mechanical properties of true formation. The materials commonly used to simulate rock sample could present the similar elastic-plastic behavior as the real rock, such as concrete, gypsum, resin and polymer. Besides, analogy method could be applied to simulate the natural fracture network in the rock (Wang et al., 2019). Different lithological combinations were used to create samples with varying ratios of mud, sand, coal and water. The samples primarily consisted of coal-shale-coal and coal-shale-limestone combination rock. Notably, the observation of natural fracture features revealed that the development of beddings in shale was a typical characteristic, while in coal, not only were bedding planes developed, but also mutually orthogonal cleat systems. To simulate natural weak planes, papers with different thicknesses were utilized in this study. The bedding plane in shale and coal was replicated using printer paper with a thickness of 0.11 mm, while the face cleat and butt cleat were replicated using two types of coated paper with

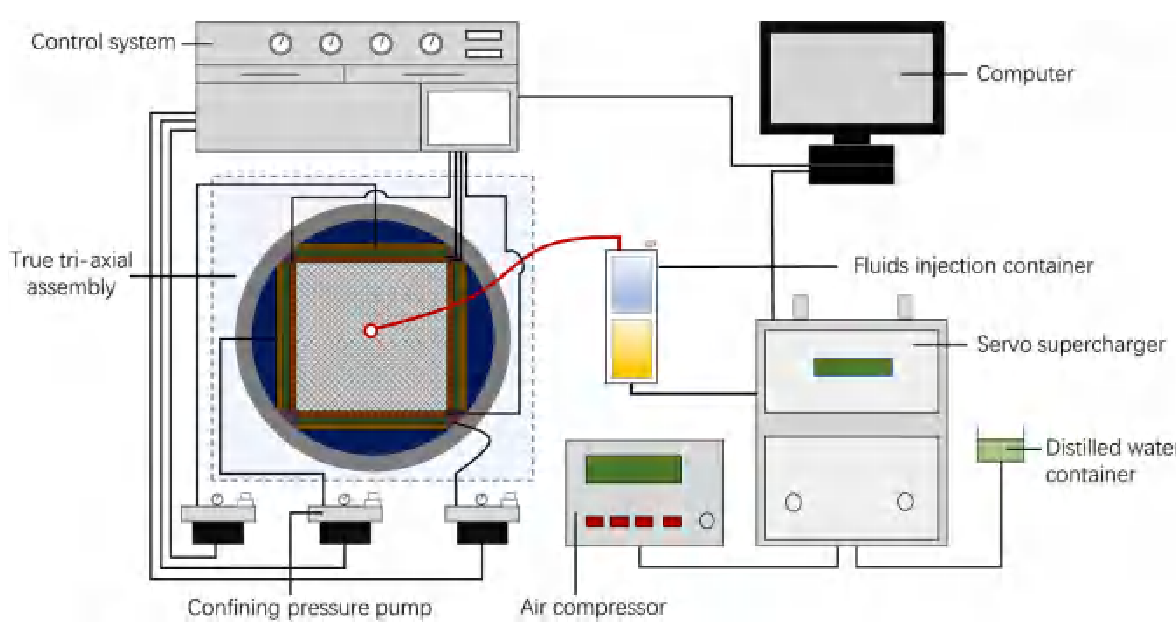

Fig. 2. True triaxial hydraulic fracturing system.

thicknesses of 0.14 mm and 0.12 mm, respectively. The following section details the procedure for preparing CMS hydraulic fracturing samples.

(1) Rock matrix preparation involved mixing single sheets of shale, coal and limestone with varying mass ratios of cement, quartz sand, coal and water to match the mechanical parameters of actual cores. Table 2 and Table 3 present the mechanical parameters of both real rock and artificial samples.
(2) To simulate natural fracture systems, coated paper was used during the preparation of coal and shale sheets to replicate cleat systems and bedding planes in coal and shale rock.
(3) Different rock sheets were stacked in a 300mm × 300mm × 300 mm square steel mold to create a combination of coal, shale and limestone. Concrete was then poured into the mold to bond the sheets and the specimens were cured at room temperature for 30 days.
(4) To simulate the wellhole, a 16 cm-long, 14 mm-diameter hole was drilled parallel or perpendicular to the bedding planes according to the horizontal and vertical well. A steel pipe was bonded with strong glue to simulate the wellbore, leaving a 2 cm open hole at the bottom. Fig. 3 illustrates the schematic drawing of a coal-shale-coal sample with a horizontal wellbore.

3.3. Experimental scheme

Based on the actual formation parameter of CMS above, the specific experimental parameters were obtained by combining the similarity criterion (Clifton and Abou Sayed, 1979) and the working capacity of the experimental system. The symbol of C, S and L indicated different slices of coal, shale and limestone, respectively (Table .4). The symbol of σ_V, σ_H, σ_h represented vertical stress, horizontal minimum stress and horizontal maximum stress. For each experiment, the fracturing fluid with yellow fluorescent tracer was injected at a constant pump rate. Under ultraviolet light, the tracer could be helpful in indicating the fracture surface generated during the experiment.

3.4. Experimental procedure

During testing, the cubic sample was placed at the center of the triaxial assembly and then loaded using three independent flat jacks to simulate in-situ stress conditions. To prevent the generation of shear stress during the in-situ stress loading process, a thin Teflon sheet, covered on both sides with Vaseline, was inserted between the sample and the flat jacks (De Pater and Beugelsdijk, 2005). To prevent mechanical shear failure in samples caused by unbalanced loading, the three in-situ stresses were simultaneously loaded to the minimum

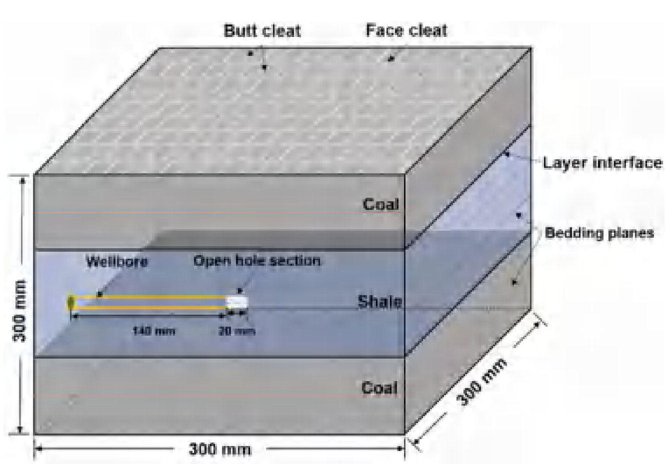

Fig. 3. Schematic drawing of coal-shale-coal sample with horizontal wellbore.

horizontal stress value first, followed by gradually increasing the vertical and maximum horizontal stresses to the maximum horizontal stress value. Finally, the vertical stress was slowly loaded to its designated value. Once all the stresses reached the desired values, it was necessary to delay for approximately 30 min to establish stress equilibrium before commencing the fracturing fluid injection process (Kim and Abass, 1991). For each experiment in this study, the sample was in a normal faulting stress regime. In both the vertical and horizontal well, the vertical stress was applied perpendicular to the layer interface, while the maximum horizontal stress was applied in the face cleat direction and the minimum horizontal stress was applied in the direction of butt cleat.

Once the stress loading was completed, the sample was injected with fracturing fluid containing luminous yellow fluorescent dye through the stimulated wellbore at a certain pump rate. Hydraulic fractures initiated once the injection pressure reached the fracturing pressure. Then propagated away from the wellbore. Injection was stopped once the hydraulic fracture was fully developed, which was ensured by adequate fracturing volume of the injected fluids. After unloading, all data were saved and the fracturing experiment was considered complete.

4. Experimental results and analysis

4.1. Experimental results

4.1.1. Fracture geometry

The hydraulic fracturing in specimens #1 and #2 was performed using a vertical well, while specimens #3 to #6 were fractured using a horizontal well. The main focus of the study was to analyze the fracture geometry and extension scale. After the experiments, each specimen was opened along the expected hydraulic fracture orientations to observe the connection degree between natural and hydraulic fractures and to analyze the fracture geometry under different experimental parameters. The fracture extension patterns observed presented a non-plane network instead of a single plane fracture. The results of the study are presented in Fig. 4.

For specimen #1 (Fig. 4(a)), the fracture initiated in the middle shale layer and propagated along the direction of minimal principal horizontal stress, resulting in a fracture with height and length. Along the direction of fracture height, the hydraulic fracture propagated to the coal layer and two parallel fractures were formed along the face cleats. Additionally, the activated face cleats were connected by butt cleats.

In specimen #2 (Fig. 4(b)), the fracture initiated from the bottom of the open hole section along the direction of maximum principal horizontal stress. As the fracture height propagated, the beddings in shale and the interface between shale and coal were activated. At the layer interface, an offset crossing of hydraulic fracture occurred and ultimately, a step-shaped fracture was formed.

In specimen #3 (Fig. 4(c)), the main fracture initiated and propagated along the direction of maximum principal horizontal stress. During fracturing fluid injection, a secondary hydraulic fracture formed along the wellbore direction. In the vertical plane, one bedding in shale was activated and the fracture height was contained by the upper- and lower-layer interface.

For specimen #4 (Fig. 4(d)), the main hydraulic fracture initiated perpendicular to the wellbore direction in the middle shale layer. As it extended upward to the layer interface between shale and coal and downward to the lower bedding in shale, the main fracture stopped. Meanwhile, the upper bedding in shale was activated.

In specimen #5 (Fig. 4(e)), the main fracture initiated and propagated along the direction of maximum principal horizontal stress. Under the effect of wellbore stress concentration, a secondary fracture was formed along the wellbore direction and the upper bedding plane in shale was activated. The vertically propagated hydraulic fracture was finally arrested by the upper and lower interfaces.

For specimen #6 (Fig. 4(f)), the main fracture initiated from the bottom of the open hole section and propagated vertically towards the

Table 4
Summary of experimental parameters.

Sample number	Well type	Rock combination	In-situ stress (MPa)			Coefficient of vertical stress difference	Flow rate (ml/min)	Viscosity (mPa·s)
			σ_V	σ_H	σ_h			
#1	Vertical well	C–S-L	22	21	20	0.1	10	3
#2		C–S-L	22	21	15	0.47	20	3
#3	Horizontal well	C–S–C	22	21	20	0.1	20	3
#4		C–S-L	22	21	20	0.1	20	3
#5		C–S–C	22	21	15	0.47	10	3
#6		C–S-L	22	21	15	0.47	20	3

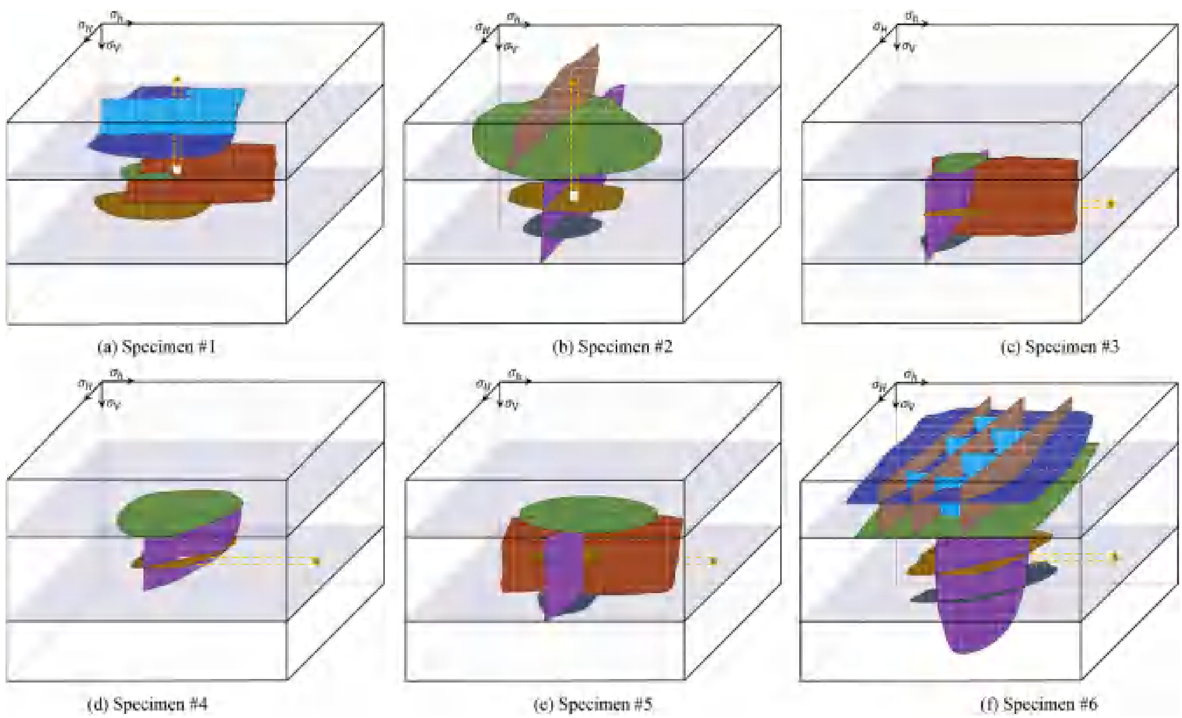

Fig. 4. The fracture geometry of different samples after fracturing.

wellbore direction, connecting the upper coal and lower limestone layers. Two bedding planes in shale and the interface between shale and limestone were activated. In the upper coal slice, the two orthotropic cleat systems were activated, resulting in the formation of a complex fracture network.

4.1.2. Stimulated rock area (SRA) and vertical fracture height (VFH)

"Stimulated Reservoir Area" (SRA) was denoted as an evaluation index for the hydraulic fracturing results (Hou et al., 2014; Wei et al., 2014). Compared with the index of "Stimulated Reservoir Volume" (SRV), SRA has a better manipulation in the laboratory hydraulic fracturing experiments. The final fracture geometry mainly includes main hydraulic fracture, activated bedding planes, cleats system, lithological interface and the combination of these planes. According the definition of SRA, each activated fracture area could be divided into five grades, including1.00 (about 300 × 300 mm), 0.8, 0.6, 0.4 and 0.2. Using specimen #4 (Fig. 4(d)) as an example, a single vertical hydraulic fracture perpendicular to the minimum horizontal stress direction was formed, accompanied by the opening of two bedding planes in the horizontal direction. The SRA values of the main hydraulic fracture and the bedding planes were 0.2 and 0.4, respectively, resulting in a total SRA value of 0.6 for this sample. Additionally, a new parameter called "Vertical Fracture Height" (VFH) was introduced in this study to evaluate the fracture propagation and penetration behavior, defined as the maximum distance of hydraulic fracture height growth. The SRA and VFH results for all samples are presented in Table 5.

4.2. Analysis on different effect factors

4.2.1. Effects of in-situ stresses

Specimens #1, #3, #4 and #2, #5, #6 were conducted under the condition that in-situ stresses were 22-21-20 and 22-21-15. Correspondingly, the vertical stress difference coefficients (Equation (1)) of the two sets of samples were 0.1 and 0.47, which was denoted as the radio between vertical in-situ stress difference and minimum horizontal in-situ stress (Tan et al., 2017).

Table 5
The value of SRA and VFH for different samples.

Specimen number	Main fracture area (mm^2)	Beddings area (mm^2)	Interface area (mm^2)	Cleats area (mm^2)	SRA (mm^2)	VFH (mm)
#1	0.2	0.6	0.4	0.6	1.8	200
#2	0.6	1	0.8	0.4	2.8	200
#3	0.6	0	0.4	0	1	100
#4	0.2	0.4	0	0	0.6	70
#5	0.6	0.2	0.4	0	1.2	100
#6	0.8	0.8	0.4	1	3	230

$$k_v = \frac{\sigma_v - \sigma_h}{\sigma_h} \tag{1}$$

Whether the slippage of natural weak plane would occur was related to the cohesion, friction coefficient and the effective normal stress loading on the weak plane based on Mohr-Coulomb law. Therefore, for a given value of cohesion, friction coefficient and roughness of the weak surface. Higher values of k_v result in a greater resistance to weak plane slippage and a higher probability of hydraulic fracture crossing layer interfaces. The experimental results demonstrate that the fracture geometry of specimens #4 and #6 were significantly different since different k_v values in these two samples. For the specimen #4 with lower k_v of 0.1 (Fig. 4(d)), the fracture geometry is characterized by the shorter vertical extension distance and larger horizontal propagation scale. In this condition, the fracturing fluid could easily diffuse to the weak discontinuities, thus the vertically propagated hydraulic fracture would be arrest or stopped at the beddings in shale or layer interface. For the specimen #6 with higher k_v of 0.47, the hydraulic fracture propagated sufficiently in the vertical direction and crossed bedding planes in shale and upper and lower lithological interfaces (Fig. 4(f)). In summary, the results indicate that the in-situ stresses have a significant impact on the vertical extension of hydraulic fractures. Additionally, the k_v parameter plays a crucial role in determining fracture patterns and layer penetration behavior. Higher values of k_v result in greater ability for fracture height growth and activation of more natural discontinuities. Conversely, lower k_v values result in a lower possibility of fracture crossing interfaces, resulting in smaller VFH and SRA values. Therefore, it can be inferred that the hydraulic fracturing design should take into consideration the in-situ stresses and k_v value to optimize the fracture pattern and ensure efficient stimulation of reservoirs.

4.2.2. *Effects of injection rate*

The injection rate of fracturing fluid is a crucial factor that affects the hydraulic fracture behavior. Changes in flow rate can directly impact the fracture propagation mode, leading to phenomena such as arrest or penetration when the fracture encounters natural fractures, bedding or interfacial interfaces. Appropriate injection rates can promote increased vertical fracture propagation height and the formation of complex fracture networks. Therefore, it is important to analyze the effect of injection rate on fracture growth behavior in CMS. In this study, two levels of injection rate (10 ml/min and 20 ml/min) were examined.

For specimen #5, which was subjected to a low injection rate of 10 ml/min, there was a higher likelihood of leakage along the beddings in shale, resulting in hindered main fracture height propagation and penetration. The hydraulic fracture propagated towards the bedding planes and easily changed direction and leading to a smaller VFH. In contrast, for specimen #6 subjected to a high injection rate of 20 ml/min, the fracture propagated vertically, connecting all layers and activating numerous cleat faces in coal seams. The stimulated area was almost oval with the long axis along the maximum principal horizontal stress direction. However, it should be noted that the ability of hydraulic fractures to cross interfaces is determined by both engineering and geological parameters, so improving the injection rate may not always aid in fracture crossing the interface. The relationship between injection rate and in-situ stress is shown in Fig. 5. It can be observed that even at higher injection rates, specimens #3 and #4 with small k_v values were unable to penetrate the lithological interface. The larger VFH and SRA were obtained under conditions of a higher vertical stress coefficient and higher flow velocity.

4.2.3. *Effects of well-type*

Experimental results showed that the hydraulic fracture propagation behavior was extremely different between the vertical and horizontal well. For the vertical well fracturing (specimen #1 and #2), the whole fracture geometry showed the " + " shaped characteristic. In the vertical plane, the hydraulic fractures could also fully communicate the bedding planes in shale. When propagated to the interface between shale and coal, the fracture turned direction firstly and then extended vertically along the face cleat direction. Finally, hydraulic fracture network with fully activated cleat system were formed (Fig. 6(a)). For the horizontal well fracturing, when encountering the beddings in shale, a large amount of fracturing fluids easily leaked off into the weak planes and pressurization rate was low in main fractures, as a result, the propagated main hydraulic fracture could stop or be arrested. Therefore, it is difficult for hydraulic fracture to penetrate bedding planes and the fracture geometry was relative sample. Generally, the main hydraulic fracture patterns presented "H" and "T" in shape (Fig. 6(b)). This may lead to complex and irregular fracture geometry, which can also be affected by the presence of natural fractures, bedding planes and lithological interfaces. Additionally, the vertical well may have a different stress regime compared to the horizontal well, leading to different fracture propagation patterns. Therefore, it is crucial to consider the wellbore geometry and the local stress field when designing and analyzing hydraulic fracturing in vertical wells. Meanwhile, fracturing fluid could flow along the interface between wellbore and rock matrix. When the injection pressure was increased, the fracture expanded dynamically and penetrated through the layered interface and formed "+" shaped fractures.

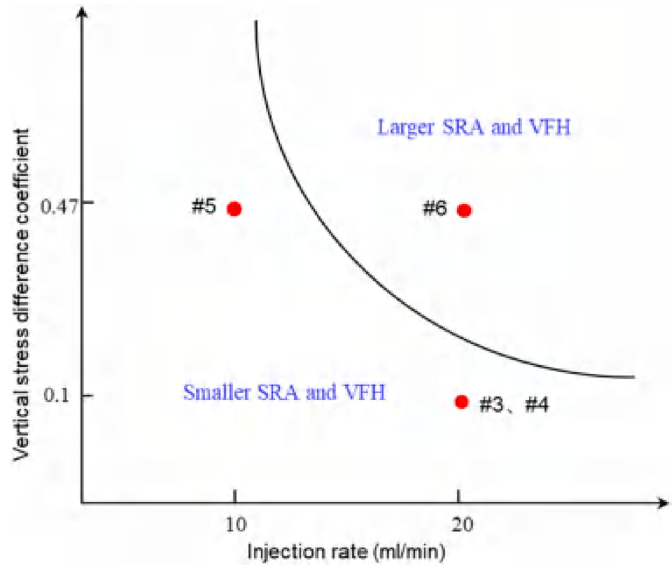

Fig. 5. The combined effects of vertical stress difference coefficient and injection rate on SRA and VFH.

4.2.4. *Effects of weak planes*

Highly developed bedding planes and cleats system were the

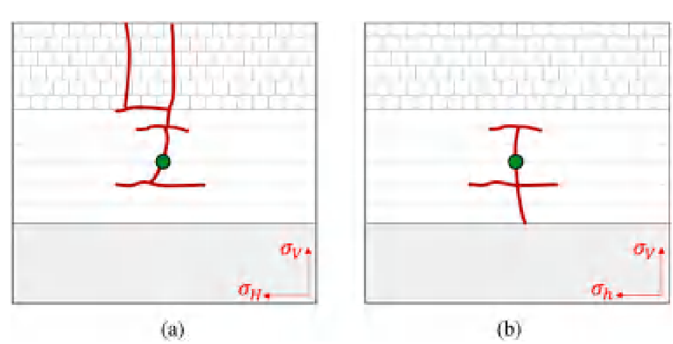

Fig. 6. The sketch of fracture geometry in the vertical profile for specimen #1 and #3. The green circle is the injection point and red line presents the main hydraulic fracture.

precondition to achieve the goal of stimulating unconventional reservoirs. Under the impact of bedding planes in shale, such as specimen #3, #4, #5, the hydraulic fracture propagated to the bedding planes and then turned to horizontal direction. Since a large amount of fracturing fluid filtrated along the bedding planes and hydraulic energy dissipation, the capacity of fracture crossing interface decreased. For specimen #1, #2 and #6, the hydraulic fracture penetrated lithological interface and connected the upper coal layer. A large number of cleats were opened and forming the complex fracture network. In addition, the propagation of hydraulic fracture followed the laws of minimum flow resistance, minimum energy dissipation and small propagation path. Hydraulic fracture extension and its communication with the upper coal seam could lead to the continuous upward flow of fracturing fluids, resulting in insufficient hydraulic energy for the downward extending fracture and incomplete connection with the limestone. Furthermore, the hydraulic fracture mainly propagated along the cleats system as it reached the coal seam, forming a complex fracture network. The tracer distribution observations after the experiments also revealed that the fracturing fluid was primarily distributed around the cleats system and did not form any fracture in the coal matrix.

Face and butt cleats as well as bedding planes were highly developed in coals and the cohesive strength of these discontinuities was lower than shale. Therefore, during the hydraulic fracturing operation, damage or breakdown of these weak structural surfaces were more prone to occur and induce the hydraulic fractures to turn and bifurcate, which led to that the propagation path of hydraulic fracture was not always perpendicular to minimum horizontal principal stress direction. Zhao and Chen (2010) used the rock fracture mechanics methods and analyzed the interaction type of hydraulic fracture and natural weak face. Their results showed that the hydraulic fracture could stop, diverse and cross lithological interface. However, it could be found in this study that except from the three basic fracture propagation types obtained by Zhao and Chen (2010), fracture behaviors such as bifurcation and offset could be also observed. Take the specimen #1 in Fig. 4(a) as example, the wing of upward hydraulic fracture bifurcated and diverted firstly and then penetrated at the upper layer interface between shale and coal. Therefore, the obtained findings in this study could enrich the fracture intersection and penetration patterns and be better used to understand the real fracture propagation behavior in unconventional fractured formations or CMS.

5. Discussions

(1) Through several groups of true tri-axial hydraulic fracturing experiments, this study analyzed the effects of various factors on hydraulic fracture geometries and penetration laws in coal-measure strata (CMS). However, due to limitations in the size and number of real reservoir cores, the study utilized artificial rock samples consisting of cement, quartz sand, and coal powder instead of real cores. This may have caused some differences in the results. To address this, the mechanical properties and natural fracture features of real formations were considered during sample preparation. Therefore, while the results may not be entirely representative or quantitatively extrapolated to field operations, the qualitative findings from the experiments provide important insights into the establishment of mathematical models and understanding of fracture height growth behavior in CMS.

(2) Previous studies showed that for tight limestone a simple fracture geometry could be formed along the maximum horizontal in-situ stress direction (Hou et al., 2018). For coal seams, hydraulic fracture mainly extended along the natural path of cleats system and finally fence-typed fracture network could be formed (Fan and Zhang, 2014). For shale formations, the bedding planes was continuously opened during the vertical propagation of hydraulic fracture, resulting in the formation of fishbone- or step-typed fracture geometry (Tan et al., 2017, 2020). Through above experiments, it could be indicated that the fracture geometry in CMS was more complex and presented huge difference compared with these single lithological formations. The typical fracture geometries in CMS, tight limestone, coal and shale were showed in Fig. 7. It could be found that for the fracture height growth of CMS it exhibited strong non planar and asymmetric penetration characteristics, which is mainly effected by the discontinuities and strong heterogeneities in the vertical profile. In addition, the hydraulic fracture extension follows the principle of least resistance, priority, and shortest propagation path. Vertical hydraulic fractures primarily propagate in the direction of minimum resistance. Hydraulic fractures tend to follow the path of least resistance, prioritizing the shortest and easiest route. In cases where resistance is equal in all directions, the fracturing fluid prefers to flow through pre-existing channels. Consequently, the hydraulic fracture extends along the path of least resistance and shortest propagation distance, and any other potential paths are delayed or stopped. Unless an abnormally high injection pressure is applied, these postponed or stopped fractures are unlikely to propagate further.

(3) Results showed that hydraulic fracture height growth was larger and had bigger chance for hydraulic fracture communicating adjacent gas bearing layers under high vertical stress difference coefficient and injection rate, which means that the final SRV and VHF was larger. Fig. 8 showed the hydraulic fracture geometry in vertical profile under different conditions of in-situ stress and flow rate. Based on the principle of co-exploitation of multiple types unconventional gases, when integrated hydraulic fracturing is performed in CMS, the hydraulic fracture height is expected to propagate longer, cross the lithological boundaries and connect more gas-production layers. According to above experimental results, the layer with higher vertical stress difference coefficient was recommended to be selected as the treatment zone. In addition, the larger injection displacement was suggested in the operation of hydraulic fracturing.

(4) The stress distribution inside the sample was complicated because of the effects of natural fracture system. The complex multi-fractures wound dissipate the hydraulic energy, limit fracture height growth and decrease the chance of layers crossing (see Fig. 4). Meanwhile, multi-fractures increased the fracture tortuosity and decreased the fracture width, which could seriously restricted proppants migration in fracture, resulting in premature sand removal. Hence, the fracture geometries should be simplified as much as possible around the wellhole. This problem could be improved by optimizing the following construction technology: Firstly, the improvement of injection rate and fracturing fluid viscosity could increase the possibility of hydraulic fracture penetrating natural weak surfaces and decrease the generation of branch fractures (Tan et al., 2020; Wan et al., 2019); Secondly, a small amount of acid fluids was suggested to be injected into the formation, which can increase the main hydraulic fracture width through acid-rock reaction (Zhang et al., 2020); Moreover, gradient sanding method could be used in field application, in which the small sized proppants were firstly employed to polish the perforating hole to reduce the proppants migration resistance. Then the large sized proppants were pumped (Tan et al., 2020).

(5) On the one hand, for the vertical well fracturing, the wellbore could easily induce the hydraulic fracture to propagate upward, cross layer interface and connect the upper layer (see Fig. 4). During the extension of main fracture, the fracturing fluids could easily leak along the natural weak planes. Finally, these natural weak planes wound be easily activated to form complex fracture network. Due to the asymmetric propagation characteristics, the hydraulic fracture mainly expanded upward in specimen #1 and

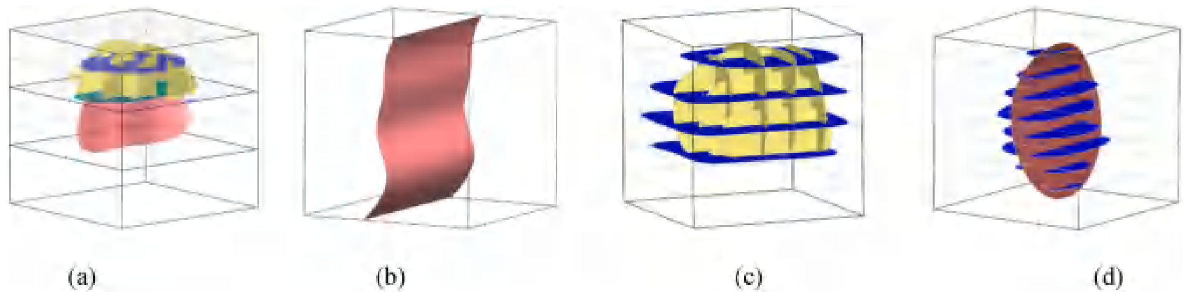

Fig. 7. Schematic diagram of fracture geometry for (a) CMS, (b) tight limestone, (c) shale and (d) coal.

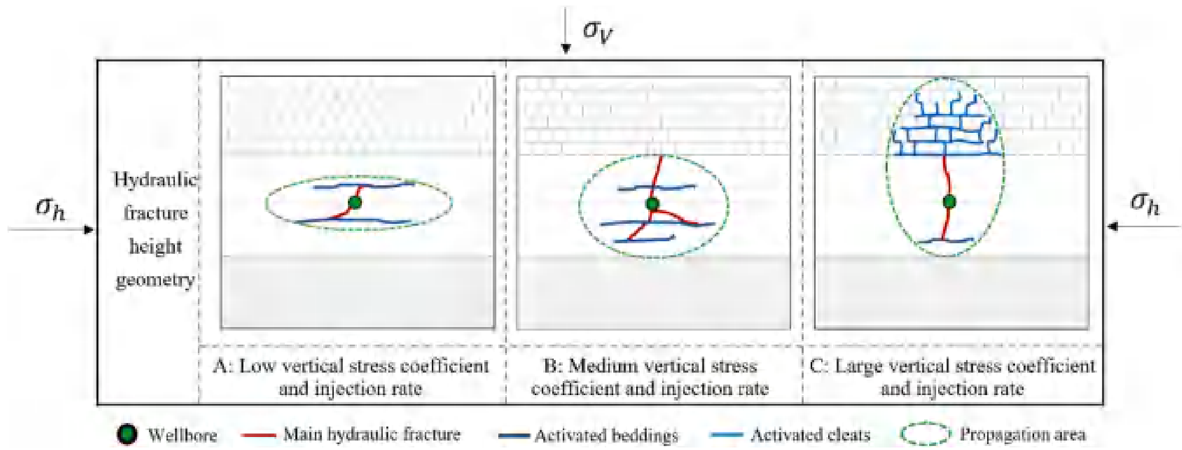

Fig. 8. Schematic diagram of hydraulic fracture geometry in vertical profile under different conditions of in-situ stress and flow rate.

#2 (see Fig. 4). Therefore, for vertical well fracturing in CMS, the downside layer was better to selected as treatment zone to improve the communication of different layers. In this condition, proppants with low density or high suspension property were suggested to be used, which could decrease the resistance of proppants upward migration and prevent premature sand plugging (Kale and Olatunji, 2017; Radwan, 2017). When the hydraulic fracture propagates upward along the wellbore, micro fractures would be easily induced in the cement sheath and its cemented surface with rock, resulting in gas channeling or casing deformation and endangering wellhead safety (Shen et al., 2016; Yu et al., 2016). So high toughness cement slurry or self-healing water mud system could be used to enhance slurry performance and cement quality in the target formation (Lee et al., 2016; Gao et al., 2019). On the other hand, for the horizontal well fracturing, the hydraulic fracture initiated from the shale layer easily turned or stopped along the beddings during extension (see Fig. 4), Therefore, it was suggested to avoid selecting the layer with high development degree of natural fractures for fracturing operation to increase the possibility of multi-layer penetration.

(1) The fracture height growth in CMS was complex, showing strong asymmetric, nonplanar extension, and unilateral expansion features due to the developed weak discontinuities and induced complicated stress field within or between layers in CMS. These factors were the main reasons for the formations of multi-fractures around the wellbore and limited layer penetration.
(2) Higher vertical stress difference coefficient and injection rate resulted in larger fracture vertical extension distance and the possibility of connecting adjacent gas bearing layers via hydraulic fractures. Thus, it is recommended to choose a fracturing layer with high vertical stress difference coefficient and increase the injection rate appropriately to promote fracture height growth.
(3) For vertical well fracturing, the main hydraulic fracture followed a "+" shape, and beddings in shale and cleats in coal could be fully activated as the fracture vertically propagated and penetrated the layer interface. For horizontal well fracturing, the hydraulic fracture was prone to turn direction when encountering weak discontinuities, leading to limited fracture height growth.
(4) Developed discontinuities could induce hydraulic fractures turning and branching to improve fracture network complexity. However, they could also cause fracturing fluid loss and dissipate hydraulic energy, making it necessary to avoid choosing shale or coal layers with developed natural fractures as treatment zones for integrated fracturing operation. Properly increasing fracturing fluid viscosity and injection rate could enhance fracturing operation efficiency.

Declaration of competing interest

We declare that we have no financial and personal relationships with other people or organizations that can inappropriately influence our work, there is no professional or other personal interest of any nature or kind in any product, service and/or company that could be construed as influencing the position presented in, or the review of, the manuscript entitled.

Data availability

No data was used for the research described in the article.

Acknowledgements

The authors gratefully acknowledge the support of the China CNPC science and technology project (2021DQ03-37, 2021DJ4706, 2021DJ4102, 2022DJ8005) and CPET science and technology project

(CPET202105).

References

Aitammar, M.J., Sharma, M.M., 2017. Effect of Geological Layer Properties on Hydraulic Fracture Initiation and Propagation: an Experimental study[C]//SPE Hydraulic Fracturing Technology Conference, Woodlands, Texas, USA.

Andra, N., Marone, C., Elsworth, D., et al., 2008. Healing of simulated fault gouges aided by pressure solution: results from rock analogue experiments[J]. J. Geophys. Res. Solid Earth 113. B4.

Abdelaziz, A., Ha, J., Li, M., et al., 2023. Understanding hydraulic fracture mechanisms: from the laboratory to numerical modelling[J]. Advances in Geo-Energy Research 7 (1), 66–68.

Clifton, R.J., Abou Sayed, A.S., 1979. On the Computation of the Three-Dimensional Geometry of Hydraulic fractures[C]//Symposium Low Permeability Gas Reservoirs, Denver, Colorado.

Chen, Z.X., Jeffrey, R.G., Zhang, X., 2015. Numerical modeling of three-dimensional T-shaped hydraulic fractures in coal seams using a cohesive zone finite[J]. Hydraulic Fracturing Journal 2 (2), 20–37.

De Pater, C.J., Beugelsdijk, L.J.L., 2005. Experiments and Numerical Simulation of Hydraulic Fracturing in Naturally Fractured rock[C]//U.S. Symposium on Rock Mechanics. Anchorage, Alaska.

Dontsov, E.V., 2022. Analysis of a constant height hydraulic fracture driven by a power-law fluid[J]. Rock Mechanics Bulletin 1 (1), 100003.

Fan, T.G., Zhang, G.Q., 2014. Laboratory investigation of hydraulic fracture networks in formations with continuous orthogonal fractures[J]. Energy 74, 164–173.

Feng, Y.C., Li, X.R., Gray, K.E., 2017. Development of a 3D numerical model for quantifying fluid-driven interface debonding of an injector well[J]. Int. J. Greenh. Gas Control 62, 76–90.

Guo, T.K., Zhang, S., Qu, Z., et al., 2014. Experimental study of hydraulic fracturing for shale by stimulated reservoir volume[J]. Fuel 128, 373–380.

Guo, Y.T., Yang, C.H., Wang, L., 2017. Study on the influence of bedding density on hydraulic fracturing in shale. Arab. J. Sci. Eng. 43, 6493–6508.

Ge, W.F., Chen, M., Jin, Y., 2011. Analysis of the external pressure on casings induced by salt-gypsum creep in build-up sections for horizontal wells[J]. Rock Mech. Rock Eng. 44, 711–723.

Gao, Y., Yang, G.G., Lu, P.Q., et al., 2019. Study and application of a large temperature difference cement slurry with good elasticity and toughness [J]. Drill. Fluid Complet. Fluid 36 (1), 97–108.

Huang, B.X., Liu, J.W., 2018. Fully Three-Dimensional Propagation Model of Horizontal Borehole Hydraulic Fractures in Strata under the Effect of Bedding planes[J]. Energy Exploration & Exploitation, 1283110222.

Haddad, M., Du, J., Vidal-gilbert, S., 2018. Integration of dynamic microseismic data with a true 3D modeling of hydraulic-fracture propagation in the vaca muerta shale [J]. SPE J. 1714–1738.

Hou, B., Chen, M., Li, Z.M., et al., 2014. Propagation area evaluation of hydraulic fracture networks in shale gas reservoirs[J]. Petrol. Explor. Dev. 41 (6), 763–768.

Hou, B., Zhang, R.X., Tan, P., et al., 2018. Characteristics of fracture propagation in compact limestone formation by hydraulic fracturing in central Sichuan, China[J]. J. Petrol. Sci. Eng. 57, 122–134.

Huang, L.K., Liu, J.J., Zhang, F.S., et al., 2019. Exploring the influence of rock inherent heterogeneity and grain size on hydraulic fracturing using discrete element modeling [J]. Int. J. Solid Struct. 176–177, 207-202.

Huang, L.K., He, R., Yang, Z.Z., et al., 2023. Exploring hydraulic fracture behavior in glutenite formation with strong heterogeneity and variable lithology based on DEM simulation [J]. Eng. Fract. Mech. 278, 109020.

Jeffrey, R.G., Bunger, A.P., 2007. A Detailed Comparison of Experimental and Numerical Data on Hydraulic Fracture Height Growth through Stress contrasts[C]//SPE Hydraulic Fracturing Technology Conference, Texas, USA.

Kim, C.M., Abass, H.H., 1991. Hydraulic Fracture Initiation from Horizontal Wellbores: Laboratory experiments[C]//U.S. Symposium on Rock Mechanics, Norman, Oklahoma.

Kale, J., Olatunji, O., 2017. Low Density Proppant in Slickwater Application Improves Reservoir Contact and Fracture Complexity- a Permian Basin Case History [C]//SPE Liquids-Rich Basins Conference - North America, Midland, Texas, USA.

Li, D.Q., Zhang, S.C., Zhang, S.A., 2014. Experimental and numerical simulation study on fracturing through interlayer to coal seam [J]. J. Nat. Gas Sci. Eng. 21, 386–396.

Liu, S.X., Valkó, P.P., 2015. An Improved Equilibrium-Height Model for Predicting Hydraulic Fracture Height Migration in Multi-Layer formations[C]//SPE Hydraulic Fracturing Technology Conference, Woodlands, Texas.

Liu, Z., Jin, Y., Chen, M., et al., 2016. Analysis of non-planar multi-fracture propagation from layered-formation inclined-well hydraulic fracturing[J]. Rock Mech. Rock Eng. 49 (5), 1747–1758.

Li, Y., Deng, J., Liu, W., 2017. Numerical simulation of limited-entry multicluster fracturing in horizontal well[J]. J. Petrol. Sci. Eng. 152, 443–455.

Li, Y.W., Long, M., Tang, J.Z., et al., 2020. A hydraulic fracture height mathematical model considering the influence of plastic region at fracture tip[J]. Petrol. Explor. Dev. 47, 184–195.

Li, Y.W., Hu, B.Q., Wu, J., et al., 2023. Optimization method of oriented perforation parameters improving uneven fractures initiation for horizontal well fracturing[J]. Fuel 349, 128754.

Lee, S.W., Minki, J., Kim, J.W., et al., 2016. Application of ca-doped mesoporous silica to well-grouting cement for enhancement of self-healing capacity[J]. Mater. Des. 89, 362–368.

Oyedokun, O., Schubert, J., 2017. A quick and energy consistent analytical method for predicting hydraulic fracture propagation through heterogeneous layered media and formations with natural fractures: the use of an effective fracture toughness [J]. J. Nat. Gas Sci. Eng. 44, 351–364.

Ouchi, H., Foster, J.T., Sharma, M.M., 2017. Effect of reservoir heterogeneity on the vertical migration of hydraulic fractures[J]. J. Petrol. Sci. Eng. 151, 384–408.

Radwan, A., 2017. A Multifunctional Coated Proppant: a Review of over 30 Field Trials in Low Permeability Formations [C]//SPE Annual Technical Conference and Exhibition, San Antonio, Texas, USA.

Shen, J., Zhang, C.J., Qin, Y., Zhang, B., 2017. Effect factors on co-mining of sandstone gas and coal bed methane in coal series and threshold of parameter in Linxing block, Ordos Basin[J]. Nat. Gas Geosci. 28 (3), 479–487.

Settgast, R.R., Fu, P., Walsh, S.D.C., et al., 2017. A fully coupled method for massively parallel simulation of hydraulically driven fractures in 3-dimensions[J]. Int. J. Numer. Anal. Methods GeoMech. 41 (5), 627–653.

Shen, X., Shen, G., Standifird, W., 2016. Numerical Estimation of Upper Bound of Injection Pressure Window with Casing Integrity under Hydraulic Fracturing [C]// Rock Mechanics/Geomechanics Symposium, Houston, Texas, USA.

Teufel, L.W., Clark, J.A., 1984. Hydraulic fracture propagation in layered rock: experimental studies of fracture containment[J]. SPE J. 19–32.

Thiercelin, M.J., Lemanczyk, Z.R., 1986. Stress Gradient Affects the Height of Vertical Hydraulic fractures[J]. SPE Production Engineering, pp. 245–254.

Tan, P., Jin, Y., Han, K., et al., 2017. Analysis of hydraulic fracture initiation and vertical propagation behavior in laminated shale formation[J]. Fuel 206, 482–493.

Tan, P., Jin, Y., Yuan, L., 2019. Understanding hydraulic fracture propagation behavior in tight sandstone–coal interbedded formations: an experimental investigation. Petrol. Sci. 16, 148–160.

Tan, P., Pang, H.W., Zhang, R.X., et al., 2020. Experimental investigation into hydraulic fracture geometry and proppant migration characteristics for southeastern Sichuan deep shale reservoirs[J]. J. Petrol. Sci. Eng. 184, 106517.

Tan, P., Jin, Y., Pang, H.W., 2021. Hydraulic fracture vertical propagation behavior in transversely isotropic layered shale formation with transition zone using XFEM-based CZM method [J]. Eng. Fract. Mech. 248, 107707.

Tien, Y.M., Kuo, M.C., Juang, C.H., et al., 2006. An experimental investigation of the failure mechanism of simulated transversely isotropic rocks[J]. Int. J. Rock Mech. Min. Sci. 43 (8), 1163–1181.

Tang, J.Z., Wu, K., Zeng, B., et al., 2018. Investigate effects of weak bedding interfaces on fracture geometry in unconventional reservoirs[J]. J. Petrol. Sci. Eng. 165, 992–1009.

Tang, J.Z., Fan, B., Xiao, L.Z., et al., 2021. A new ensemble machine learning framework for searching sweet spots in shale reservoirs[J]. SPE J. 26 (1), 482–497.

Warpinski, N.R., Clark, J.A., Schmidt, R.A., et al., 1982. Laboratory investigation on the effect of in-situ stresses on hydraulic fracture containment[J]. Int. J. Rock Mech. Min. Sci. Geomech. Abstracts 19 (6), 333–340.

Wan, L.M., Hou, B., Tan, P., et al., 2019. Observing the effects of transition zone properties on fracture vertical propagation behavior for coal measure strata[J]. J. Struct. Geol. 126, 69–82.

Wang, D.J., Tang, H.M., Shen, P.W., et al., 2019. Co-effects of bed-ding planes and parallel flaws on fracture evolution in ani-sotropic rocks[J]. Eng. Geol. 264, 105382.

Wei, D., Gao, Z.Q., Fan, T.L., 2014. Experimental hydraulic fracture propagation on naturally tight intra-platform shoal carbonate[J]. J. Petrol. Sci. Eng. 157, 980–989, 2017.

Wang, W., Zheng, D., Sheng, G., et al., 2017. A review of stimulated reservoir volume characterization for multiple fractured horizontal well in unconventional reservoirs [J]. Advances in Geo-Energy Research 1 (1), 54–63.

Wang, X.H., Zhang, F.S., Tang, M.R., et al., 2021. Effect of stress shadow caused by multi-stage fracturing from multiple well pads on fracture initiation and near-wellbore propagation from infill wells. SPE J. 27 (1), 204–225.

Xing, P.J., Yoshiok, A.K., Adachi, J., et al., 2018a. Laboratory demonstration of hydraulic fracture height growth across weak discontinuities. [J]. Geophysics 83 (2), 93–105.

Xing, P.J., Yoshiokab, K., Adachib, J., 2018b. Lattice simulation of laboratory hydraulic fracture containment in layered reservoirs[J]. Computer and Geotechnics 100, 62–75.

Yu, Y.J., Jin, J.Z., Qi, F.Z., 2016. Progress of study on functional cementing fluids[J]. Drill. Fluid Complet. Fluid 33 (4), 1–7.

Zhao, H.F., Chen, M., 2010. Extending behavior of hydraulic fracture when reaching formation interface[J]. J. Petrol. Sci. Eng. 74 (1–2), 26–30.

Zhao, H.F., Wang, X.F., Liu, Z.Y., 2019. Experimental investigation of hydraulic sand fracturing on fracture propagation under the influence of coal macrolithotypes in Hancheng block, China[J]. J. Pet. Sci. Eng. 175, 60–71.

Zhao, X.Z., Jin, F.M., Liu, X.W., et al., 2022. Numerical study of fracture dynamics in different shale fabric facies by integrating machine learning and 3-D lattice method: a case from Cangdong Sag, Bohai Bay basin, China[J]. J. Petrol. Sci. Eng. 218, 110861.

Zou, Y.S., Zhang, S.C., Qu, Z.Q., et al., 2016a. Experimental investigation into hydraulic fracture network propagation in gas shales using CT scanning technology[J]. Rock Mech. Rock Eng. 49, 33–45.

Zou, Y.S., Ma, X.F., Zhang, S.C., et al., 2016b. Numerical investigation into the influence of bedding plane on hydraulic fracture network propagation in shalefFormations[J]. Rock Mechancis and Rock Engineering 49, 3597–3614.

Zhang, X., Jeffrey, R.G., 2007. Hydraulic Fracture Propagation across Frictional interfaces[C]/. U.S. Rock Mechanics Symposium, Vancouver, Canada.

Zhu, H.Y., Deng, J.G., Zhao, J., et al., 2014. Cementing failure of the casing-cement-rock interfaces during hydraulic fracturing. Comupt. Concr. 14 (1), 91–107.

Zhang, F.S., Dontsov, E., Mack, M., 2017. Fully coupled simulation of hydraulic fracture interacting with natural fractures with a hybrid discrete-continuum method[J]. Int. J. Numer. Anal. Methods GeoMech. 41 (13), 1430–1452.

Zhang, F.S., Damjanac, B., Maxwell, S., 2019. Investigating hydraulic fracturing complexity in naturally fractured rock masses using fully coupled multiscale numerical modeling[J]. Rock Mech. Rock Eng. 52 (12), 5137–5160.

Zhang, R.X., Hou, B., Shan, Q.L., et al., 2018. Hydraulic fracturing initiation and near-wellbore nonplanar propagation from horizontal perforated boreholes in tight formation[J]. J. Nat. Gas Sci. Eng. 55, 337–349.

Zhang, R.X., Hou, B., Tan, P., et al., 2020. Hydraulic fracture propagation behavior and diversion characteristic in shale formation by temporary plugging fracturing [J]. J. Petrol. Sci. Eng. 177, 442–451.

Zhang, J., Li, Y.W., Pan, Y.S., et al., 2021. Experiments and analysis on the influence of multiple closed cemented natural fractures on hydraulic fracture propagation in a tight sandstone reservoir[J]. Eng. Geol. 281, 105981.

引文： 陈朝伟, 周文高, 项德贵, 等. 预防页岩气套变的橡胶组合套管研制及其抗剪切性能评价[J]. 天然气工业, 2023, 43(11): 131-136.
CHEN Zhaowei, ZHOU Wengao, XIANG Degui, et al. Development of rubber composite casing for preventing shale gas casing deformation and its shear resistance evaluation[J]. Natural Gas Industry, 2023, 43(11): 131-136.

预防页岩气套变的橡胶组合套管研制及其抗剪切性能评价

陈朝伟[1,2] 周文高[3] 项德贵[1,2] 谭 鹏[1,2] 宋 建[1,2] 陈晓军[1,2] 任乐佳[1,4] 黄 浩[1,4]

1. 中国石油工程技术研究院有限公司 2. 油气钻完井技术国家工程研究中心
3. 中国石油川庆钻探工程有限公司 4. 中国石油大学（北京）

摘要： 页岩气是目前天然气勘探开发的重点和热点，但页岩气在开发过程中经常会遇到套管变形问题，套管变形不仅影响单井产量，还将缩短井筒生命周期，严重制约着我国页岩气的规模效益开发。为此，利用橡胶吸收裂缝 / 断层的滑动位移原理，创新设计了一种橡胶组合套管；在综合套管变形量、橡胶膨胀率、下套管摩阻、水泥浆通道和吸水膨胀效率等因素基础上，优选了橡胶胶种，设计橡胶筒成槽孔结构；并利用物理模拟试验系统对橡胶组合套管进行了抗剪切试验，最后利用 ABAQUS 有限元软件建立了橡胶组合套管位移加载三维力学模型，评价了橡胶组合套管的抗剪切能力。研究结果表明：①膨胀橡胶通过变形和破碎吸收了地层位移载荷，保护了套管，吸收地层滑动量可达到 37.2 ～ 40.0 mm；②当橡胶筒厚度增加时，套管的变形量随之减小，当橡胶筒厚度达到 21.7 mm 时，橡胶可以完全吸收施加的位移，避免套管发生变形。结论认为，橡胶组合套管可以有效吸收裂缝 / 断层的滑动位移，从而保护了内层套管不受影响，进而提高了页岩气井的压裂施工效率，缩短了投产周期，可为我国页岩气的效益开发提供重要的技术支撑。

关键词： 页岩气；套管变形；大位移量；橡胶组合套管；剪切试验
DOI: 10.3787/j.issn.1000-0976.2023.11.012

Development of rubber composite casing for preventing shale gas casing deformation and its shear resistance evaluation

CHEN Zhaowei[1,2], ZHOU Wengao[3], XIANG Degui[1,2], TAN Peng[1,2], SONG Jian[1,2], CHEN Xiaojun[1,2], REN Lejia[1,4], HUANG Hao[1,4]

(1. *CNPC Engineering Technology R & D Co., Ltd., Beijing* 102206, *China*; 2. *National Engineering Research Center for Oil & Gas Drilling and Completion Technology, Beijing* 102206, *China*; 3. *CNPC Chuanqing Drilling Engineering Company Limited, Chengdu, Sichuan* 610051, *China*; 4. *China University of Petroleum, Beijing* 102249, *China*)

Natural Gas Industry, Vol.43, No.11, p.131-136, 11/25/2023. (ISSN 1000-0976; In Chinese)

Abstract: Shale gas is the current focus and hotspot of natural gas exploration and development, but casing deformation happens frequently during it development, which not only impacts single well production, but also shortens the service life of wellbore, seriously restricting the large-scale benefit development of shale gas in China. In this paper, a rubber composite casing is designed according to the principle that rubber can absorb the sliding displacement of fracture/fault. Then, an optimal rubber is selected by taking into account the factors comprehensively such as casing deformation, rubber expansion rate, casing running friction, cement slurry channel, and water absorption and expansion efficiency. In addition, a slotted hole structure is designed for the rubber cylinder, and shear tests are conducted on the rubber composite casing using a physical simulation test system. Finally, a three-dimensional mechanical model for displacement loading of the rubber composite casing is established using ABAQUS finite element software, and the shear resistance of the rubber composite casing is evaluated. And the following research results are obtained. First, the expanded rubber absorbs the displacement load of the formation through deformation and fragmentation, so as to protect the casing. And it can absorb the formation sliding as large as 37.2–40.0 mm. Second, the casing deformation decreases with the increase of rubber cylinder thickness. When the rubber cylinder is 21.7 mm thick, the rubber can absorb all displacement loads, to avoid casing deformation. In conclusion, the rubber composite casing can absorb the sliding displacement of fracture/fault effectively, so as to protect the inner casing from damage and consequently improve the fracturing construction efficiency of shale gas well and shorten the commissioning cycle, which provides an important technical support for the benefit development of shale gas in China.

Keywords: Shale gas; Casing deformation; Large displacement; Rubber composite casing; Shear test

---

基金项目： 国家自然科学基金项目“流体注入引起的深部页岩断层激活与变形滑移机理研究”（编号：42077247）、“山地页岩水力压裂引起断层活化机理与诱发地震灾害防控”（编号：52179114），中国石油油田技术服务有限公司项目“深层页岩气体积压裂关键技术研究与应用”（编号：2022T-002-001），中国石油工程技术研究院有限公司课题“页岩气套变机理与风险预测技术研究”（编号：CPET202224）。

作者简介： 陈朝伟，1979 年生，正高级工程师，博士，本刊编委；主要从事石油工程地质力学技术研究工作。地址：（102206）北京市昌平区沙河中国石油科技园。ORCID: 0000-0002-0692-9203。E-mail: chenzwdri@cnpc.com.cn

0　引言

四川盆地页岩气在开发过程中遇到了套管变形问题，套管变形不仅影响单井产量，还将缩短井筒生命周期，严重制约着我国页岩气的高效开发。泸州地区深层页岩气不仅套变率高（超过 46.5%），而且套管变形量更大。截至 2021 年 9 月，共发现 A 类套变井（套变量小于 29 mm）6 口，B 类套变井（套变量 29 ～ 60 mm）4 口，C 类套变井（套变量大于 60 mm）20 口，过大的套管变形量使得现场没有办法继续进行压裂作业。

目前，套管变形的机理已达成共识，即水力压裂诱发断层 / 天然裂缝滑动，从而对穿过其中的套管施加了剪切位移 [1-11]。为了解决套管变形问题，现场采取了包括提高套管钢级、增加套管壁厚、优化固井质量、压裂降排量和减液量等多种措施，但都未取得实质性的效果 [12-15]。2023 年，中国石油西南油气田公司在泸州地区深层页岩气井开展了“空心微珠”固井工艺现场试验，其效果还有待于检验 [16]。可以预见，向固井水泥中添加空心微珠等材料，随着添加量的增加，水泥石的密度和抗压强度将随之降低，进而影响固井质量。因此，这种方法比较适合于套管变形量较小的情况，对于较大变形量，需要寻找其他的解决方法。

为解决较大变形量的套管变形问题，笔者团队研制了一种新型的橡胶组合套管，其工作原理是在高风险断层 / 裂缝处下入橡胶组合套管，压裂诱发裂缝 / 断层滑动时，橡胶吸收裂缝 / 断层的滑动位移，从而保护内层套管不受影响。本文介绍了橡胶组合套管的结构设计，包括优选膨胀橡胶和优化尺寸等，对加工的橡胶组合套管短节进行了抗剪切性能试验，并对橡胶组合套管的抗剪切性能进行了数值模拟，研究了其吸收剪切位移的效果。

1　橡胶组合套管结构设计

橡胶组合套管由页岩气井常用的钢制套管和橡胶筒组成，通过热硫化方法可将橡胶牢固地粘贴在套管的外表面。套管外增加橡胶筒，增加了下套管的阻力，为了尽可能减少阻力，橡胶设计为遇水膨胀橡胶，即下套管过程中橡胶筒不膨胀（油基钻井液），而在固井过程中吸水膨胀。

为了选择适宜的橡胶胶种（有一定的膨胀率，但膨胀后环空应足够大，确保水泥浆有足够的流动通道），优选了 6 种橡胶，进行了浸泡膨胀试验。在 100 ℃的 0.9% 盐溶液和 100 ℃的清水中浸泡 4 h，膨胀率测试结果如图 1 所示。试验数据表明，6 种胶种中 WSR Ⅰ、WSR Ⅳ和 WSR Ⅵ膨胀率过大，膨胀后发生糯化，强度不满足要求；WSR Ⅱ加工性能未满足要求，成形性能以及加工强度与预期有所差距；WSR Ⅴ膨胀率较低，未达到要求。综合成型条件、膨胀后弹性要求及水泥浆正常固化等多方面考虑，最终优选出 WSR Ⅲ作为候选胶种。

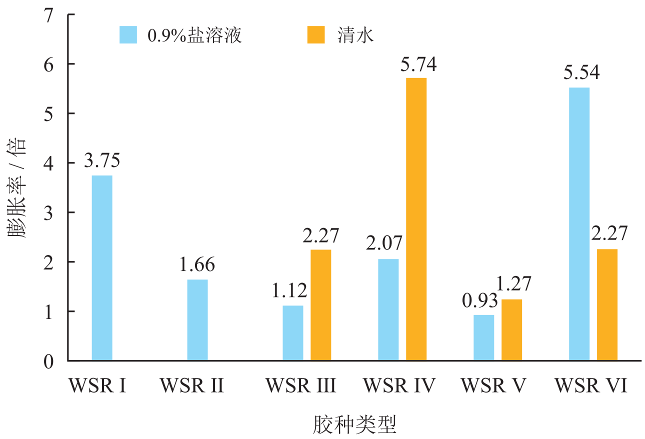

图 1　不同胶种在两种介质中浸泡 4 h 的膨胀率柱状图

进一步将胶种 WSR Ⅲ分别在清水、不同比例的盐溶液以及油液中进行浸泡试验，其在油液中的膨胀率小于 0.1 倍，满足在油基钻井液中不膨胀的要求（图 2）。

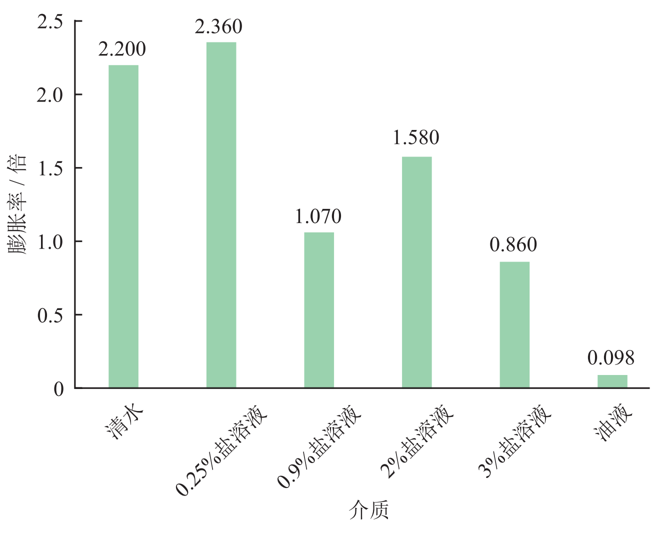

图 2　胶种 WSR Ⅲ在不同介质中浸泡 4 h 的膨胀率柱状图

综合套管变形量、橡胶膨胀率和下套管工艺情况，设计橡胶筒厚度为 12.7 mm，可根据需要进一步优化。为了保留固井水泥浆的流动通道以及橡胶组合套管在水泥浆凝固过程中吸水膨胀的效果，将膨胀橡胶筒设计成槽孔结构，其中槽宽 10 mm，槽深 6 mm，橡胶组合套管的结构如图 3 所示。

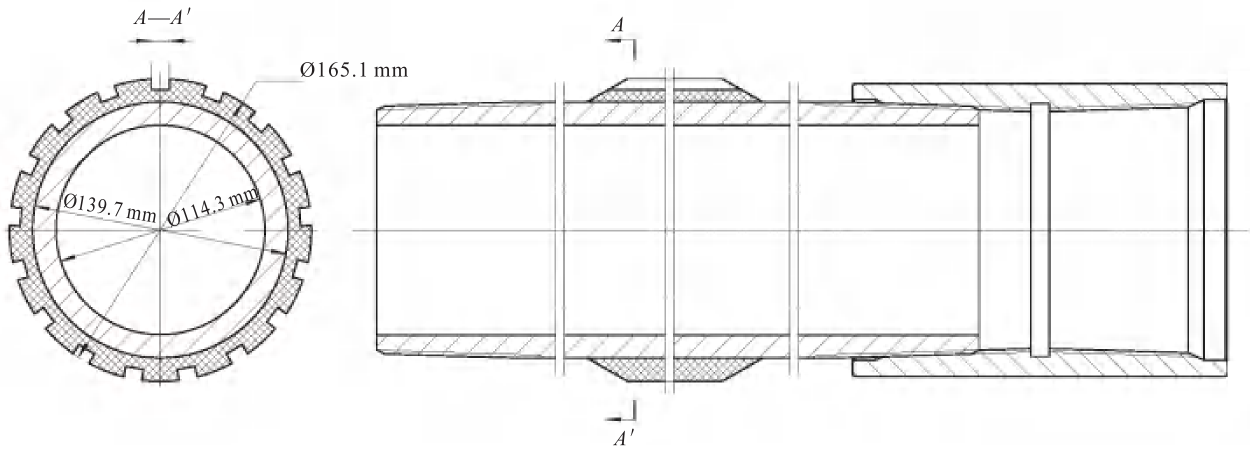

图 3　槽孔组合橡胶套管结构图

2　橡胶组合套管抗剪切性能试验

为了评价橡胶组合套管吸收地层位移的能力，加工了橡胶组合套管短节（图 4），利用 UTG 物理模拟试验系统对橡胶组合套管进行了抗剪切试验 [17]，共分 4 组试验，3 组为橡胶组合套管，1 组为常规套管。

图 4　槽孔组合膨胀橡胶套管样机照片

将套管短节（橡胶组合套管）做成试验样品，置于内径为 215.9 mm 套筒中，套筒的尺寸和页岩气现场井眼尺寸一致，并确保居中。将调配好的水泥浆浇筑到套筒和套管之间的环空，水泥浆按四川页岩气井现场用的配方调配：100% 嘉华 G 级水泥 +1% 降失水剂 +1% 缓凝剂 +0.2% 消泡剂 +0.7% 分散剂 +44% 水。候凝期间橡胶吸水膨胀，水泥浆凝固，7 天后水泥浆完全固结成水泥石，测量膨胀橡胶筒壁厚，厚度如表 1 所示。可见橡胶组合套管可通过吸收水泥浆中的水分而膨胀，膨胀率为 0.43 ～ 0.51，远低于清水中的膨胀率，但接近于 3% 盐溶液的膨胀率。最终的试样由套管、橡胶套筒、水泥石和套筒 4 层结构组成（图 5）。

将样品置于试验机上进行位移加载（图 6），用于模拟断块滑移过程 [18]。在加载过程中，仪器上下两端做相对运动，即样品左右两侧受到向上的位移

表 1　套管试验数据表

套管类型	橡胶筒壁厚 /mm		套管内径 /mm		套管变形量 / mm
	膨胀前	膨胀后	试验前	试验后	
常规	—	—	114.3	104.0	10.3
组合 1	12.7	18.2	114.3	114.0	0.3
组合 2	12.7	18.7	114.3	114.2	0.1
组合 3	12.7	19.2	114.3	114.1	0.2

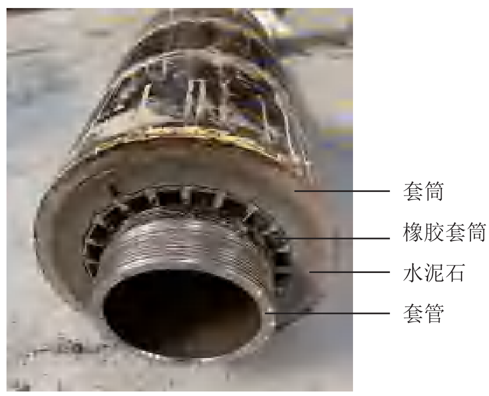

图 5　橡胶组合套管试样照片

图 6　位移加载试验照片

载荷，中部受向下的位移载荷，其中一个样品的位移载荷加载曲线如图 7 所示。位移加载量根据长宁—威远和泸州区块套管变形量设计，本实验位移加载量均取为 40.0 mm[2,19]。

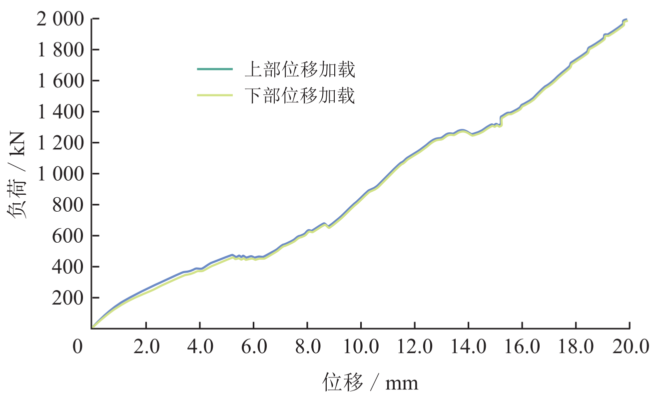

图 7　某样品的位移载荷加载曲线图

当位移加载达到设定的 40.0 mm 时，停止加载，保持状态 10 min，卸载后取出试验样品进行观察和测量。试验后的试样发生了错位（以 1 号橡胶组合套管样品为例），如图 8 所示，用内径规测量套管内径为 114.0 mm，表明套管完好，没有发生变形。

a. 样品　　b. 套管内径测量

图 8　试样试验后照片

打开外层套筒，去除水泥石，可见套管外层橡胶破损严重，残余厚度几乎为零，如图 9 所示。按照相同的方法，测得其他 3 组试验数据（表 1）。可以看到，3 组橡胶组合套管基本完好，而常规套管发生了变形，变形量为 10.3 mm。可见，膨胀橡胶通过变形和破碎吸收了位移载荷，保护了套管。

对比常规套管变形量发现，橡胶组合套管能够吸收 10.0 mm 的位移，该数值可作为吸收能力的下限；从加载 40.0 mm 位移下里层套管未发生变形来看，橡胶组合套管结合水泥石能够吸收地层位移 40.0 mm，该值可作为吸收能力的上限值。

值得说明的是，观察试验后的样品，还可以看

a. 中部橡胶吸收变形情况　　b. 上、下部橡胶吸收变形情况

图 9　试验后的橡胶破坏情况照片

到有少量橡胶和或水泥石从端面被挤出的情况，这是由于端面是自由端没有施加约束造成的。实际上，井下套管和水泥石在轴向方向受到约束。因此，试验结果可能会夸大橡胶组合套管吸收地层位移的能力。

3　橡胶组合套管抗剪切性能数值模拟

为了弥补室内试验的不足，开展了数值模拟研究。利用 ABAQUS 有限元软件建立了橡胶组合套管位移加载三维力学模型，如图 10 所示。其中套管、橡胶套筒、水泥石和套筒 4 层结构的几何结构和尺寸与试验样品保持一致，施加位移载荷装置用上下两个夹具来模拟，上下夹具宽 180.0 mm，上下夹具中心间距为 240.0 mm。

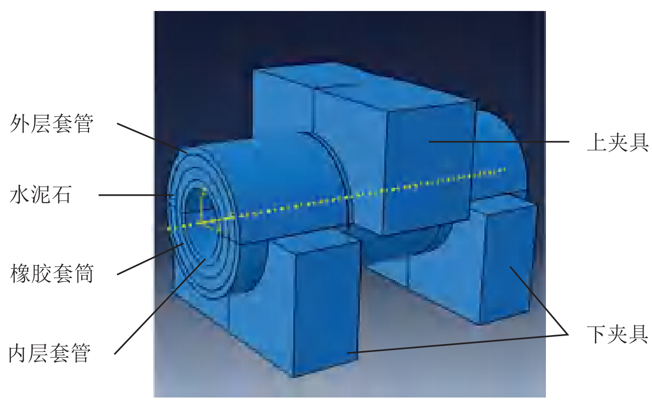

图 10　橡胶组合套管位移加载三维力学模型图

模型中包括钢材、橡胶和水泥石 3 种材料。值得说明的是橡胶材料采用常用的 Mooney—Rivlin 本构模型 [20]：

$$U = C_{10}(I_1 - 3) + C_{01}(I_2 - 3) \tag{1}$$

式中 U 表示应变势能，MPa；I_1 和 I_2 表示基本应变

不变量，无量纲；C_{10}、C_{01} 表示橡胶力学特性系数，MPa，可由试验确定。Mooney—Rivlin 模型几乎可以模拟所有橡胶材料的力学行为，适合于中小变形，一般适用于应变约为 100 %(拉伸)和 30%(压缩)的情况。本文取参数 C_{10} 为 0.289 7 MPa，C_{01} 为 0.059 9 MPa。

材料的屈服准则，套管采用广义 Mises 准则，橡胶和水泥石均采用德拉克—普拉格模型，具体数值见表 2。

表 2　模型屈服准则参数表

材料	屈服准则	杨氏模量 / GPa	泊松比	屈服强度 / MPa	摩擦角 / (°)
水泥	德拉克—普拉格	10	0.2	12	23
橡胶	德拉克—普拉格	1	0.2	5	—
套管	广义 Mises 准则	210	0.3	965	—

上下夹具设置为刚体，对各管体侧面施加 Y 方向约束，以防橡胶和水泥从两端挤出。分别对上下两个夹具各施加 20.0 mm 的位移载荷，共计 40.0 mm 的位移。

膨胀橡胶厚度设置为 18.7 mm，利用模型计算得到套管的变形量见图 11，其中最大值为 2.8 mm。因此，考虑管体侧面约束，橡胶组合套管结合水泥石能够吸收位移量为 37.2 mm。在其他条件相同的情况下，数值模拟结果比试验结果更准确地给出吸收的位移量。

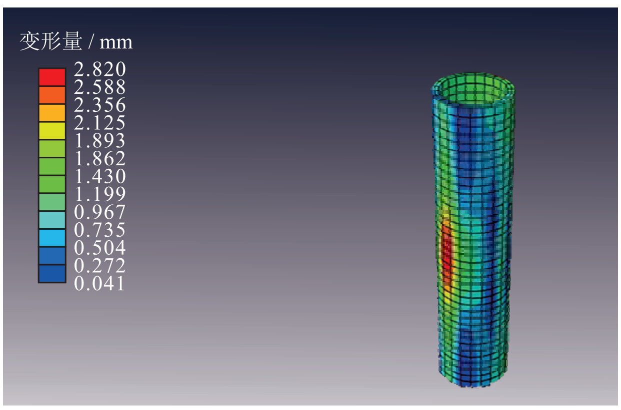

图 11　套管变形量模拟结果图

为了探讨橡胶筒的厚度对套管变形量的影响规律，按同样的方式，分别设置橡胶厚度为 12.7 mm、15.7 mm 和 21.7 mm，通过数值模拟计算得到套管变形量分别为 15.00 mm、11.10 mm 和 0.01 mm。可见，当橡胶筒厚度增加时，套管的变形量随之减小。当橡胶筒厚度达到 21.7 mm 时，橡胶可以完全吸收施加的位移，避免套管发生变形。该数据可为优化橡胶筒厚度提供依据。

根据橡胶组合套管吸收位移能力，预计可将潜在的 A 类套变降低为不发生套变，将潜在的 B 类套变降低为 A 类套变或不套变，将潜在的 C 类套变降低为B类套变，如果联合空心微珠固井和扩眼等技术，有希望将 C 类套变降低为 A 类套变，保证压裂作业的正常进行。

4　结论和建议

1）针对大变形量套管变形问题，创造性地提出了一种槽孔结合的遇水膨胀橡胶筒组合套管，综合套管变形量、橡胶的膨胀率、下套管工艺情况、固井水泥浆通道和吸收膨胀效率等因素，对该产品进行了结构和尺寸的优化设计。

2）对橡胶组合套管短节进行了抗剪切试验，并利用 ABAQUS 有限元软件建立了橡胶组合套管位移加载三维力学模型，评价橡胶组合套管的抗剪切能力，结果表明膨胀橡胶通过变形和破碎吸收了位移载荷，和普通套管相比，橡胶组合套管可以有效地吸收断层滑移，吸收变形量可达到 37.2 ～ 40.0 mm。

3）根据橡胶组合套管吸收位移能力，其可将潜在的套变等级降低至少一个等级，有望成为一种解决套管变形问题的行之有效的工具，建议尽快开展现场试验。

参　考　文　献

[1] 陈朝伟 , 石林 , 项德贵 . 长宁—威远页岩气示范区套管变形机理及对策 [J]. 天然气工业 , 2016, 36(11): 70-75.
CHEN Zhaowei, SHI Lin, XIANG Degui. Mechanism of casing deformation in the Changning-Weiyuan National shale gas project demonstration area and countermeasures[J]. Natural Gas Industry, 2016, 36(11): 70-75.

[2] 陈朝伟 , 王鹏飞 , 项德贵 . 基于震源机制关系的长宁—威远区块套管变形分析 [J]. 石油钻探技术 , 2017, 45(4): 110-114.
CHEN Zhaowei, WANG Pengfei, XIANG Degui. Analysis of casing deformation in the Changning-Weiyuan block based on focal mechanism[J]. Petroleum Drilling Techniques, 2017, 45(4): 110-114.

[3] 童亨茂 , 张平 , 张宏祥 , 等 . 页岩气水平井开发套管变形的地质力学机理及其防治对策 [J]. 天然气工业 , 2021, 41(1): 189-197.
TONG Hengmao, ZHANG Ping, ZHANG Hongxiang, et al. Geomechanical mechanisms and prevention countermeasures of casing deformation in shale gas horizontal wells[J]. Natural Gas Industry, 2021, 41(1): 189-197.

[4] 高利军 , 柳占立 , 乔磊 , 等 . 页岩气水力压裂中套损机理及其数值模拟研究 [J]. 石油机械 , 2017, 45(1): 75-80.

GAO Lijun, LIU Zhanli, QIAO Lei, et al. Mechanism analysis and numerical simulation of casing failure in hydraulic fracturing of shale gas formation[J]. China Petroleum Machinery, 2017, 45(1): 75-80.

[5] GUO Xueli, LI Jun, LIU Gonghui, et al. Numerical simulation of casing deformation during volume fracturing of horizontal shale gas wells[J]. Journal of Petroleum Science and Engineering, 2019, 172: 731-742.

[6] 陈朝伟 , 曹虎 , 周小金 , 等 . 四川盆地长宁区块页岩气井套管变形和裂缝带相关性 [J]. 天然气勘探与开发 , 2020, 43(4): 123-130.
CHEN Zhaowei, CAO Hu, ZHOU Xiaojin, et al. Correlation between casing deformation and fracture zones in Changning shale gas block, Sichuan Basin[J]. Natural Gas Exploration and Development, 2020, 43(4): 123-130.

[7] YIN Fei, HAN Lihong, YANG Shangyu, et al. Casing deformation from fracture slip in hydraulic fracturing[J]. Journal of Petroleum Science and Engineering, 2018, 166: 235-241.

[8] XI Yan, LI Jun, LIU Gonghui, et al. Numerical investigation for different casing deformation reasons in Weiyuan−Changning shale gas field during multistage hydraulic fracturing[J]. Journal of Petroleum Science and Engineering, 2018, 163: 691-702.

[9] ZHANG Fengshou, YIN Zirui, CHEN Zhaowei, et al. Fault reactivation and induced seismicity during multistage hydraulic fracturing: Microseismic analysis and geomechanical modeling[J]. SPE Journal, 2020, 25(2): 692-711.

[10] 陈朝伟 , 曹虎 , 石元会 . 四川长宁区块地应力特征及裂缝带活化分析 [J]. 工程地质学报 , 2020, 28(增刊 1): 86-95.
CHEN Zhaowei, CAO Hu, SHI Yuanhui. In-situ stress characteristics and fracture zone activation analysis of Changning shale gas in Sichuan Province[J]. Journal of Engineering Geology, 2020, 28(S1): 86-95.

[11] 李皋 , 李泽 , 简旭 , 等 . 页岩膨胀应变及固井质量对套管变形的影响研究 [J]. 特种油气藏 , 2021, 28(3): 139-143.
LI Gao, LI Ze, JIAN Xu. Study on the effect of shale expansion strain and cementing quality on casing deformation[J]. Special Oil & Gas Reservoirs, 2021, 28(3): 139-143.

[12] CHEN Zhaowei, ZHOU Lang, WALSH R, et al. Case study: Casing deformation caused by hydraulic fracturing-induced fault slip in the Sichuan Basin[C]//SPE/AAPG/SEG Unconventional Resources Technology Conference. Houston: SPE, 2018: URTEC-2882313-MS.

[13] CHEN Zhaowei, FAN Yu, HUANG Rui, et al. Case study: Fault slip induced by hydraulic fracturing and risk assessment of casing deformation in the Sichuan Basin[C]//SPE/AAPG/SEG Asia Pacific Unconventional Resources Technology Conference. Brisbane: SPE, 2019: URTEC-198212-MS.

[14] ZENG Bo, ZHANG Haozhe, ZHOU Xiaojin, et al. Microseismic characteristics of shale gas wells with casing deformation in Sichuan Basin[C]//55th U.S. Rock Mechanics/Geomechanics Symposium. Virtual: American Rock Mechanics Association, 2021: ARMA-2021-1825.

[15] 陈朝伟 , 黄锐 , 曾波 , 等 . 四川盆地长宁页岩气区块套管变形井施工参数优化分析 [J]. 石油钻探技术 , 2021, 49(1): 93-100.
CHEN Zhaowei, HUANG Rui, ZENG Bo, et al. Analysis and optimization of construction parameters for preventing casing deformation in the Changning shale gas block, Sichuan Basin[J]. Petroleum Drilling Techniques, 2021, 49(1): 93-100.

[16] 张平 , 何昀宾 , 刘子平 , 等 . 页岩气水平井套管的剪压变形试验与套变预防实践 [J]. 天然气工业 , 2021, 41(5): 84-91.
ZHANG Ping, HE Yunbin, LIU Ziping, et al. Shear compression deformation test and deformation prevention practice of casing in shale gas horizontal wells[J]. Natural Gas Industry, 2021, 41(5): 84-91.

[17] 韩礼红 , 杨尚谕 , 魏风奇 , 等 . 复杂压裂页岩气井套管变形机制及控制方法 [J]. 石油管材与仪器 , 2020, 6(4): 16-23.
HAN Lihong, YANG Shangyu, WEI Fengqi, et al. Casing deformation mechanism and controlling method for shale gas well under complex fracture environment[J]. Petroleum Tubular Goods & Instruments, 2020, 6(4): 16-23.

[18] 蒋振源 , 陈朝伟 , 张平 , 等 . 断块滑动引起的套管变形及影响因素分析 [J]. 石油管材与仪器 , 2020, 6(4): 30-37
JIANG Zhenyuan, CHEN Zhaowei, ZHANG Ping, et al. Casing deformation and its influencing factors caused by block sliding[J]. Petroleum Tubular Goods & Instruments, 2020, 6(4): 30-37.

[19] 陈朝伟 , 房超 , 朱勇 , 等 . 四川页岩气井套管变形特征及受力模式 [J]. 石油机械 , 2020, 48(2): 126-134.
CHEN Zhaowei, FANG Chao, ZHU Yong, et al. Deformation characteristics and stress modes of casings for shale gas wells in Sichuan[J]. China Petroleum Machinery, 2020, 48(2): 126-134.

[20] 李卓 , 黄琳 , 刘彦奎 , 等 . 基于 Mooney−Rivlin 本构模型的捣固凸轮橡胶弹簧变形分析 [J]. 燃料与化工 , 2022, 53(6): 10-14.
LI Zhuo, HUANG Lin, LIU Yankui, et al. Deformation analysis of cam rubber spring for stamping machine based on M−R constitutive model[J]. Fuel & Chemical Processes, 2022, 53(6): 10-14.

（修改回稿日期 2023-09-20 编辑 王 斌）

本文互动

· 微地震 · 文章编号:1000-7210(2021)06-1286-07

四川长宁页岩气套管变形井微地震特征分析

陈朝伟*① 张浩哲② 周小金③ 曹 虎②

(①中国石油集团工程技术研究院有限公司,北京 102206;②中国石油大学(北京),北京 102249;
③中国石油西南油气田公司页岩气研究院,四川成都 610051)

陈朝伟,张浩哲,周小金,曹虎. 四川长宁页岩气套管变形井微地震特征分析. 石油地球物理勘探,2021,56(6):1286-1292.

摘要 针对四川页岩气井套管变形问题,利用通过的小桥塞尺寸和多臂井径测井(MIT)数据计算了 H19 平台套管变形的变形量,同时分析了套管变形点处微地震事件点的时空分布和矩震级大小特征。然后在识别出的天然裂缝空间分布特征基础上建立了裂缝面模型,并利用该模型分析了套管变形量、天然裂缝尺度和微地震地震矩之间的定量关系。该平台共测得 9 个套管变形点的变形量,最小变形量为 6.10mm,最大为 50.43mm,平均为28.03mm,分析后得到天然裂缝的微地震时空特征:①微地震事件关于井筒不对称;②不同压裂段的微地震事件点大部分重叠,呈线性分布;③出现了较多的大矩震级事件;④时间上,大矩震级事件点出现在压裂中后期的频率较高。根据裂缝面模型,计算出引起长宁地区页岩气套管变形的裂缝面积为 40000~70000m^2,地震矩为 2.57×10^9~7.57×10^{10} N·m,矩震级范围为−1.16~0.79。研究结果对利用微地震实时监测、预警套管变形和判断天然裂缝尺度、预防套管变形具有指导作用。

关键词 四川盆地 页岩气 套管变形 水力压裂 天然裂缝 微地震 套管变形量

中图分类号:P631 文献标识码:A doi:10.13810/j.cnki.issn.1000-7210.2021.06.010

0 引言

四川长宁—威远页岩气示范区页岩气井在开发过程中套管变形问题突出。截至 2018 年 10 月,该区块已完成压裂的 187 口井中,发生套管变形的井总计 75 口,套变比例达 40%。套管变形导致井下工具下入困难,施工成本和难度增加,单井产能降低,压裂段数减少,从而影响了页岩气开发的整体经济效益。统计数据表明,长宁—威远地区 61.7%的套管变形点与天然裂缝或者层理弱面有关,并且表现出剪切变形的特点[1-5]。目前,多数学者对套管变形机理方面达成了共识:水力压裂过程中,大量压裂液可以通过不同途径进入天然裂缝,从而使天然裂缝内孔隙压力上升、有效应力下降,导致裂缝被激活而产生滑移,进而造成套管剪切变形[6-15]。

关于套管变形井的微地震特征,很多学者做了研究。陈朝伟等[2]利用圆形断层模型,初步分析了断层半径、滑移距离与地震矩的关系;储仿东等[16]针对页岩各向异性强、天然裂缝发育,水力压裂时容易发生套管形变而影响施工进度问题,利用微地震监测技术识别可能造成套管形变的天然裂缝空间位置,降低施工风险;康亮等[17]在四川威远地区根据微地震震源机制,从定性的角度分析了套管变形处的微地震特征。上述研究初步地探讨了套管变形井的微地震特征,但还不够全面,也缺乏理论认识。

本文以 H19 平台井为例,首先介绍该平台套管变形情况并计算了套管变形量;其次,分析套管变形点附近的微地震事件点空间和时间分布特征;最后根据裂缝面模型,利用地震矩公式分析了天然裂缝尺度、地震矩与变形量之间的关系。

*北京市昌平区沙河镇西沙屯桥西中国石油创新基地 34 地块工程技术研究院 A609,102206。Email:chenzwdri@cnpc.com.cn
本文于 2021 年 3 月 11 日收到,最终修改稿于同年 9 月 22 日收到。
本项研究受国家科技重大专项"页岩气水平井体积压裂及排采技术研究与试验"(2016ZX05062-004)和中国石油股份有限公司重大技术现场试验项目"页岩气水平井套变防范与治理技术攻关"(2019F-3105)联合资助。

1　H19 平台套管变形情况

位于四川盆地页岩气开发区块的 H19 平台的 H19-4、H19-5、H19-6 三口井在压裂施工期间发生了严重的套管变形，变形点共计 12 处，套管变形的深度和遇阻压裂段见图 1 和表 1。该平台三口井共设计压裂 84 段，因套管变形丢段数达 20 段，实际压裂 64 段。

套管变形的深度是通过下桥塞遇阻位置判断，原尺寸桥塞在套管变形点无法通过时，需要更换较小尺寸的桥塞，完成套变段的压裂作业。

利用通过变形点的最小桥塞的尺寸可以计算套管变形量[2]。以 H19-6 井第 4 个套管变形点（表 1 中序号为 12）为例，套管内径为 114.3mm，先使用 105mm 桥塞不能通过，最终选择 90mm 桥塞才能正常通过套管变形点进行压裂施工，则计算该处套管变形量为 24.3mm。

另一种确定套管变形量的方法是利用多臂井径测井（MIT）数据。H19-4、H19-5 井的部分井段实施了多臂井径测井，以 H19-5 井 3501m 处套管变形点数据为例（表 1 中序号为 7），结果如图 2 所示。从井径曲线可以看出，变形深度范围约为 4m，属于典型的局部变形。以图中黑色虚线为分界线，上部的井径曲线向左弯曲扩径，指示该部分套管受力向左变形，而下部的井径曲线向右弯曲缩径，指示该部分套管受力向右变形，整体呈 S 型剪切变形。该特征与裂缝上下两盘相对错动的剪切特征一致。由图可见，在深度 3501m 处，最小内径为 63.87mm，由此可知最大变形量为 50.43mm（图 2）。

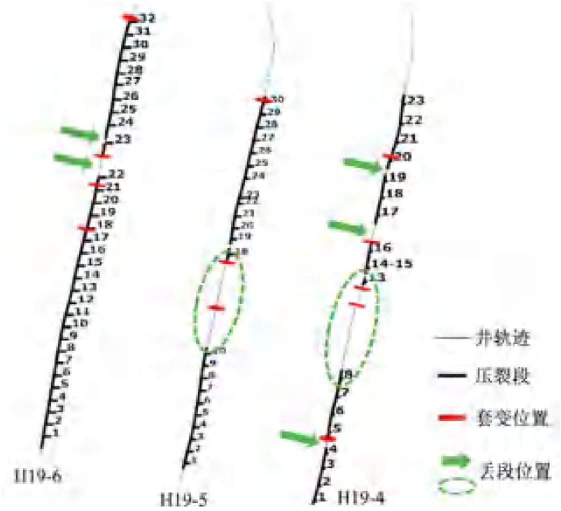

图 1　H19 平台套管变形情况与压裂施工段示意图

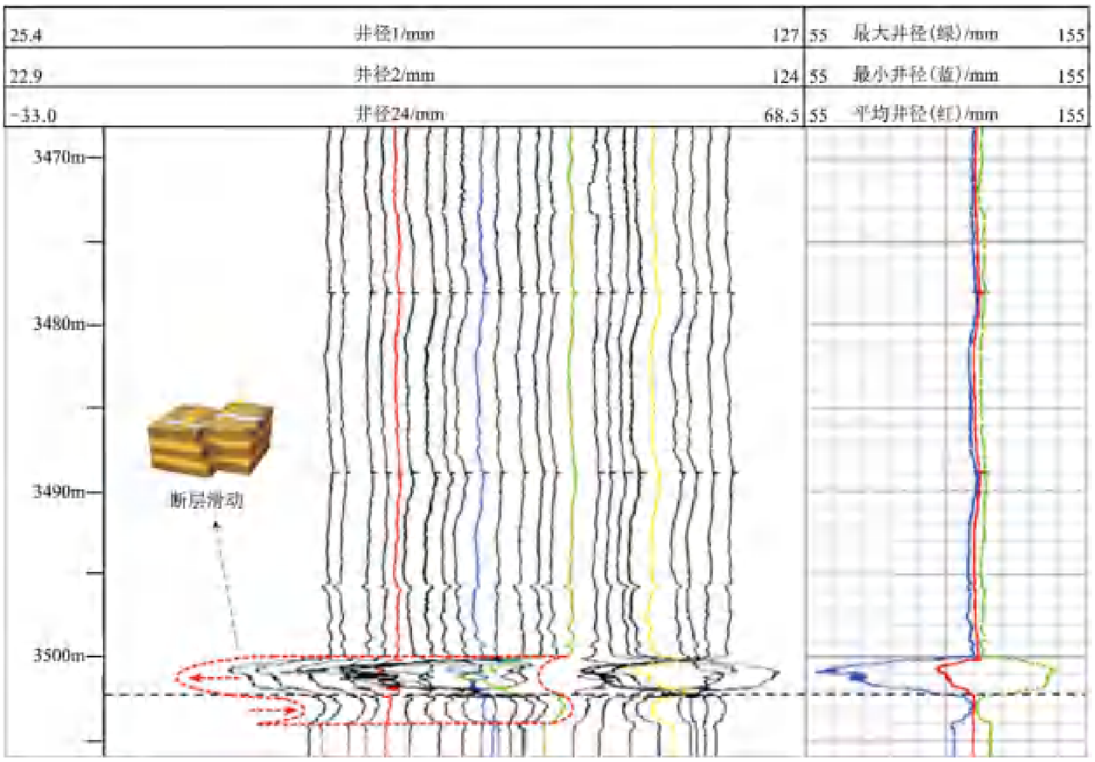

图 2　H19-5 井部分井段多臂井径测井曲线

H19 平台 12 个套管变形点之中求得变形量的有 9 个，其中最小值为 6.10mm，最大值为50.43mm，平均值为 28.03mm(表 2)。

表 1 H19 平台套管变形的深度和遇阻压裂段

序号	井名	遇阻深度/m	遇阻压裂段	序号	井名	遇阻深度/m	遇阻压裂段
1	H19-4	4331	5	7	H19-5	3501	18
2	H19-4	3840	12	8	H19-5	2925	30
3	H19-4	3779	13	9	H19-6	3352	18
4	H19-4	3610	16	10	H19-6	3195	22
5	H19-4	3303	20	11	H19-6	3094	23
6	H19-5	3667	14	12	H19-6	2615	32

表 2 H19 平台套管变形参数

序号	套管内径/mm	桥塞外径/mm	桥塞确定的变形量/mm	MIT 确定的变形量/mm
1	114.3	—	—	—
2	114.3	86.64	27.66	24.26
3	114.3	—	—	6.10
4	114.3	85.00	29.30	—
5	114.3	—	—	—
6	114.3	63.87	50.43	—
7	114.3	—	—	50.43
8	114.3	85.00	29.30	—
9	114.3	95.00	19.30	—
10	114.3	95.00	19.30	—
11	114.3	—	—	—
12	114.3	90.00	24.30	—

2 H19 平台微地震特征

H19 平台实施了微地震监测，本文分析了与套管变形相关的微地震事件点，观察微地震事件点的空间和时间分布特征。

以 H19 平台第 6 个套管变形点处的微地震事件点为例(图 3)，从第 4 段开始，微地震事件点沿着一条近乎垂直的平面向井筒逼近，在第 9 段和第 10 段到达近井筒附近，最终与井筒相交的位置出现在套管变形点附近。

由图 3 可以看出，这几段微地震事件点与常见的微地震事件点在空间分布上明显不同，具有以下特征：(1)微地震事件点与井筒不对称；(2)不同压裂段的微地震事件点大部分重叠，呈线性分布；(3)出现了较多的大矩震级事件。

基于微地震事件点特征和套管变形的剪切特征，可以认为水力压裂激活了一条天然裂缝，天然裂缝错动引起套管发生剪切变形。

按照上述思路，对 H19 平台的每一个套管变形点的微地震数据进行分析，观察到了相同的空间分布特征，共识别出 14 条裂缝，12 个套管变形点均与裂缝相关(图 4)，从统计上再次说明套管变形是水力压裂激活裂缝导致。

微地震事件点是在压裂过程中，按时间先后顺序出现的，因此可以将微地震事件点投射到压裂施工曲线上，得到微地震事件随时间的分布。以 H19-5 井第 4 至第 10 压裂段为例，如图 5 所示。

由图 5 可以看出，微地震事件点有以下几个特点。

(1)H19 平台采用了地面微地震监测，总体上事件点数量偏少，但是出现了矩震级相对较大的微

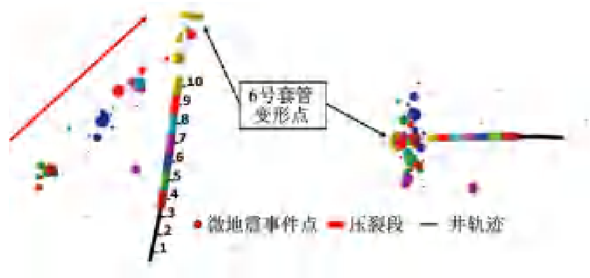

图 3 激活天然裂缝微地震事件点空间分布俯视图(左)和侧视图(右)
图中数字表示压裂段段号，其中第 4 至第 10 压裂段的微地震事件点用不同颜色圆点表示

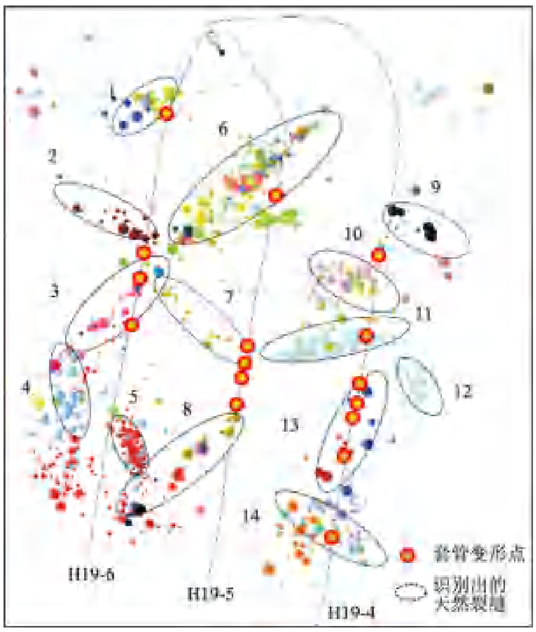

图 4 H19 平台微地震事件点与套管变形点的位置关系

地震事件，矩震级范围为－0.98～0.92。H19-5 井最大矩震级出现在第 6 段，为 0.92；在引发套变的第 10 段，最大矩震级为 0.79；各段矩震级大于－0.5微地震事件如表 3 所示。

（2）总体上，大矩震级事件点出现在压裂中后期的频率较高。Maxwell 等[18] 在统计北美页岩气微地震和压裂施工数据后观察到相似的特征，指出注入初期和注入后期出现大矩震级微地震事件是由激

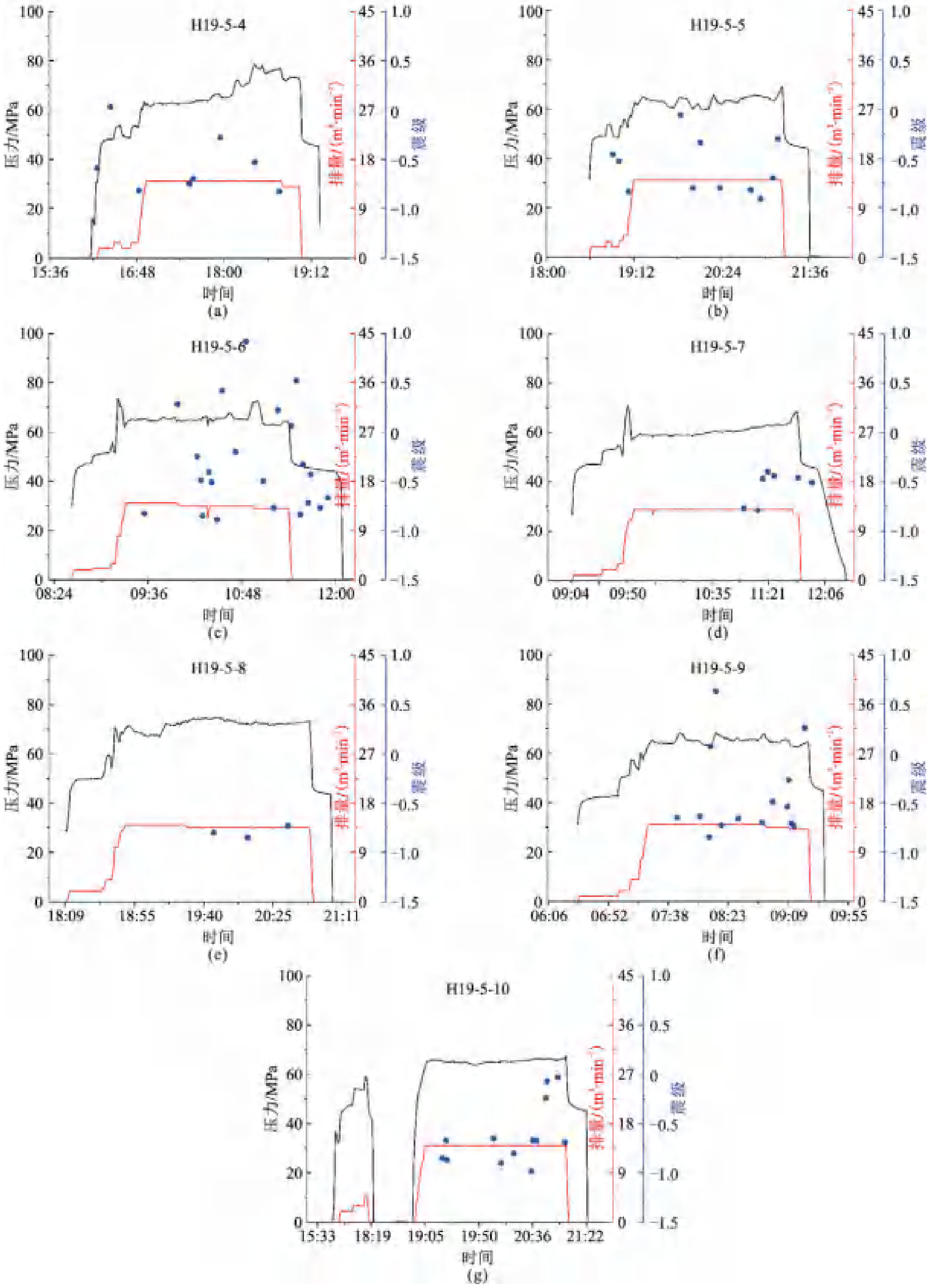

图 5　H19-5 井第 4 至第 10 压裂段（a～g）压裂曲线及微地震事件点随时间分布

黑色为压力曲线；红色为排量曲线；蓝点为微地震事件点

活了天然裂缝引发的，与图 5 的认识一致。

综上所述，套管变形点位置数据是通过桥塞遇阻深度或多臂井径测井数据得到的，是客观的实测数据。在确定套管变形点的位置之后，仔细观察每一段压裂产生的微地震事件点的时间和空间分布规律，从而总结出微地震的特征。实际上，套管变形点数据和微地震数据都是相互独立得到的，两组数据对应得如此之好充分说明套管变形是由裂缝滑动引起的，这个结论是可信的。事实上，在其他钻井平台依然可观察到相似的现象，得到相同的认识。因此，套管变形微地震的空间和时间分布特征，可为判断压裂时是否激活裂缝提供依据。

表 3　H19-5 井第 4～第 10 压裂段大于－0.5 级矩震级微地震事件统计

微地震事件序号	段号	地震矩 N·m	矩震级	微地震事件序号	段号	地震矩 N·m	矩震级
1	4	3.31×10^{9}	0.03	17	6	2.57×10^{8}	0.52
2	4	5.31×10^{8}	－0.28	18	6	1.60×10^{9}	－0.33
3	5	2.32×10^{8}	－0.46	19	6	1.11×10^{10}	－0.43
4	5	3.05×10^{8}	－0.06	20	7	2.32×10^{8}	－0.47
5	5	5.37×10^{9}	－0.34	21	7	4.95×10^{8}	－0.40
6	5	6.31×10^{8}	－0.30	22	7	3.09×10^{9}	－0.44
7	6	3.02×10^{10}	0.28	23	7	5.50×10^{8}	－0.46
8	6	2.24×10^{8}	－0.25	24	9	1.93×10^{10}	0.07
9	6	2.69×10^{9}	－0.49	25	9	9.89×10^{8}	0.63
10	6	1.55×10^{9}	－0.41	26	9	1.14×10^{9}	－0.49
11	6	7.59×10^{9}	0.42	27	9	3.31×10^{9}	－0.27
12	6	4.03×10^{8}	－0.20	28	9	5.31×10^{8}	0.26
13	6	2.85×10^{8}	0.92	29	10	2.32×10^{8}	－0.24
14	6	2.48×10^{8}	－0.50	30	10	3.05×10^{8}	0.79
15	6	3.16×10^{8}	0.22	31	10	5.37×10^{9}	－0.07
16	6	2.75×10^{8}	0.06	32	10	6.31×10^{8}	－0.03

3　对裂缝面模型的理论分析

通过对微地震事件点空间分布特征的分析（图 3 和图 4），可知这些微地震事件点组合成了一条裂缝面。依据震源模型，每一个事件点可看作一个圆形平面[2]，则多个事件点对应多个圆形平面，组合在一起，则构成一条裂缝面，该裂缝面可近似用矩形面表示[19-20]，如图 6 所示。

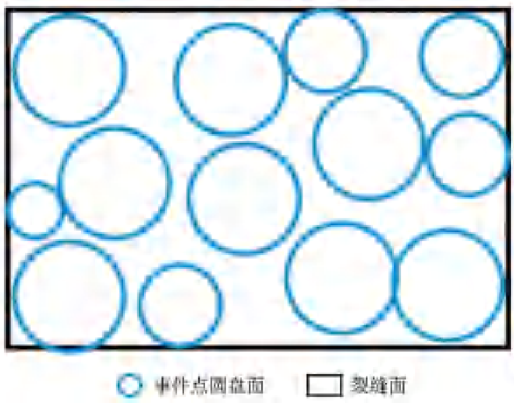

图 6　裂缝面模型

利用该裂缝面模型，可建立地震矩、裂缝面面积和裂缝面滑动量之间的关系[2]，即

$$M_0 = \mu AD \tag{1}$$

式中：M_0 为地震矩；A 为裂缝面积；D 为断层滑移量，可将套管变形量近似看作断层滑动量；μ 为裂缝岩石的剪切模量。

该裂缝面内所有事件点都与该裂缝面有关，因此，该裂缝面对应的地震矩可认为是所有微地震事件点的地震矩之和。矩震级 M_W 与地震矩之间关系[2]为

$$M_W = \frac{2}{3}(\lg M_0 - 9.1) \tag{2}$$

通过裂缝面模型，建立了套管变形量与裂缝面积、微地震地震矩和矩震级之间的关系。

以 H19 平台第 6 个套变点为例，由于套管变形点出现时间在第 10 段压裂施工之后，根据裂缝整体趋势与空间位置，使用 FracMan 软件中插入轨迹平面功能，可建立由第 10 段微地震事件点组合成的裂缝面，如图 7 所示。通过测量矩形边长，可得裂缝面长为 262m，宽为 153m，面积为 40086m^2。

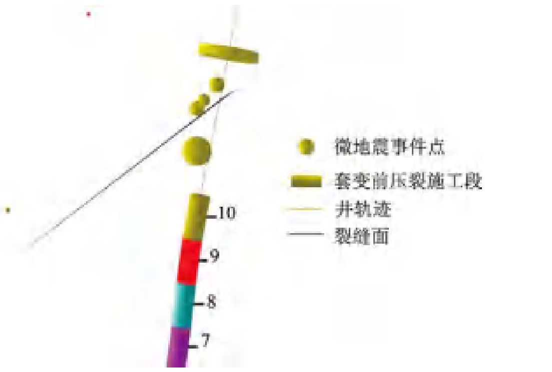

图 7　H19-5 井第 10 段压裂微地震事件点组成的裂缝面

通过对该裂缝面内所有微地震事件点的地震矩求和,可得该裂缝面的地震矩为 2.29×10^{10} N·m。由桥塞尺寸计算可得,该处套管变形量为 50.43mm,可认为裂缝滑动量为 50.43mm。则由式(1)可确定岩石剪切模量为 1×10^{7} Pa。

对所有套管变形点计算,结果如表 4 所示,除第一个值偏低外,其他 6 个数值的平均单段地震矩为 2.04×10^{10} N·m,平均剪切模量 $\mu=1\times10^{7}$ Pa = 10MPa。需要说明的是,由于 MIT 数据是压裂后测得的,无法还原套变时所对应的压裂段及该段的微地震数据,因此,在这种情况下,不能确定裂缝面和地震矩。所以该表的数据仅包含能够用桥塞确定变形量的套管变形点。

式(1)有 3 个变量,给定断层滑动量,则由该式可建立断层面积和地震矩之间的线性关系。当滑动量 D 为 5、10、20 和 50mm 时,绘制的地震矩和断层面积之间的关系如图 8 所示。

由图 8 可以看出,该平台引起套管变形的裂缝面积为 40000～70000m², 则裂缝尺度范围为 200～264m,引发套管变形的地震矩范围为 2.57×10^{9}～7.57×10^{10} N·m,矩震级范围为 −1.16～0.79,引发的套管变形量集中在 20～50mm 之间。

表 4　由套管形变和微地震事件计算的岩石剪切模量

套变点序号	裂缝面积 m²	单段地震矩 N·m	套管变形量 mm	剪切模量 Pa
2	57000	7.55×10^{8}	27.66	5×10^{5}
4	120150	7.57×10^{10}	29.30	2×10^{7}
6	40086	2.29×10^{10}	50.43	1×10^{7}
8	55660	2.57×10^{9}	29.30	1×10^{7}
9	65151	6.72×10^{9}	19.30	7×10^{6}
10	67100	9.19×10^{9}	19.30	5×10^{6}
12	51120	1.29×10^{10}	24.30	1×10^{7}

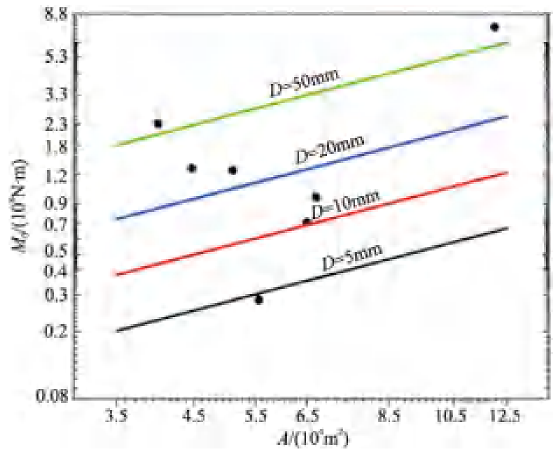

图 8　不同变形量下裂缝面积与地震矩的关系

综上所述,利用裂缝面模型,建立了套管变形量和天然裂缝尺度,以及裂缝滑动时的微地震地震矩之间的定量关系,对进一步利用微地震数据预防和预警套管变形有指导作用。

4　结论与建议

(1)本文利用通过的小桥塞尺寸和 MIT 数据计算了套管变形量,12 个套管变形点中测得变形量的有 9 个,其中最小值 6.10mm,最大值 50.43mm,平均值 28.03mm。

(2)通过分析套管变形附近的微地震数据,得到了天然裂缝的微地震时空特征:①微地震信号与井筒不对称;②不同压裂段的微地震事件点大部分重叠,呈线性分布;③出现了较多的大矩震级事件;④时间上,大矩震级事件点出现在压裂中后期的频率较高。建议在压裂过程中实时监测微地震事件,观察其是否具有天然裂缝特征,及时处理,防止套管变形。

(3)在了解天然裂缝空间分布的基础上,建立了裂缝面模型。利用该模型,明确了套管变形量与天然裂缝尺度和裂缝滑动时的微地震地震矩之间的定量关系。结果表明引起长宁地区页岩气套管变形的裂缝面积为 40000～70000m²,引发套管变形地震矩为 2.57×10^{9}～7.57×10^{10} N·m,引发的矩震级为 −1.16～0.79,引发的套管变形量集中在 20～50mm。

本文研究对进一步利用微地震数据预防和预警套管变形具有指导作用。

参考文献

[1] 陈朝伟,石林,项德贵. 长宁—威远页岩气示范区套管变形机理及对策[J]. 天然气工业,2016,36(11):70-75.
CHEN Zhaowei,SHI Lin,XIANG Degui. Mechanism of casing deformation in the Changning-Weiyuan national shale gas project demonstration area and countermeasures[J]. Natural Gas Industry,2016,36(11):70-75.

[2] 陈朝伟,王鹏飞,项德贵. 基于震源机制关系的长宁—威远区块套管变形分析[J]. 石油钻探技术,2017,45(4):110-114.
CHEN Zhaowei,WANG Pengfei,XIANG Degui. Analysis of casing deformation in the Changning-Weiyuan block based on focal mechanism[J]. Petroleum Drilling Techniques,2017,45(4):110-114.

[3] 陈朝伟,项德贵,张丰收,等. 四川长宁—威远区块水力压裂引起的断层滑移和套管变形机理及防控策略[J]. 石油科学通报,2019,4(4):364-377.
CHEN Zhaowei,XIANG Degui,ZHANG Fengshou, et al. Fault slip and casing deformation caused by hydraulic fracturing in Changning-Weiyuan block, Sichuan:Mechanism and prevention strategy[J]. Petroleum Science Bulletin,2019,4(4):364-377.

[4] 陈朝伟,宋毅,青春,等. 四川长宁页岩气水平井压裂套管变形实例分析[J]. 地下空间与工程学报,2019,15(2):513-524.
CHEN Zhaowei, SONG Yi, QING Chun. A case study on casing deformation of horizontal well during hydraulic fracturing in Sichuan Changning[J]. Chinese Journal of Underground Space and Engineering,2019,15(2):513-524.

[5] Chen Z,Shi L,Xiang D. Mechanism of casing deformation in the Changning-Weiyuan national shale gas demonstration area and countermeasures[J]. Natural Gas Industry B,2017,4(1):1-6.

[6] Yin F,Han L,Yang S,et al. Casing deformation from fracture slip in hydraulic fracturing[J]. Journal of Petroleum Science and Engineering, 2018, 166:235-241.

[7] Qian B,Yin C,Li Y,et al. Diagnostics of casing deformation in multi-stage hydraulic fracturing stimulation in Lower Silurian marine shale play in Southwestern China[C]. Unconventional Resources Technology Conference,2015,402-415.

[8] Xi Y,Li J,Liu G,et al. Numerical investigation for different casing deformation reasons in Weiyuan-Changning shale gas field during multistage hydraulic fracturing[J]. Journal of Petroleum Science and Engineering,2018,163:691-702.

[9] Zhang F,Yin Z,Chen Z,et al. Fault reactivation and induced seismicity during multistage hydraulic fracturing:Microseismic analysis and geomechanical modeling[J]. SPE Journal,2020, 25(2):692-711.

[10] Zoback M D著;石林,陈朝伟,刘玉石,译. 储层地质力学[M]. 北京:石油工业出版社,2011.

[11] Barton C A,Zoback M D,Moos D. Fluid flow along potentially active faults in crystal line rock[J]. Geology,1995,23(8):683-686.

[12] Walsh F R,Zoback M D. Probabilistic assessment of potential fault slip related to injection-induced earthquakes: Application to north-central Oklahoma,USA[J]. Geology,2016,44(12):991-994.

[13] Chen Z,Zhou L,Walsh F R,et al. Case study: Casing deformation caused by hydraulic fracturing induced fault slip in the Sichuan Basin[C]. Unconventional Resources Technology Conference, Houston, 2018.

[14] Liu K,Gao D,Wang Y,et al. Effect of local loads on shale gas well integrity during hydraulic fracturing process[J]. Journal of Natural Gas Science and Engineering,2017,37:291-302.

[15] 林鹤,李德旗,周博宇,等. 天然裂缝对压裂改造效果的影响[J]. 石油地球物理勘探,2018,53(增刊2):156-161.
LIN He,LI Deqi,ZHOU Boyu,et al. Influences of natural cracks on fracturing[J]. Oil Geophysical Prospecting,2018,53(S2):156-161.

[16] 储仿东,焦亚军,杨立峰,等. 利用微地震识别水力压裂井旁天然裂缝[J]. 石油地球物理勘探,2018,53(增刊2):143-147.
CHU Fangdong,JIAO Yajun,YANG Lifeng,et al. Natural fracture identification at hydraulic fracturing wells with microseismic[J]. Oil Geophysical Prospecting,2018,53(S2):143-147.

[17] 康亮,刘丽婷,秦俐,等. 浅析水力压裂施工中套管变形在微地震中的特征表现[C]. 中国石油学会2019年物探技术研讨会论文集,2019.

[18] Maxwell S著;李彦鹏,王熙明,徐刚,等译. 非常规储层水力压裂微地震成像[M]. 北京:石油工业出版社,2015.

[19] 刘星,金衍,林伯韬,等. 利用微地震事件重构三维缝网[J]. 石油地球物理勘探,2019,54(1):102-111.
LIU Xing,JIN Yan,LIN Botao,et al. A 3D fracture network reconstruction method based on microseismic events[J]. Oil Geophysical Prospecting,2019,54(1):102-111.

[20] 李亚龙,刘先贵,胡志明,等. 页岩储层压裂缝网模拟研究进展[J]. 石油地球物理勘探,2019,54(2):480-492.
LI Yalong,LIU Xiangui,HU Zhiming,et al. Research progress on fracture network simulation in shale reservoirs[J]. Oil Geophysical Prospecting,2019,54(2):480-492.

(本文编辑:宜明理)

作者简介

陈朝伟　教授级高级工程师,1979年生;2001年毕业于湖南大学,获工程力学专业学士学位;2007年获北京大学固体地球物理学专业博士学位;现在中国石油集团工程技术研究院主要从事钻完井工程地质力学方面的研究。

cal Prospecting, 2021, 56(6): 1279-1285.

As an effective method to apply surface seismic data to development seismology, logging-while-drilling (LMD) processing plays an important role in avoiding drilling risk and improving the drilling success rate. The core problem is how to use the measured data while drilling to improve the accuracy of the surface seismic velocity model and further promote the accuracy of seismic data imaging and guide the adjustment of drilling trajectories. Therefore, this paper proposed the correction method for the well-driven seismic velocity model. Specifically, given the traditional pre-stack depth migration velocity model, we presume the velocity and depth information of the drilled formations while drilling as constraints and rapidly correct the existing seismic velocity model combined with the logging and VSP data of drilled wells in the surrounding area. In this way, more accurate seismic underground imaging can be obtained, and the geological description and prediction of the undrilled formations can be realized to improve the drilling success rate. Oilfield examples show that this method shortens the update and iteration time of the velocity model and can meet the accuracy and timeliness requirements of LWD processing. The proposed method plays an important role in improving the accuracy of real-time pre-drilling prediction while drilling.

Keywords: logging-while-drilling, velocity modeling, velocity model correction, pre-stack depth migration, well-driven

1. Northwest Branch, Research Institute of Petroleum Exploration & Development, PetroChina, Lanzhou, Gansu 730020, China

Microseismic characteristics of shale gas wells with casing deformation in Changning, Sichuan. CHEN Zhaowei[1], ZHANG Haozhe[2], ZHOU Xiaojin[3], and CAO Hu[2]. Oil Geophysical Prospecting, 2021, 56(6): 1286-1292.

To address the casing deformation of shale gas wells in Sichuan Basin, this paper calculates the casing deformation of the H19 platform with a small bridge plug size and multi-finger image tool (MIT) data and analyzes the characteristics of the spatial and temporal distribution and moment magnitude of microseismic events at casing deformation points. The fracture surface model is established depending on the spatial distribution characteristics of identified natural fractures. The quantitative relationship among casing deformation, natural fracture scale and microseismic moment is analyzed by the model. There were 9 deformation values, with the minimum of 6.10mm and the maximum of 50.43mm, averaged to be 28.03mm. The spatial and temporal distribution characteristics of microseismic events are as follows: ①The microseismic events are not symmetric about the wellbore; ②most of the microseismic events in different fracturing stages are overlapped spatially, showing linear distribution; ③ there are many large-moment-magnitude events; ④ the frequency of large-moment-magnitude events is relatively high in the middle or late fracturing period. According to the calculation with the fracture surface model, the area of the fractures causing casing deformation in shale gas wells in the Changning area is $40000 \sim 70000 m^2$, the seismic moment $2.57 \times 10^9 \sim 7.57 \times 10^{10}$ N·m, and the moment magnitude range is $-1.16 \sim 0.79$. These results have guiding significance for real-time monitoring and early warning of casing deformation according to microseismic events and prevention of casing deformation via the judgment of natural fracture scale.

Keywords: Sichuan Basin, shale gas, casing deformation, hydraulic fracturing, natural fracture, microseismic, casing deformation value

1. CNPC Engineering Technology R & D Company Limited, Beijing 102206, China
2. China University of Petroleum (Beijing), Beijing 102249, China
3. Shale Gas Research Institute, PetroChina Southwest Oil & Gasfield Company, Chengdu, Sichuan 610051, China

AVF inversion based on analytical solution of viscous acoustic equation. YANG Wuyang[1], LI Yuanqiang[2], HUANG Yan[3], LI Jingye[2], WANG Enli[1], and ZHOU Chunlei[1]. Oil Geophysical Prospecting, 2021, 56(6): 1293-1300.

The P-wave attenuation and dispersion are the main reasons for the attenuation of PP wave seismic records. Therefore, in theory, only the post-stack seismic data of the PP wave is required for AVF inversion and the subsequent acquisition of P-wave dispersion factor that can indicate the fluid area. However, the AVF inversion method based on the traditional single-interface assumption is not satisfactory and is controversial in many aspects. So, an AVF inversion method based on the analytical solution of the zero-offset viscous acoustic equation is proposed. The process is as follows: ① The time-frequency spectra of seismic records are calculated by a time-frequency spectrum method. ②With seismic records, wavelets are extracted to eliminate the wavelet overprints in seismic data and thereby obtain the time-frequency spectra of the reflection coefficients. ③According to the viscous acoustic equation, wave impedance inversion is carried out to obtain more accurate impedance parameters and thus to calculate the Fréchet derivative. ④An AVF inversion equation is formulated in view of the derivative matrix. Then, appropriate reference frequency points and frequency points involved in the calculation are selected to acquire the high-precision dispersion attributes through inversion. Numerical simulation and actual data tests show that interface dispersion has little effect on seismic records and the AVF effect of the propagation process is much greater than that caused by interface dispersion. The accuracy and resolution

工程哲学

DOI: 10.3724/j.issn.1674-4969.20240095
CSTR: 32282.14.JES.20240095

解决工程问题的通用方法和哲学思考——以四川页岩气开发套管变形问题为例

陈朝伟

中国石油集团工程技术研究院有限公司 钻井工艺研究所，北京 102206

摘要：大型工程施工作业中难题时有发生，为了快速高效地找到解决工程问题的思路和方法，提高经济效益，本文对页岩气开发套管变形问题的攻关过程进行了梳理，并应用辩证唯物主义哲学去观察和提炼，分析总结了解决工程问题的一般流程和方法（PRIS）。（1）提出问题（P）指通过调查分析，从工程问题中提炼科学问题；（2）研究机理（R）指通过建立模型、试验数值模拟和矛盾分析，探索问题的本质原因；（3）研发手段（I）指根据问题的机理和矛盾，探索解决问题的思路，研发具体的技术手段；（4）试验推广（S）指把新工艺和新技术推广到现场，解决生产问题。PRIS 的底层逻辑契合辩证唯物主义的认识论和方法论，作为一种体现了哲学规律性的工程流程方法，PRIS 可以在工程实践中为解决工程问题提供指导。

关键词：石油工程；工程问题；哲学思考；页岩气开发；套管变形

中图分类号：TE34 **文献标识码：**A **文章编号：**1674-4969(2025)03-0387-10

引言

石油工程是根据油气和储层特性建立适宜的流动通道并优选举升方法，经济有效地将深埋于地下油气从油气藏中开采到地面所实施的一系列工程和工艺技术的总称，包括油藏、钻井、采油和石油地面工程等。

石油工程是和地下岩石打交道，常常遇到诸多问题，比如，钻井破岩问题、井壁失稳问题、井漏问题、套管变形问题和水力压裂造缝问题等等。每个问题都有各自的特殊性，分析方法都有所不同，解决思路也差异很大。当面对一个新问题时，能否快速找到分析方法和解决思路呢？或者说，对于这些问题有没有一个通用的分析和解决方法呢？

针对这一问题，本文以四川页岩气开发套管变形问题为典型案例，简要介绍了技术攻关过程，并通过

收稿日期：2024-07-21； **修回日期：**2025-05-08
作者简介：陈朝伟（1979—），男，博士，正高级工程师，研究方向为石油工程技术。E-mail: chenzwdri@cnpc.com.cn
引用格式：陈朝伟. 解决工程问题的通用方法和哲学思考——以四川页岩气开发套管变形问题为例[J]. 工程研究——跨学科视野中的工程, 2025, 17(3): 387-396. DOI: 10.3724/j.issn.1674-4969.20240095. CSTR: 32282.14.JES.20240095
Chen Zhaowei. General Methods and Philosophical Thinking for Solving Engineering Problems: Taking the Issue of Casing Deformation in Sichuan Shale Gas Development As an Example[J]. Journal of Engineering Studies, 2025, 17(3): 387-396. DOI: 10.3724/j.issn.1674-4969.20240095. CSTR:

对工程问题研究方法的总结与思考，形成了一套系统的工程问题解决流程和方法。该流程方法的底层逻辑与马克思主义认识论和唯物辩证法相契合，因而使其具备了工程方法论的普遍意义。这套方法和流程可为工程实践提供有效参考与指导。

1　典型案例

为保障国家能源安全并实现"双碳"目标，中国石油天然气集团有限公司通过评层选区、先导试验、示范区建设和规模上产四个阶段，目前已成功实现四川地区页岩气的效益开发[1]。

四川页岩气开发的主体技术包括水平井和分段体积压裂技术。水平井按丛式井组部署，采用常规双排布井方式，水平巷道间距为300～400 m，水平段长度1500～2000 m。井身结构采用“三开三完”①方式，水平井井眼直径215.9 mm，固井采用φ139.7 mm×Q125×12.7 mm气密封扣油层套管②。完井方案采用套管射孔完井工艺，压裂均采用电缆泵送桥塞分簇射孔分段工艺（图1），按照从“脚趾”（水平井B点）到“脚跟”（水平井A点）的顺序压裂。簇间距按20~25 m设计，考虑到每段分3簇，每簇间距20~25 m，段长为60~75 m。

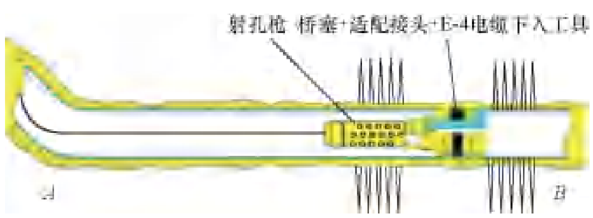

图1　水平井和分段体积压裂技术示意图

Figure 1　Schematic diagram of horizontal well and segmented volumetric tracturing technology

不同于美国巴内特等页岩气区块，川南页岩气区块地质条件更为复杂，钻完井工程中常面临多种技术难题，包括井壁失稳、井漏及压裂期间的套管变形等问题。其中，套管变形问题尤为突出，是当前页岩气开发过程中最严峻的工程挑战。

以四川长宁区块第一口页岩气水平井宁201-H1井为例（2011年），该井分12段，压裂施工作业前，使用118 mm钻头钻井底水泥塞过程无阻卡现象。随后顺利完成了第1段压裂施工作业。但是，在下入2号桥塞过程中，在井深3490 m处桥塞遇阻，而其设计井深为3577 m，距离其设计井深87 m。现场取出桥塞，使用114.3 mm铣锥通井仍然遇阻，起出后发现铣锥单侧存在划痕。根据桥塞遇阻及铣锥划痕状态，判定宁201-H1井在井深3490 m发生了套管变形问题。最后，在变形处就地坐封桥塞，设计施工12段调整到实际施工10段，完成了后续的压裂施工作业。

截至2019年9月6日，四川长宁区块已完成压裂井161口，发生套管变形井共计55口，套管变形比例34.16%。威远区块套管变形比例为52.3%，近几年才开发的泸州深层页岩气，套管变形比例也高达40%。套管变形导致压裂段数减少，降低单井产量，处理套管变形也会增加作业成本，而且，套管变形还影响二次压裂，缩短井的生命周期。因此，套管变形从多个方面制约着页岩气的高效开发。

笔者在2014年4月开始接触页岩气开发套管变形问题，并把解决套管变形问题作为个人和团队的重点攻关方向。在近10年的时间里，按攻关方向可以分成三个阶段。

第一阶段，2014—2016年底，主要研究套管变形的原因和机理。经过近两年的调查研究发现，套管变形的地质原因为断层/裂缝，工程原因则是水力压裂。基于地质力学原理，研究建立了流体通道-断层激活模型。该模型揭示了压裂引发套管变形的过程：压裂液沿流体通道进入断层/天然裂缝，导致其孔隙压力上升；当压力达到临界值时，将激发断层/天然裂缝滑动，进而引发套管变形。相关研究成果在

① 在页岩气开发中，“三开三完”是指一口水平井的钻井作业分三个阶段（三开）完成，并确保每个阶段一次性顺利完工（三完），以提高效率、降低成本。

② 套管参数解析：139.7 mm外径、12.7 mm壁厚，属于API标准常规尺寸，适用于中深井（3000~5000 m）；钢级Q125，高强度套管，适合高压、含腐蚀性流体或地应力复杂地层；气密封扣为特殊螺纹设计，通过金属/弹性密封确保高压气井的密封性，需严格检测上扣扭矩和密封脂涂覆。

2016年11期的《天然气工业》上刊出[2]，截至目前该论文已被引用150余次，成为页岩气领域套管变形研究中的高被引论文。

第二阶段，2017年初—2022年，主要研究如何解决套管变形的问题。利用断层激活理论与定量风险分析方法，提出了断层滑动风险评估和套管变形预测方法[3-4]，并开发了套管变形风险预测软件。建立了断块滑动和套管相互作用数值模型，定量分析了套管变形的影响因素，提出了“以柔克刚”的套管变形预防理念[5-6]，基于该理念，发明了橡胶组合套管等工具[7]，以及研发了超低弹性模量材料等大变形固井用材料。研究了套管变形井微地震和施工曲线特征，提出了套管变形预警方法[8]。建立了水力压裂激发断层活化的数值模型，研究了排量、液量和流体黏度对断层滑动的影响规律，提出了高风险断层降液量，中风险降排量的套管变形控制方法[9]。综合来看，形成了涵盖钻前预测、压前预防、压裂预警及压裂控制的一体化套管变形防控技术方案[10]。相关研究成果已汇编为专著《四川页岩气套管变形机理与防控技术》[11]，并于2022年底由科学出版社出版。

第三阶段，2023年初至今，主要工作是完善软件、加工产品、室内试验和现场试验等[12-13]，努力把防控技术推到现场，最终解决套管变形问题。

2 解决工程问题的通用流程和方法

通过对页岩气套管变形问题以及其他工程问题研究过程的梳理，可以总结出一套共性的流程和方法，包括提出问题、研究机理、研发手段和试验推广4个阶段（图2）。

2.1 提出问题

解决工程问题的第一步是从工程问题中提炼科学问题。提出科学问题，是解决问题的起点，相当于指明方向，重要程度不言而喻。钱学森指出：“数学方法只是技术科学研究中的工具，不是真正关键的部分。那么，关键的是什么呢？技术科学工作中最主要的一点是对所研究问题的认识。只有对一个问题认识

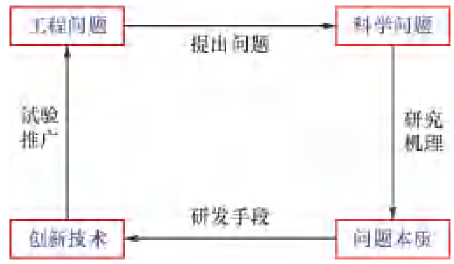

图2 解决工程问题的流程和方法

Figure 2 Processes and methods for solving engineering problems

了以后才能开始分析，才能开始计算。”[14]

怎样才能正确地提出科学问题呢？首先是做调查。围绕工程问题，尽可能收集现场资料，特别是现场第一手数据资料。以石油工程问题为例，资料包括地震、地球物理和测井等地质资料，也包括钻井、压裂、测试、录井等工程资料。还要在现场和相关技术人员面谈，了解他们对问题的认识，听取他们的意见。

接着利用“解剖麻雀”的方法对资料作分析。所谓“解剖麻雀”的方法，就是选好一两个或几个数据资料比较全的典型案例，对其进行全面且详细的剖析，根据问题发生的时空，分析每一个因素（各类资料）和问题之间的相关性，判断什么是问题的主要因素，什么是次要因素，哪些因素虽然也存在，可是它们对问题本身不起多大作用，因而这些因素就可以忽略不计。

接下来是真正创造性的工作，即结合这些因素和自然科学及工程专业知识，提炼出工程问题背后的科学问题。科学问题代表了研究者们对工程问题的认识、对现象机理的初步了解。提出科学问题的过程并非一蹴而就。当发现科学问题存在偏差时，必须暂停理论工作，重返现场进行观察，收集必要的新数据，继而重新构建科学问题。这种做法既能避免将个别现象误认为普遍规律而导致片面性错误，又能防止错将支流视作主流而造成重大判断失误。

套管变形问题的科学问题是怎么提出来的呢？笔者收集了与套管变形相关的所有资料，包括套管变形检测资料（井径测井数据、铅印资料）、地质资料（蚂蚁体、曲率体、似然体等）、测井数据、钻井资料（井轨迹、狗腿度）、固井质量资料和压裂资料（微地

震监测数据、压裂施工曲线等），并以宁201-H1井和长宁H19平台为典型案例，对套变相关的每一个因素进行解剖分析，并将初步的结论和其他所有井进行对比分析，最早提出套管变形是由温度应力效应引起的，但后来根据新的套管变形实测资料否定了这个认识，前后经历了两年的时间，最终认识到断层/裂缝是套管变形的地质原因，水力压裂是套管变形的工程原因，并结合地质力学原理，提出了“在四川页岩气长宁-威远等区块，水力压裂为什么能引起断层/裂缝滑动”的科学问题。

2.2　研究机理

解决工程问题的第二步是通过对科学问题进行研究，探索问题的本质原因。

最常用的科学方法是模型法，即针对科学问题，结合典型案例和专业理论知识，建立一幅关联各主要因素的“图画”。因此，模型是对现场工程问题发生过程的一种合理正确的抽象，是科研工作者的创造性工作，既体现了本质的、内部联系的东西，又与实际过程相比，具有简化和理想化的特点。通过模型，可以对问题形成一般性的定性认识，并为工程问题提供定性解释。需要说明的是：对于同一过程，在不同问题中，若关注其本质的不同方面，可以构建出截然不同的模型。

模型也是进行定量研究的新起点。基于模型，可以利用理论推导、室内试验或数值模拟等方法对问题进行研究。通过理论推导，能够得到理论结果是最理想的，但由于工程问题的复杂性，得到理论结果的情况还是很少见的。因此，室内试验和数值模拟是更常用的方法。室内试验和数值模拟方法都是要设计一个和现场相似的过程，让问题在实验室或电脑上重现，利用现场典型案例数据设计室内试验或数值模型的数据，得到定量的数据结果。通过对比结果和现场实际数据，可以检验模型正确与否。通过人为控制变量（因素变化），利用试验或数值模拟得到对应的结果，了解不同因素对问题的影响程度，判断问题发生的主控因素，基于问题发生过程中不同因素之间的定量关系，得到过程中各因素的内在联系。

事物的本质是由主要矛盾以及矛盾的主要方面决定的[15]，因此，接下来利用模型分析问题发生的矛盾运动过程，分析过程有哪几个阶段，每个阶段矛盾的特殊性，主要矛盾和次要矛盾，矛盾的主要方面和次要方面（因素），每个因素之间是怎么连接的，矛盾各个方面各占何种地位、对抗情况以及各自的变化情况，从而最终揭示问题发生的本质原因。石油工程中的很多工程问题是与力学相关的，而力学中的基本矛盾是作用力和反作用力。因此，分析这类问题的内在矛盾时，需要利用油气田地质力学、井筒流体力学和井筒管柱力学中的相关原理，分析问题发生过程中的作用力和反作用力，并了解这些作用力之间是怎么联系在一起的。

在研究套管变形问题的过程中，基于现场调查分析结果和地质力学原理，建立了流体通道-断层滑动模型[2]（图3）。然后在该模型的基础上，建立了水力压裂激活断层/裂缝数值模型，讨论了压裂施工参数和断层/裂缝之间的定量关系；建立了断块滑动和套管相互作用的数值模型，讨论了套管钢级、套管壁厚、固井水泥石弹性模量和厚度对套管变形量的影响规律等[6]。在这些规律认识的基础上，进一步理清了套管变形过程的几个矛盾，即井底压力和地层闭合压力、断层/裂缝的剪应力和滑动阻力、滑动的断层/天然裂缝和套管之间的相互作用，以及井底压力和滑动阻力存在定量的依存关系[13]。进而，结合四川页岩气地质和工程特征，揭示了页岩气套管变形的本质原因。

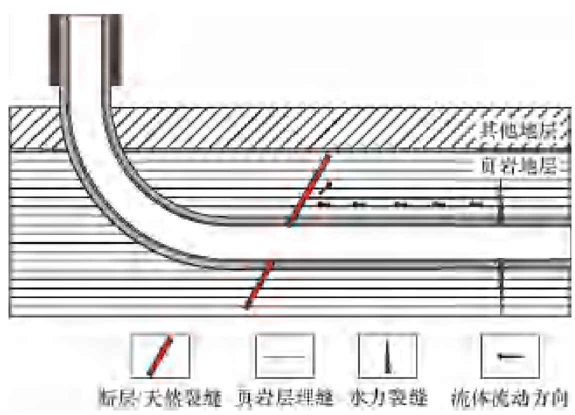

图3　流体通道-断层滑动模型[10]

Figure 3　Fluid channel-fault slip model[10]

2.3　研发手段

解决工程问题的第三步是在机理和矛盾认识的基础上，探索解决问题的思路，进而围绕具体的技术问题，研发解决工程问题的技术手段。

揭示了问题发生的矛盾运动过程，就掌握了问题发生的必然性，从而可以实现对工程问题的预测。具体的方法，就是对矛盾的各个方面（因素）以及各自的变化有一个定量的认识，进而根据矛盾的转化条件对问题进行预测。为了方便工程应用，常见的做法是基于模型开发一套关联各主要因素的工程软件，利用该软件，可以方便地进行预测、评估和优化设计等。有些情况下，为了实时掌握关键因素的数值变化，需要研发具有能够对该数据进行实时测量和监测功能的技术，从而实现现场问题的实时预警。

解决工程问题需要具体的技术手段，实现预防和控制的目的。不同的矛盾，要用不同的方法来解决，即具体问题具体分析。其中一种常见的问题是在矛盾转化过程中发生的，这种问题的解决，需要通过分析矛盾两个方面的转化条件入手，研究解决问题的具体思路。唯物辩证法认为，外因是问题发生的条件，内因是问题发生的根据，外因通过内因而起作用。石油工程问题的内因往往是地质原因，外因是工程原因，地质因素是客观的，不可改变的，工程因素是可改变的。在了解工程问题的地质和工程的内在联系后，通过改变工程中可控因素，从而可以避免矛盾双方发生转换。根据该目标，可以提出解决问题的方向。而改变可控因素的具体方法有很多，可以从工艺上改变，也可以开发新产品，包括研发新工具和新材料等。

仍以套管变形问题为例说明研发手段的思路和方法。断层/裂缝面上的剪切力和滑动阻力这对矛盾的转化会引起运动状态的变化。当剪切力小于滑动阻力时，断层/裂缝是稳定的；当剪切力大于滑动阻力时，断层/裂缝发生滑动。根据井底压力和滑动阻力之间的关系，通过改变井底压力，可以控制滑动阻力始终大于剪切力，这种解决套管变形问题的思路可称为“均衡压裂”理念，主要手段包括“控液量和控排量”的双控技术、“一堵一疏”和“一簇一压”等具体策略。此外，根据断层/天然裂缝和套管之间的相互作用这一对矛盾，应该免“硬碰硬”，而应该采用“以柔克刚”的预防理念。具体的技术手段包括“低弹模”水泥石固井法，即水泥石的抗压强度在满足要求的情况下，弹性模量尽可能低的预防套管变形方法[6]，或应用一种外层膨胀橡胶组合套管工具[7]。基于上述理念，还可以进一步探索更多的手段或者技术。

2.4　试验推广

解决工程问题的第四步是在对新工艺和新技术进行试验的过程中，针对系统配套带来的新问题进行测试和分析，对产品进行优化改进，提高技术成熟度，最终解决工程问题。

首先要进行室内试验和测试。对于新工具和新材料等技术手段，在应用到原系统时，可能带来新的问题。这就要求新产品的设计要考虑全面：一方面，通过试验和数值模拟等方法，对新产品进行功能测试；另一方面，还要结合现场工艺，进行安全方面的考虑，进行安全性测试。

在现场试验前要做好现场试验方案，考虑整个现场施工工艺过程，注意每一个细节，并做好安全预案。 当顺利完成现场试验后，及时对其效果进行评价。值得说明的是，新技术往往不是一帆风顺的，出现这样那样的问题是正常的。这时要对问题及时进行总结，对产品进行优化设计。

目前，针对套管变形问题，现场主要采取“双控”的技术方法，即对裂缝发育带穿过的压裂段降低液量 200~300 m^3，降低排量 2 m^3/min，通过对比可知，优化施工参数对套管变形的减缓取得了一定的效果，但仍有部分井的停泵压力数值较大，仍能够激活断层/裂缝。另外，先后在威远区块高风险区域威204H38-4井、威204H18-5井和威204H40-3井开展了“高强度微珠固井”工艺现场试验，这3口井都是位于套管变形高风险区域的高风险井，目前威204H38-4井已经顺利完成压裂，没有发生套变[16]。2024年，对原创的橡胶组合套管技术在新疆油田JHW69-13等6口井进行了现场试验，总计下入38根，下入过程安全可靠，固井和压裂作业正常，对比试验结果证实了

防套管变形能力显著。

3　哲学思考

笔者在思考解决工程问题方法论的过程中，也在不断思考其背后的哲学基础。为了表述方便，用“PRIS”来描述上述流程，其中P（problem）表示提出问题，R（research）表示研究机理，I（innovation）表示研发创新手段，S（service）表示试验推广。

3.1　PRIS蕴含着辩证唯物主义认识论思想

PRIS的各个环节组成一个前后联系、不可分割的整体。提出问题和研究机理，是对客观实际问题从感性认识到理性认识的过程，最终目的是解释问题（解释世界）。研发手段和试验推广是在理性认识的基础上，形成解决问题的理念和具体手段，并回到现场去解决工程问题，最终目的是解决问题（改造世界），如果遇到新问题，再进入下一个循环。PRIS四个环节是“实践—认识—再实践—再认识”的辩证唯物主义认识论的过程[17]。

PRIS体现了理论和实践的辩证关系。PRIS是从工程问题出发，通过研究和研发，最终要回到解决工程问题上去。一方面，体现了实践对认识的决定性作用，即实践是认识的来源、动力、目的和检验标准。另一方面，也说明认识对实践的反作用，即正确的认识，科学的理论对实践有巨大的指导作用，而没有理论指导的实践，就是盲目的实践[17]。在解决工程问题过程中，往往需要不断重复PRIS的过程，即由实践到认识，由认识到实践这样多次的反复，才能够完成。

3.2　PRIS蕴含着唯物辩证法思想

PRIS遵循了特殊和一般的辩证关系。从套管变形研究实例到PRIS，是一个特殊到一般的过程，当利用PRIS研究其他的石油工程问题，甚至其他行业的工程问题时，是一般到特殊的过程。相似地，PRIS和辩证唯物主义认识论也是特殊和一般的关系，PRIS是辩证唯物主义认识论在工程领域的体现，在其他领域也可以推广和借鉴[18]。

PRIS的过程，是从工程问题出发，分析矛盾，解决矛盾，从而最终解决工程问题的过程。工程问题是一种现象，是矛盾的表现形式。唯物辩证法认为，事物是运动变化发展的，事物的运动变化发展是由矛盾运动的结果。如果矛盾双方的对立统一关系以对立为主，矛盾双方处于尖锐激化的状态，或者矛盾的两个方面向着它的对立面所处的地位转化时，事物的运动状态就发生了变化。这两种情形都有可能“事与愿违”，在外部可能表现为问题。因此，PRIS遵循了问题和矛盾之间、现象和本质之间的辩证关系。PRIS过程就是在利用矛盾分析法研究工程问题的过程。

4　现实意义

PRIS为科研工作者提供了一套科研工作方法论。

4.1　知道干什么和知道怎么干

科技研究的最高境界，可归纳为十个字：知道干什么，知道怎么干[19]。根据PRIS，科研工作者要干的工作主要就是解决工程问题。因此，科研工作必须坚持问题导向，要研究真问题，真研究问题[20]。

PRIS还可告诉科研工作者如何解决工程问题。关键在于明确自己所处的解决阶段，并通过发挥主观能动性，将科研工作从一个阶段推进到下一阶段。

在提出问题的过程中，广泛调查和收集数据，学会解剖麻雀的工作方法，坚持理论和实际相结合，锻炼从现场资料中提炼科学问题的思维能力，避免从论文中寻找科学问题。

在研究机理的过程中，学会模型研究法，锻炼抽象思维能力，提高试验或数值模拟能力，善于寻找和发现规律，养成矛盾分析思维。对问题的规律性认识及时总结，积极撰写论文。主动和现场人员交流，积极参加学术会议，听取不同的意见和建议，丰富认识。

在研发手段的过程中，要从问题的矛盾出发，提出切实可行的解决思路和理念，及时撰写专利。积极地把专利转化成技术产品，并努力把产品推广到现场去，以求真正解决问题，不仅把论文写在祖国的大地

上，而且实现技术创新，推动技术进步。

总之，提出问题、研究机理、研发手段、试验推广等阶段都是主动探索的过程，正体现了毛泽东思想阐述的“实事求是”的“求”的过程[21]。

4.2 知道学什么和知道怎么学

一般地，工程问题是多学科交叉的，解决问题往往不是一蹴而就的。解决问题的过程中需要不断学习。要学习什么呢?

从PRIS过程可知，一方面要学习正确的思维方法。主要的是要学习马克思主义哲学，以便更好地了解和掌握解决问题的思维过程。要养成抽象思维能力，研究问题要追求认识问题的本质，主动寻找问题的矛盾以及矛盾的两个方面；以及不同矛盾方面之间的关系。另一方面，认识问题的本质，解决问题的理念，以及研究具体的解决问题的技术手段，包括工具和材料等，这些都离不开专业知识，因此，要学习相关专业知识，提高运用专业知识的能力。此外，做研究，还需要掌握或了解工程分析的数学方法、工程问题的科学基础、工程设计的原理和实践等。

5 结论

通过对10年科研经验的总结，形成了一条解决工程问题的流程和方法——PRIS理念，包括提出问题、研究机理、研发手段、试验推广4个阶段。

（1）PRIS揭示了科学、技术和工程之间的内在联系。工程问题具有复杂性、现实性和特殊性，而科学问题具有一般性，提出问题是从工程问题提炼科学问题的过程，是由个性到共性的过程。而研究机理的过程是基于工程问题的本质，研发手段，试验推广的过程，是从共性到个性的过程。工程问题是目的，科学问题是方法，技术问题是手段，科学、技术和工程是目的和手段的统一、理论与实践的统一。

（2）PRIS可为培养卓越工程师提供一套可行的方法论，在解决具体的工程问题过程中，按照PRIS流程，坚持干中学，学中干，边干边学，进而可以不断提高技术创新能力和工程思维水平，最终成长为善于解决复杂工程问题的工程师。

参考文献

[1] 何骁, 吴建发, 雍锐, 等. 四川盆地长宁: 威远区块海相页岩气田成藏条件及勘探开发关键技术[J]. 石油学报, 2021, 42(2): 259-272.
He X, Wu J F, Yong R, et al. Accumulation conditions and key exploration and development technologies of marine shale gas field in Changning-Weiyuan block, Sichuan Basin[J]. Acta Petrolei Sinica, 2021, 42(2): 259-272.

[2] 陈朝伟, 石林, 项德贵. 长宁—威远页岩气示范区套管变形机理及对策[J]. 天然气工业, 2016, 36(11): 70-75.
Chen Z W, Shi L, Xiang D G. Mechanism of casing deformation in the Changning—Weiyuan national shale gas project demonstration area and countermeasures[J]. Natural Gas Industry, 2016, 36(11): 70-75.

[3] Chen Z W, Zhou L, Walsh R, et al. Case study: Casing deformation caused by hydraulic fracturing-induced fault slip in the Sichuan Basin [C]//Proceedings of the 6th Unconventional Resources Technology Conference. Houston, Texas, USA. Tulsa, OK, USA: American Association of Petroleum Geologists, 2018, 6: 23-25.

[4] Chen Z W, Fan Y, Huang R, et al. Case study: Fault slip induced by hydraulic fracturing and risk assessment of casing deformation in the Sichuan basin[C]//Proceedings of the SPE/AAPG/SEG Asia Pacific Unconventional Resources Technology Conference. Brisbane, Australia. Tulsa, OK, USA: Unconventional Resources Technology Conference, 2019.

[5] 陈朝伟, 房超, 朱勇, 等. 四川页岩气井套管变形特征及受力模式[J]. 石油机械, 2020, 48(2): 126-134.
Chen Z W, Fang C, Zhu Y, et al. Deformation characteristics and stress modes of casings for shale gas wells in Sichuan[J]. China Petroleum Machinery, 2020, 48(2): 126-134.

[6] 蒋振源, 陈朝伟, 张平, 等. 断块滑动引起的套管变形及影响因素分析[J]. 石油管材与仪器, 2020, 6(4): 30-37.
Jiang Z Y, Chen Z W, Zhang P, et al. Casing deformation and its influencing factors caused by block sliding[J]. Petroleum Tubular Goods & Instruments, 2020, 6(4): 30-37.

[7] 项德贵, 陈朝伟. 一种含膨胀橡胶外层的组合套管: CN 106761442B[P]. 2019-06-11.
Xiang D G, Chen Z W. A combination casing with an expansive rubber outer layer: CN 106761442B[P]. 2019-06-11.
[8] 陈朝伟, 张浩哲, 周小金, 等. 四川长宁页岩气套管变形井微地震特征分析[J]. 石油地球物理勘探, 2021, 56(6): 1286-1292, 1198.
Chen Z W, Zhang H Z, Zhou X J, et al. Microseismic characteristics of shale gas wells with casing deformation in Changning, Sichuan[J]. Oil Geophysical Prospecting, 2021, 56(6): 1286-1292, 1198.
[9] 陈朝伟, 黄锐, 曾波, 等. 四川盆地长宁页岩气区块套管变形井施工参数优化分析[J]. 石油钻探技术, 2021, 49(1): 93-100.
Chen Z W, Huang R, Zeng B, et al. Analysis and optimization of construction parameters for preventing casing deformation in the Changning shale gas block, Sichuan Basin[J]. Petroleum Drilling Techniques, 2021, 49(1): 93-100.
[10] 陈朝伟, 项德贵. 四川盆地页岩气开发套管变形一体化防控技术[J]. 中国石油勘探, 2022, 27(1): 135-141.
Chen Z W, Xiang D G. Integrated prevention and control technology of casing deformation in shale gas development well in Sichuan Basin [J]. China Petroleum Exploration, 2022, 27(1): 135-141.
[11] 陈朝伟. 四川页岩气套管变形机理和防控技术[M]. 北京: 科学出版社, 2022.
Chen Z W. Deformation Mechanism and Prevention and Control Technology of Shale Gas Casing in Sichuan[M]. Beijing: Science Press, 2022.
[12] 陈朝伟, 周文高, 项德贵, 等. 预防页岩气套变的橡胶组合套管研制及其抗剪切性能评价[J]. 天然气工业, 2023, 43(11): 131-136.
Chen Z W, Zhou W G, Xiang D G, et al. Development of rubber composite casing for preventing shale gas casing deformation and its shear resistance evaluation[J]. Natural Gas Industry, 2023, 43(11): 131-136.
[13] 陈朝伟, 曹虎, 石元会. 四川长宁区块地应力特征及裂缝带活化分析[J]. 工程地质学报, 2020, 28(增刊): 86-95.
Chen Z W, Cao H, Shi Y H. *In-situ* stress characteristics and fracture zone activation analysis of Changning shale gas in Sichuan Province [J]. Journal of Engineering Geology, 2020, 28(S): 86-95
[14] 钱学森. 论技术科学[J]. 科学通报, 1957, 4: 97-104.
Qian X S. On technical science[J]. Science Bulletin, 1957, 4: 97-104.
[15] 毛泽东. 矛盾论[M]//毛泽东选集:第1卷. 北京: 人民出版社, 1991: 299-337.
Mao Z D. Theory of contradiction[M]//Selected Works of Mao Zedong: Volume 1. Beijing: People's Publishing House, 1991: 299-337.
[16] 张平, 何昀宾, 刘子平, 等. 页岩气水平井套管的剪压变形试验与套变预防实践[J]. 天然气工业, 2021, 41(5): 84-91.
Zhang P, He Y B, Liu Z P, et al. Shear and compression deformation test of casing in horizontal shale gas wells and casing variation prevention practice[J]. Natural Gas Industry, 2021, 41(5): 84-91.
[17] 毛泽东. 实践论[M]//毛泽东选集:第1卷. 北京: 人民出版社, 1991: 282-298.
Mao Z D. Theory of practice[M]//Selected Works of Mao Zedong: Volume 1. Beijing: People's Publishing House, 1991: 282-298.
[18] 毛泽东. 反对本本主义[M]//毛泽东选集:第1卷. 北京: 人民出版社, 1991: 109-118.
Mao Z D. Opposition to capitalism[M]//Selected Works of Mao Zedong: Volume 1. Beijing: People's Publishing House, 1991: 109-118.
[19] 苏义脑. 关于工程科技创新的哲学思考[J]. 石油科技论坛, 2020, 39(1): 10-14.
Su Y N. Philosophical thoughts on engineering technological innovation[J]. Petroleum Science and Technology Forum, 2020, 39(1): 10-14.
[20] 习近平. 努力实现高水平科技自立自强. 习近平著作选读(第二卷)[M]. 北京: 人民出版社, 2021: 468-475.
Xi J P. Endeavouring to Achieve a High Level of Scientific and Technological Self-reliance and Self-improvement. Selected Writings of Xi Jinping (Volume 2) [M]. Beijing: People’s Publishing House, 2021: 468-475.
[21] 毛泽东. 改造我们的学习. 毛泽东选集:第3卷[M]. 北京: 人民出版社, 1991: 795-803.
Mao Z D. Transforming our learning[M]//Selected Works of Mao Zedong: Volume 3. Beijing: People's Publishing House, 1991: 795-803.

General Methods and Philosophical Thinking for Solving Engineering Problems: Taking the Issue of Casing Deformation in Sichuan Shale Gas Development As an Example

Chen Zhaowei

Drilling Teohnology Research Institute, CNPC Engineering Technology R&D Company Limited, Beijing 102206*, China*

Highlights

- Summarizing 10 years of scientific research experience, a process and method for solving engineering problems were proposed, which includes four stages: problem posing, research mechanism, R&D technical means, and product promotion.
- The underlying logic of PRIS aligns with the epistemology and methodology of dialectical materialism. The four stages of PRIS are the process of dialectical materialist epistemology of "practice cognition re-practice cognition". PRIS follows a dialectical relationship between particularity and generality, problem and contradiction, phenomenon and essence.
- PRIS reveals the intrinsic connections between science, technology, and engineering, providing researchers with a methodology for research and graduate education.

Graphical Abstract

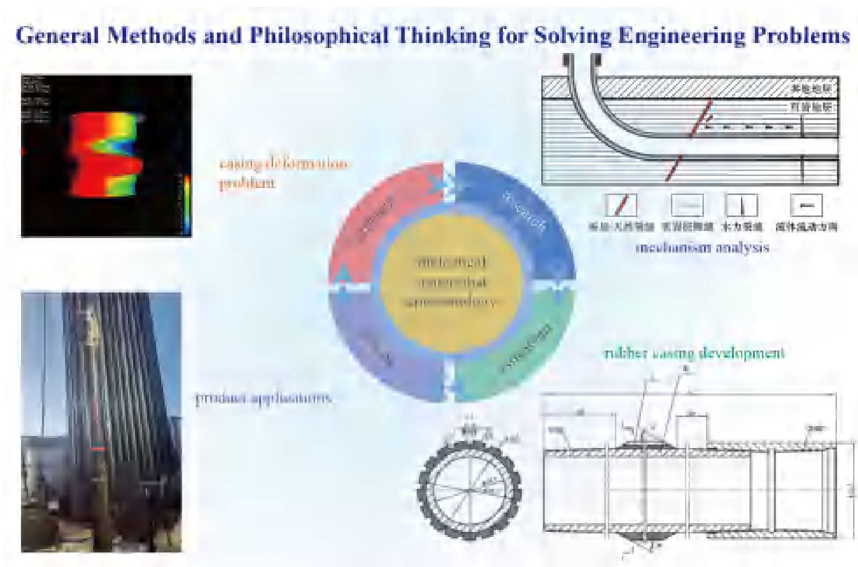

Abstract: Problems often arise in large-scale engineering construction operations. In order to quickly and efficiently find ideas and solutions to solve engineering problems and improve economic benefits, this paper sorts out the research process of shale gas casing deformation problems, and applies dialectical materialism philosophy to observe and refine. The general process and method for solving engineering problems are analyzed and summarized:

(1) Problems posing: through comprehensive investigation, typical case analysis, as well as refining the rough and accurate, and combining professional theoretical knowledge to extract scientific problems from engineering problems.

(2) Research mechanism: Based on scientific problems, a reasonable abstraction of the occurrence process of on-site engineering problems is carried out, and a model related to various main factors is established. Using the model, theoretical/numerical/experimental research is conducted to clarify the main controlling factors of scientific problems and the inherent connections between each factor. Using a model, analyze the process of contradictory movements that occur in a problem, clarify which stages the process has, the particularity of each stage's contradiction, the main and secondary contradictions, the main and secondary aspects (factors) of the contradiction, how each factor is connected, the position of each aspect of the contradiction, the situation of confrontation, and their respective changes, in order to ultimately reveal the essential causes of the problem.

(3) Research and development innovation meass: Based on the understanding of the contradictions that arise, analyze the conditions for the transformation of contradictions, explore ways to solve problems, and then develop specific technical methods to solve engineering problems around technical issues such as prediction, warning, control, and prevention.

(4) Experimentation and extension services: In the process of testing new processes and technologies, analyze and test the new

problems brought by system matching, optimize and improve the product, improve technical maturity, and ultimately solve engineering problems.

The above process can be described using PRIS, whose underlying logic aligns with the epistemology and methodology of dialectical materialism. On the one hand, PRIS contains the epistemological ideas of dialectical materialism, that is, the four stages of PRIS are the process of dialectical materialist epistemology of “practice cognition re practice cognition”. On the other hand, PRIS contains the dialectical thinking of materialism, which follows the dialectical relationship between special and general, problem and contradiction, phenomenon and essence. As an engineering process method that embodies philosophical regularity, PRIS can not only provide guidance for solving engineering problems in engineering practice, but also reveal the inherent connections between science, technology, and engineering, and provide a feasible methodology for cultivating outstanding engineers.

Keywords: hollow microspheres; shell structure; lightweight; divisional design; structural stability; functionality regulation

引用：陈朝伟，项德贵．四川盆地页岩气开发套管变形一体化防控技术 [J]. 中国石油勘探，2022,27(1):1-11.
Chen Zhaowei, Xiang Degui. Integrated prevention and control technology of casing deformation in shale gas development well in Sichuan Basin[J]. China Petroleum Exploration, 2022,27(1):1-11.

四川盆地页岩气开发套管变形一体化防控技术

陈朝伟　项德贵

（中国石油集团工程技术研究院有限公司）

摘　要：针对四川盆地长宁—威远国家级页岩气示范区开发过程中出现的套管变形问题，提出了地质工程一体化防控技术。在流体通道—断层激活模型的基础上，结合断层滑动力学条件和定量风险评估方法（QRA），对套管变形风险段进行预测；分析断层滑动和套管相互作用的规律，用“以柔克刚”的方法对套管变形进行预防；基于套管变形井微地震特征，压裂实时监测微地震信号，对套管变形进行预警；基于流体通道和压裂模型，可通过优化压裂施工参数和多簇射孔＋暂堵孔眼工艺对套管变形进行控制。综合起来，形成了钻前预测、压前预防、压裂预警和压裂控制的一体化套管变形防控策略，为解决页岩气开发套管变形问题提供了依据。

关键词：页岩气；套管变形；压裂；一体化；套损

中图分类号：TE256　　**文献标识码**：A　　DOI：10.3969/j.issn.1672-7703.2022.01.001

Integrated prevention and control technology of casing deformation in shale gas development well in Sichuan Basin

Chen Zhaowei, Xiang Degui

(*CNPC Engineering Technology R&D Company Limited*)

Abstract: With regard to the casing deformation in shale gas development wells in Changning-Weiyuan national demonstration area in Sichuan Basin, an integrated prevention and control technology is proposed. By using the fluid channel-fault activation model and combining with mechanics condition of fault slip and quantitative risk assessment (QRA), the section with casing deformation risk is predicted; The law of interaction between fault slip and casing is analyzed to prevent casing deformation by method of “overcoming hardness with softness”; The microseismic characteristics are analyzed in wells with casing deformation, and the microseismic signals are monitored in real time during fracturing, so as to early warn the casing deformation; Based on fluid channel and fracturing model, casing deformation is controlled by optimizing fracturing parameters and technology of multi-cluster perforation + temporary plugging. To sum up, an integrated casing deformation prevention and control strategy is formed, including pre-drilling prediction, pre-fracturing prevention, early warning and control in fracturing, which provides a basis for solving the problem of casing deformation in shale gas development wells.

Key words：shale gas, casing deformation, fracturing, integration, casing damage

0 引言

四川盆地已初步建成长宁—威远国家级页岩气示范区，但 30% 以上的水平井在压裂过程中出现套管变形问题，套管变形不仅影响单井产量，还缩短井筒生命周期，严重制约着我国页岩气的高效开发。

针对造成页岩气开发套管变形的原因，许多学者开展了研究，提出了温度应力效应 [1-3]、非对称压裂 [4-9]、固井质量 [10-15] 和断层滑动 [16-30] 等原因。目前，大多数学者认识到水力压裂过程中的断层激活可能是导致套管变形的主控因素 [17-29]，这也得到了越来越

基金项目：中国石油天然气股份有限公司重大技术现场试验项目“页岩气水平井套变防范与治理技术攻关”（2019F-3105）。
第一作者简介：陈朝伟（1979-），男，辽宁葫芦岛人，博士，2007 年毕业于北京大学，教授级高级工程师，现主要从事钻完井工程地质力学技术研究工作。地址：北京市昌平区沙河中石油科技园 A34 地块，邮政编码：102206。E-mail：chenzwdri@cnpc.com.cn
收稿日期：2021-06-09；修改日期：2021-12-04

多现场数据的验证。这些研究认识为现场提供了理论指导，但套管变形仍时有发生，还缺乏解决问题的具体措施，有待于进一步研究。

本文从套管变形的机理出发，分析套管变形的防控技术。首先，基于套管变形的地质和工程原因，建立了流体通道—断层激活模型，揭示了套管变形机理。其次，在该模型的基础上，从钻井、固井、压裂等方面提出了套管变形的防控策略，实现钻前预测、压前预防、压裂预警和压裂控制的一体化套管变形防控策略，为解决页岩气开发套管变形问题提供了依据。

1 套管变形机理

四川盆地页岩气开发套管变形具有三大特征，其一，具有天然裂缝／断层相关性的套管变形点数量占套管变形总数的 61.7%，这是地质特征[16,31−32]。其二，套管变形均发生在水力压裂期间，井底施工压力均较大，这是工程特征[33]。其三，具有剪切特征的变形点数量占 73%，这是套管变形形状特征[34]。因此，断层／天然裂缝是套管变形的地质原因，水力压裂是套管变形的工程原因。

基于套管变形的地质和工程原因，利用断层激活地质力学原理，建立流体通道—断层激活模型（图 1）。该模型包含几个矛盾运动过程：其一，水力压裂过程中，压裂液通过孔眼进入地层，在井底压力和地层闭合压力这两个相反的作用力的作用下，水力裂缝向地层深处不断扩展；其二，压裂液通过某条流体通道进入断层／天然裂缝，造成断层／天然裂缝内流体压力增加，滑动阻力减小，当滑动阻力小于断层／天然裂缝面的剪应力时，断层／天然裂缝发生滑动，同时伴随着能量释放，流体压力降低，滑动阻力增加，达到新的平衡状态；其三，断层／天然裂缝滑动过程中，对穿过断层／天然裂缝的套管施加剪切作用，引起套管变形。该模型将水力裂缝扩展、断层被激活、断层和套管相互作用这 3 个过程联系在一起，其中断层被激活的过程是该模型的核心。

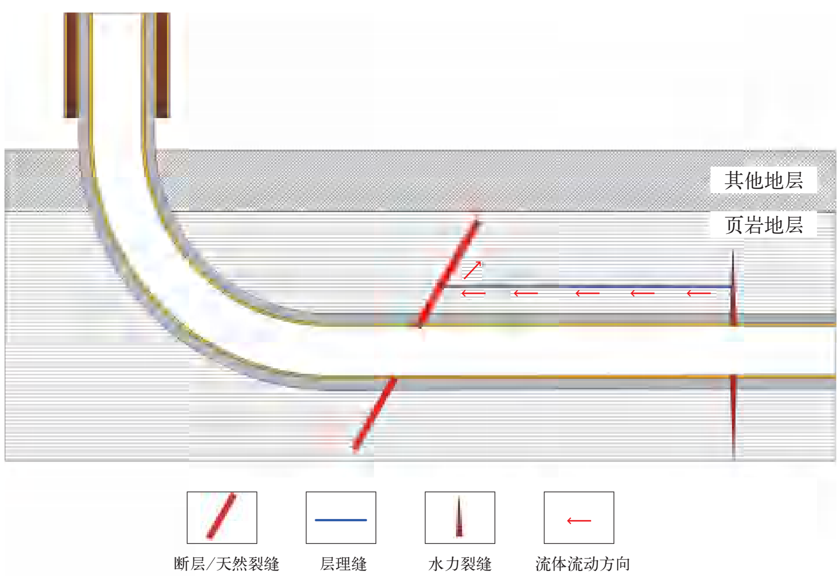

图 1 流体通道—断层激活模型示意图

Fig.1 Schematic diagram of fluid channel−fault activation model

流体通道—断层激活模型揭示了压裂时引起套管变形的发生过程和机理：压裂液沿着某条流体通道进入断层／天然裂缝，造成断层／天然裂缝内孔隙压力增加，当达到临界值时，激发断层／天然裂缝滑动，造成套管变形。流体通道可以是水力裂缝、井壁通道和层理裂缝[35−36]，或者是由这几种通道组合形成的综合通道[37]。该模型为套管变形防控方法提供了理论依据。

2 套管变形风险预测技术

依据断层激活地质力学原理，断层是否激活主要取决于地应力场的方向与大小、断层的方位、孔隙压力及摩擦系数等因素。通常获取这些参数存在一定的误差，在参数不确定的背景下，利用蒙特卡洛方法可

以真实地模拟实际物理过程的优势，评估断层/天然裂缝滑动概率，以此表征其滑动风险，其分析流程如下：

（1）基于高分辨率地震资料，利用最大似然体属性方法，识别研究区内断层/天然裂缝分布特征；

（2）通过地质、钻井、测井等资料，获取研究区内基础的地应力场及孔隙压力数据；

（3）基于临界应力断层/天然裂缝假说原理，评估原始条件下研究区中断层/天然裂缝力学活动状态；

（4）基于压裂施工资料确定研究区孔隙压力变化规律；

（5）采用定量风险评估方法（QRA），确定研究区中断层/天然裂缝随地层孔隙压力变化的滑动概率。

断层/天然裂缝滑动风险是在考虑地层参数不确定性的基础上，以断层/天然裂缝滑动概率来表征的。当断层/天然裂缝滑动概率为50%时，表明该断层/天然裂缝处于即将滑动状态，但是在地层参数误差范围内，断层/天然裂缝滑动风险是应力状态中心值偏离临界破坏线的距离所决定的，所以以摩尔圆与临界破坏线交点为中心，将断层/天然裂缝滑动风险划分为3个等级：低风险（滑动概率小于30%）、中风险（滑动概率为30%～70%）、高风险（滑动概率大于70%），如图2所示。

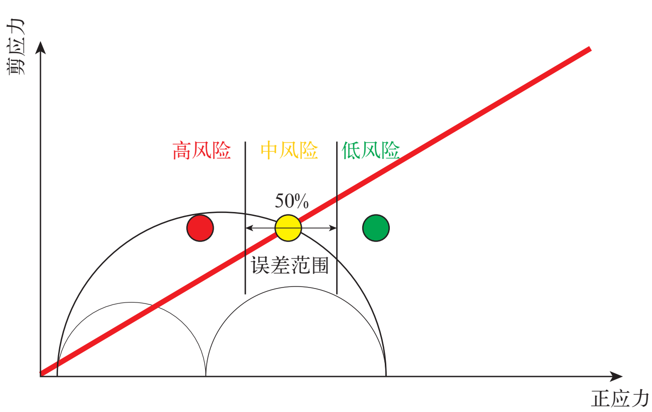

图2 不同滑动风险断层/天然裂缝的应力状态

Fig.2 Stress state of faults/natural fractures with various slip risks

利用该方法，评估了宁201-H1井[38]、H19平台[39]的断层/天然裂缝滑动风险，评估结果和现场实际情况吻合较好。最近利用该方法对宁209井区进行了断层/天然裂缝滑动风险预测，结果如图3所示。

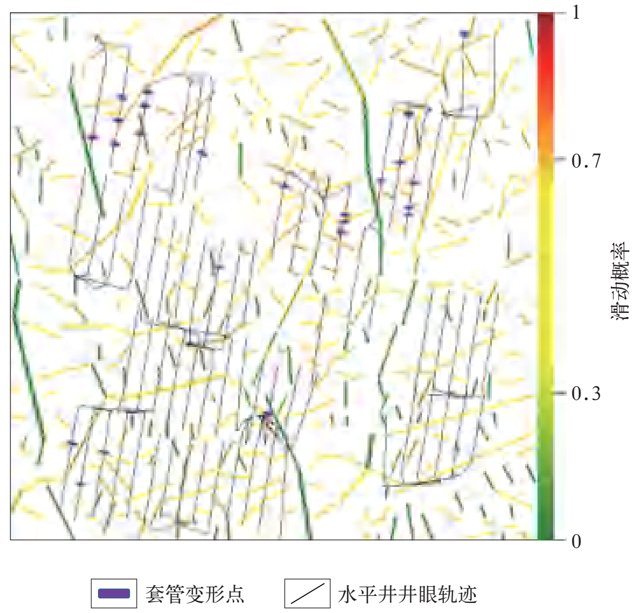

图3 宁209井区断层/天然裂缝滑动风险预测图

Fig.3 Prediction of slip risks of faults/fractures in Ning 209 well block

3 套管变形预防技术

在断层/天然裂缝滑动过程中，会对穿过断层/天然裂缝的套管施加一个巨大的作用力和位移，2009—2016年现场采用了提高套管钢级和增加套管壁厚等措施，以抵抗这种外挤力。但现场实践表明，提高套管钢级和增加套管壁厚对减少套管变形的效果非常有限。为了分析影响套管变形的因素，从而寻找有效的预防方法，建立了断块滑动引起套管剪切变形的断块—水泥环—套管模型，实现了对断块滑动的数值模拟，并对套管钢级、套管壁厚和固井水泥弹性模量等参数的影响规律进行分析[40]。

计算结果表明，当提高套管钢级，屈服强度从655MPa上升至965MPa时，断层滑动30mm导致的套管变形量降低了1.31%；当套管壁厚从9.15mm上升至13.15mm时，断层滑动30mm导致的套管变形量降低了7.47%。这说明，提高套管钢级和壁厚对套管变形影响较小，这在理论上解释了这两种方法不能有效缓解套管变形的原因[40]。

在断块滑动量s=30mm的情况下，当固井水泥弹性模量从10GPa降低到5GPa和2GPa时，套管变形量分别减小了13.56%、41.83%（图4）。若采用超柔性固井材料（弹性模量为0.1GPa），甚至不固井的措施（弹性模量为0.01GPa），套管变形量可控制在2mm以内[40]。

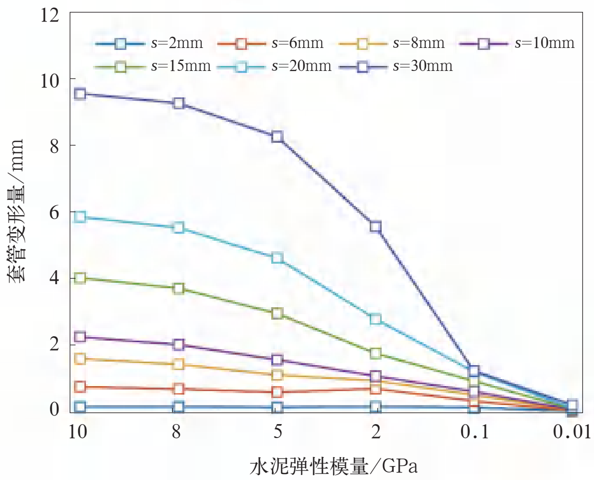

图 4　水泥弹性模量对套管变形量的影响[40]

Fig.4 Influence of elastic modulus of cement sheath on casing deformation[40]

基于上述实践和数值分析，为了预防套管变形，避免“硬碰硬”，应该采用“以柔克刚”的预防方法。基于该理念，提出了用“低弹模”水泥石，即水泥石的抗压强度在满足要求的情况下其弹性模量尽可能低的预防套管变形方法；在高风险井段下入膨胀橡胶组合套管等特殊工具，用于吸收套管变形，保护套管。最近，先后在威远区块高风险区域威 204H38−4 井、威 204H18−5 井和威 204H40−3 井开展了“高强度微珠固井”工艺现场试验，目前威 204H38−4 井已经顺利完成压裂，没有发生套管变形[41]。

4 套管变形预警技术

断层／天然裂缝滑动过程伴随着能量释放，产生了微地震信号。对长宁 H19 平台实施微地震监测，提取了与套管变形点相关的微地震事件点，发现微地震在空间和时间上具有如下特征：(1) 微地震信号与井筒不对称；(2) 不同压裂段的微地震事件点大部分重叠，呈线性分布；(3) 出现了较多的大矩震级事件；(4) 时间上，大矩震级事件点出现在压裂中后期的频率较高；(5) 微地震 b 值（b 为震级和频度关系式中的比例系数）较小，接近于 1。基于微地震信号特征和套管变形的剪切特征，这些微地震信号可以解释为激活的断层／天然裂缝，正是这些断层／天然裂缝的错动引起了套管发生剪切变形[42−43]。通过上面分析可以看出，套管变形时微地震特征很显著，可以将其作为套管变形发生的前兆信号，作为套管变形预警的手段。

对长宁区块的微地震数据进行统计，可分成以下 3 级：高风险对应震级 $M_w \geqslant -0.46$，中等风险对应 $-1.3 < M_w < -0.46$，低风险对应 $M_w \leqslant -1.3$。同理 b 值也可分成 3 级：高风险对应 $b \leqslant 1.02$，中等风险对应 $1.02 < b < 1.11$，低风险对应 $b \geqslant 1.11$。将高风险、中等风险和低风险分别对应“红、黄、绿”3 个等级，建立分级预警标准（图 5）。当达到红色级别时，停止施工；当达到黄色级别时，调整施工参数，如降低排量、减小规模，同时继续观察，不升级为红色级别即可；当为绿色级别时，可继续施工不受影响。因此，通过实时监测微地震信号并处理分析，可实现套管变形预警。

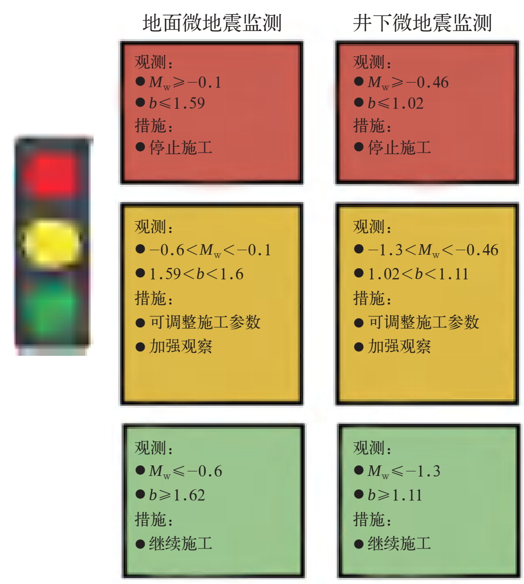

图 5　基于微地震监测的套管变形“红黄绿灯”预警标准

Fig.5 Early warning standard of “Red−Yellow−Green Light” for casing deformation based on microseismic monitoring

5 套管变形压裂控制技术

压裂液通过孔眼进入地层，再通过某条流体通道进入断层／天然裂缝，流体通道不仅传递了压裂液，还传递了流体压力，地面施工压力改变了断层／天然裂缝面上的滑动阻力与剪应力之间的平衡，引起断层／天然裂缝滑动，造成套管变形。

基于上述原理，有两种控制套管变形的思路：第一种是优化压裂施工参数。为此，建立断层滑动的水力压裂数值模型，利用压裂数值模拟建立压裂施工参数与断层激活之间的定量联系。模拟分析的结果表明，降低排量和液量均能降低断层激活的长度，从而

能在一定程度上控制断层滑动，进而控制套管变形。宁 201 井区套管变形比例为 22%，而宁 209 井区采取了降排量和（或）降液量的措施后套管变形比例为 13%[44]。

第二种方法是阻断流体通道。其原理如下，当水力裂缝沟通断层／天然裂缝后，通道内阻力减小，缝内净压力降低，井筒内的压裂液向其汇集，形成一条高速流动的流体通道；在压裂液中投放一定数量的暂堵球，暂堵球根据流速进行分配，倾向于流速大的孔眼，从而堵住与断层／天然裂缝沟通的孔眼，切断井筒和断层／天然裂缝的连接通道，从而控制住断层／天然裂缝的滑动（图 6）。因此，多簇射孔＋暂堵孔眼可控制排量和液量分配，是一种有效的平衡套管变形和页岩气产量之间矛盾的手段。截至 2020 年底，威远区块 28 口井采用“裂缝暂堵＋长段多簇”压裂工艺，只有 4 口井发生套管变形，套管变形比例从研究前 54% 降低到 14.3%[41]。

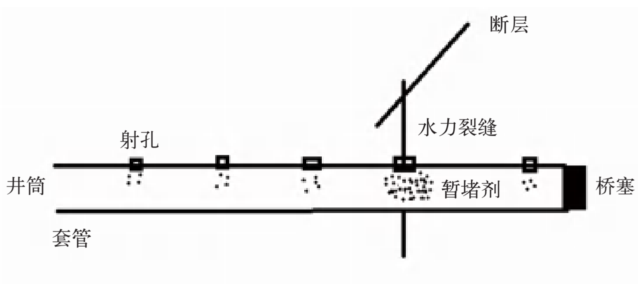

图 6 多簇射孔＋暂堵孔眼控制套管变形示意图

Fig.6 Schematic diagram of multi-cluster perforation + temporary plugging for casing deformation controlling

6 结论

基于套管变形的地质、工程和形状特征，利用断层激活地质力学原理，建立了流体通道—断层激活模型，从而将水力裂缝扩展、断层／天然裂缝被激活、断层／天然裂缝和套管相互作用 3 个过程联系了起来。

流体通道—断层激活模型揭示了套管变形的发生过程和原因：压裂液沿着某条流体通道进入断层／天然裂缝，造成断层／天然裂缝内孔隙压力增加，当达到临界值时，激发断层／天然裂缝滑动，造成套管变形。

在流体通道—断层激活模型的基础上，分析断层滑动力学条件、断层滑动和套管相互作用规律、套管变形井微地震特征、优化压裂施工参数和多簇射孔＋暂堵孔眼工艺，形成了钻前预测、压前预防、压裂预警和压裂控制一体化套管变形防控策略。

本文研究结果能对四川盆地页岩气开发套管变形问题的解决提供指导，也能为其他盆地套管变形问题的研究提供参考。

参考文献

[1] Sugden C, Johnson J, Chambers M, *et al*. Special considerations in the design optimization of the production casing in high-rate, multistage-fractured shale wells[J]. SPE Drilling & Completion, 2012,27(4):459-472.

[2] 田中兰，石林，乔磊．页岩气水平井井筒完整性问题及对策 [J]. 天然气工业，2015,35(9):70-76.
Tian Zhonglan, Shi Lin, Qiao Lei. Research of and countermeasure for wellbore integrity of shale gas horizontal well[J]. Nature Gas Industry, 2015,35(9):70-76.

[3] Yin F, Gao D. Prediction of sustained production casing pressure and casing design for shale gas horizontal wells[J]. Journal of Natural Gas Science and Engineering, 2015,25:159-165.

[4] Daneshy A A. Impact of off-balance fracturing on borehole stability and casing failure[C]. SPE Western Regional Meeting. Richardson: Society of Petroleum Engineers, 2005.

[5] 于浩，练章华，林铁军，等．页岩气体积压裂过程中套管失效机理研究 [J]. 中国安全生产科学技术，2016,12(10):37-43.
Yu Hao, Lian Zhanghua, Lin Tiejun, *et al*. Study on failure mechanism of casing in stimulated reservoir volume fracturing of shale gas[J]. Journal of Safety Science and Technology, 2016,12(10):37-43.

[6] 于浩，练章华，林铁军．页岩气压裂过程套管失效机理有限元分析 [J]. 石油机械，2014,42(8):84-88.
Yu Hao, Lian Zhanghua, Lin Tiejun. Finite element analysis of failure mechanism of casing during shale gas fracturing[J]. China Petroleum Machinery, 2014,42(8):84-88.

[7] 于浩，练章华，徐晓玲，等．页岩气直井体积压裂过程套管失效的数值模拟 [J]. 石油机械，2015,43(3):73-77.
Yu Hao, Lian Zhanghua, Xu Xiaoling, *et al*. Numerical simulation for casing failure during volumetric fracturing of shale gas vertical wells[J].China Petroleum Machinery, 2015, 43(3):73-77.

[8] Lian Z H, Yu H, Lin T J, *et al*. A study on casing deformation failure during multi-stage hydraulic fracturing for the stimulated reservoir volume of horizontal shale wells[J]. Journal of Natural Gas Science and Engineering, 2015,23:538-546.

[9] 刘伟，陶长洲，万有余，等．致密油储层水平井体积压裂套管变形失效机理数值模拟研究 [J]. 石油科学通报，2017,2(4):466-477.
Liu Wei, Tao Changzhou, Wan Youyu, *et al*. Numerical analysis of casing deformation during massive hydraulic fracturing of horizontal wells in a tight-oil reservoir[J]. Petroleum Science Bulletin, 2017,2(4): 466-477.

[10] 于浩，练章华，林铁军．油田固井质量对套管损坏影响的数值仿真 [J].

计算机仿真，2014,31(9):161-164.
Yu Hao，Lian Zhanghua，Lin Tiejun. Numerical simulation of influence of cementing quality on casing failure for oil field[J]. Computer Simulation，2014,31(9):161-164.

[11] 蒋可，李黔，陈远林，等. 页岩气水平井固井质量对套管损坏的影响 [J]. 天然气工业，2015,35(12):77-82.
Jiang Ke，Li Qian，Chen Yuanlin，*et al*. Influence of cementing quality on casing failures in horizontal shale gas wells[J]. Natural Gas Industry，2015,35(12):77-82.

[12] 范明涛，柳贡慧，李军，等. 页岩气井温压耦合下固井质量对套管应力的影响 [J]. 石油机械，2016,44(8):1-5.
Fan Mingtao，Liu Gonghui，Li Jun，*et al*. Effect of cementing quality on casing stress of shale gas well under heat-mechanical coupling[J]. China Petroleum Machinery，2016,44(8):1-5.

[13] Liu K，Gao D，Wang Y，*et al*. Effect of local loads on shale gas well integrity during hydraulic fracturing process[J]. Journal of Natural Gas Science and Engineering，2017,37:291-302.

[14] 刘奎，高德利，王宴滨，等. 局部载荷对页岩气井套管变形的影响 [J]. 天然气工业，2016,36(11):76-82.
Liu Kui，Gao Deli，Wang Yanbin，*et al*. Effects of local load on shale gas well casing deformation[J]. Natural Gas Industry，2016,36(11):76-82.

[15] 刘奎，王宴滨，高德利，等. 页岩气水平井压裂对井筒完整性的影响 [J]. 石油学报，2016,37(3):406-414.
Liu Kui，Wang Yanbin，Gao Deli，*et al*. Effects of hydraulic fracturing on horizontal wellbore for shale gas[J]. Acta Petrolei Sinica，2016,37(3):406-414.

[16] 陈朝伟，石林，项德贵. 长宁—威远页岩气示范区套管变形机理及对策 [J]. 天然气工业，2016,36(11):70-75.
Chen Zhaowei，Shi Lin，Xiang Degui. Mechanism of casing deformation in the Changning-Weiyuan national shale gas demonstration area and countermeasures[J]. Natural Gas Industry，2016,36(11):70-75.

[17] Yin F，Han L，Yang S，*et al*. Casing deformation from fracture slip in hydraulic fracturing[J]. Journal of Petroleum Science and Engineering，2018,166:235-241.

[18] Qian B，Yin C，Li Y，*et al*. Diagnostics of casing deformation in multi-stage hydraulic fracturing stimulation in lower silurian marine shale play in southwestern China[C]. Unconventional Resources Technology Conference，Society of Exploration Geophysicists，American Association of Petroleum Geologists，Society of Petroleum Engineers，2015:402-415.

[19] Xi Y，Li J，Liu G，*et al*. Numerical investigation for different casing deformation reasons in Weiyuan-Changning shale gas field during multistage hydraulic fracturing[J]. Journal of Petroleum Science and Engineering，2018,163:691-702.

[20] Zhang F，Yin Z，Chen Z，*et al*. Fault reactivation and induced seismicity during multistage hydraulic fracturing: microseismic analysis and geomechanical modeling[J]. SPE Journal，2019,25(2):692-711.

[21] Yan X，Jun L，Chunqing Z，*et al*. A new investigation on casing shear deformation during multistage fracturing in shale gas wells based on microseism data and calliper surveys[J]. Journal of Petroleum Science and Engineering，2019,180:1034-1045.

[22] Xi Y，Li J，Liu G，*et al*. Mechanisms and influence of casing shear deformation near the casing shoe，based on MFC surveys during multistage fracturing in shale gas wells in Canada[J]. Energies，2019,12(3):372.

[23] Yin F，Xiao Y，Han L，*et al*. Quantifying the induced fracture slip and casing deformation in hydraulically fracturing shale gas wells[J]. Journal of Natural Gas Science and Engineering，2018，60:103-111.

[24] Yin F，Deng Y，He Y，*et al*. Mechanical behavior of casing crossing slip formation in water flooding oilfields[J]. Journal of Petroleum Science and Engineering，2018,167:796-802.

[25] Li H，Deng J，Liu W，*et al*. Research on casing deformation failure mechanism during volume fracturing for tight oil reservoir of horizontal wells[C]. 51st US Rock Mechanics/Geomechanics Symposium. American Rock Mechanics Association，2017.

[26] 高利军，柳占立，乔磊，等. 页岩气水力压裂中套损机理及其数值模拟研究 [J]. 石油机械，2017,45(1):75-80.
Gao Lijun，Liu Zhanli，Qiao Lei，*et al*. Mechanism analysis and numerical simulation of casing failure in hydraulic fracturing of shale gas formation[J]. China Petroleum Machinery，2017，45(1):75-80.

[27] 高利军，乔磊，柳占立，等. 页岩储层剪切套损的数值模拟及固井对策研究 [J]. 石油机械，2016,44(10):6-10,16.
Gao Lijun，Qiao Lei，Liu Zhanli，*et al*. Numerical modeling and cementing countermeasure analysis of casing shear damage in shale reservoir[J]. China Petroleum Machinery，2016,44(10):6-10,16.

[28] Guo X，Li J，Liu G，*et al*. Shale experiment and numerical investigation of casing deformation during volume fracturing[J]. Arabian Journal of Geosciences，2018,11(22):723.

[29] Guo X，Li J，Liu G，*et al*. Numerical simulation of casing deformation during volume fracturing of horizontal shale gas wells[J]. Journal of Petroleum Science and Engineering，2019，172:731-742.

[30] 舒红林，王利芝，尹开贵，等. 地质工程一体化实施过程中的页岩气藏地质建模 [J]. 中国石油勘探，2020,25(2):84-95.
Shu Honglin，Wang Lizhi，Yin Kaigui，*et al*. Geological modeling of shale gas reservoirs during the implementation process of geology-engineering integration[J]. China Petroleum Exploration，2020,25(2):84-95.

[31] 周小金，雍锐，范宇，等. 天然裂缝对页岩气水平井压裂的影响及工艺调整 [J]. 中国石油勘探，2020,25(6):94-104.
Zhou Xiaojin，Yong Rui，Fan Yu，*et al*. Influence of natural fractures on fracturing of horizontal shale gas wells and process adjustment[J]. China Petroleum Exploration，2020,25(6):94-104.

[32] 陈朝伟，曹虎，周小金，等 . 四川盆地长宁区块页岩气井套管变形和裂缝带相关性 [J]. 天然气勘探与开发，2020,23(4):123-130.
Chen Zhaowei, Cao Hu, Zhou Xiaojin, *et al*. Correlation between casing deformation and fracture zones in Changning shale gas block, Sichuan Basin[J]. Natural Gas Exploration and Development, 2020,23(4):123-130.

[33] 陈朝伟，曹虎，石元会 . 四川长宁区块地应力特征及裂缝带活化分析 [J]. 工程地质学报，2020,28(增刊 1):86-95.
Chen Zhaowei, Cao Hu, Shi Yuanhui. In-situ stress characteristics and fracture zone activation analysis of Changning shale gas in Sichuan Province[J]. Journal of Engineering Geology, 2020, 28(S1):86-95.

[34] 陈朝伟，房超，朱勇，等 . 四川页岩气井套管变形特征及受力模式 [J]. 石油机械，2020,48(2):126-131.
Chen Zhaowei, Fang Chao, Zhu Yong, *et al*. Deformation characteristics and stress modes of casing for shale gas wells in Sichuan[J]. China Petroleum Machinery, 2020,48(2):126-131.

[35] 陈朝伟，宋毅，青春，等 . 四川长宁页岩气水平井压裂套管变形实例分析 [J]. 地下空间与工程学报，2019,15(2):513-524.
Chen Zhaowei, Song Yi, Qing Chun, *et al*. A case study on casing deformation of horizontal well during hydraulic fracturing in Sichuan Changning[J]. Chinese Journal of Underground Space and Engineering, 2019,15(2):513-524.

[36] 张华礼，陈朝伟，石林，等 . 流体通道形成机理及在四川页岩气套管变形分析中的应用 [J]. 钻采工艺，2018,41(4):8-11.
Zhang Huali, Chen Zhaowei, Shi Lin, *et al*. Mechanism of how fluid passage formed and application in Sichuan shale gas casing deformation analysis[J]. Drilling & Production Technology, 2018,41(4):8-11.

[37] 童亨茂，张平，张宏祥，等 . 页岩气水平井开发套管变形的地质力学机理及其防治对策 [J]. 天然气工业，2021,41(1):189-197.
Tong Hengmao, Zhang Ping, Zhang Hongxiang, *et al*. Geomechanical mechanisms and prevention countermeasures of casing deformation in shale gas horizontal wells[J]. 2021,41(1): 189-197.

[38] Chen Zhaowei, Zhou Lang, Walsh F R, *et al*. Case study: casing deformation caused by hydraulic fracturing induced fault slip in the Sichuan Basin[C]. Unconventional Resources Technology Conference, 2018.

[39] Chen Zhaowei, Fan Yu, Huang Rui, *et al*. Case study: fault slip induced by hydraulic fracturing and risk assessment of casing deformation in the Sichuan Basin[C]. SPE/AAPG/SEG Asia Pacific Unconventional Resources Technology Conference, 2019.

[40] 蒋振源，陈朝伟，张平，等 . 断块滑动引起的套管变形及影响因素分析 [J]. 石油管材与仪器，2020,6(4):30-37.
Jiang Zhenyuan, Chen Zhaowei, Zhang Ping, *et al*. Casing deformation and its influencing factors caused by block sliding[J]. Petroleum Tubular Goods & Instruments, 2020,6(4): 30-37.

[41] 张平，何昀宾，刘子平，等 . 页岩气水平井套管的剪压变形试验与套变预防实践 [J]. 天然气工业，2021,41(5):84-91.
Zhang Ping, He Yunbin, Liu Ziping, *et al*. Shear compression deformation test and deformation prevention practice of casing in shale gas horizontal wells[J]. Natural Gas Industry, 2021,41(5):84-91.

[42] Zeng Bo, Zhang Haozhe, Zhou Xiaojin, *et al*. Microseismic characteristics of shale gas wells with casing deformation in Sichuan Basin[C]. 55^{th} US Rock Mechanics/Geomechanics Symposium, 2021.

[43] 陈朝伟，王鹏飞，项德贵 . 基于震源机制关系的长宁—威远区块套管变形分析 [J]. 石油钻探技术，2017,45(4):110-114.
Chen Zhaowei, Wang Pengfei, Xiang Degui. Analysis of casing deformation in the Changning-Weiyuan Block based on focal mechanism[J]. Petroleum Drilling Techniques, 2017,45(4): 110-114.

[44] 陈朝伟，黄锐，曾波，等 . 四川盆地长宁页岩气区块套管变形井施工参数优化分析 [J]. 石油钻探技术，2021,49(1):93-100.
Chen Zhaowei, Huang Rui, Zeng Bo, *et al*. Analysis and optimization of construction parameters for preventing casing deformation in the Changning shale gas block, Sichuan Basin[J]. Petroleum Drilling Techniques, 2021,49(1):93-100.

Zhaowei Chen · Degui Xiang ·
Qing Zhao · Peng Tan

Casing Deformation Induced by Fault Slip During Shale Hydraulic Fracturing

Mechanism and Solutions

Science Press
Beijing

Springer

四川页岩气套管变形机理和防控技术

陈朝伟 等 著

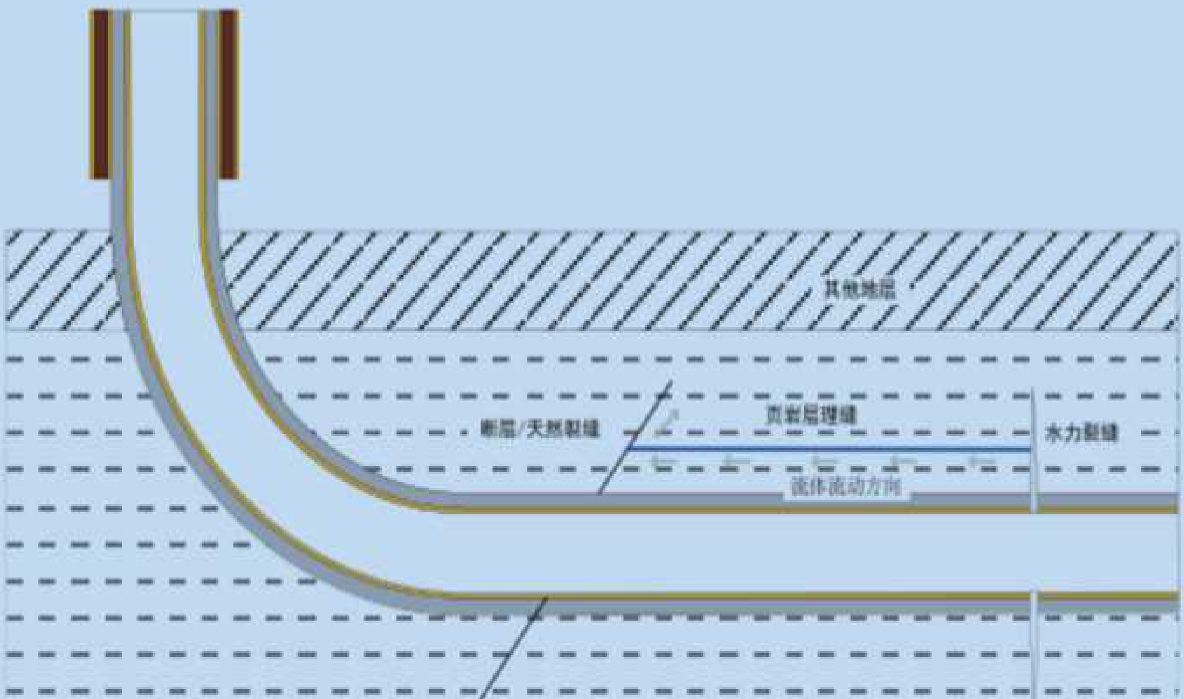

科学出版社

证书号第8720688号

专利公告信息

发明专利证书

发明名称：一种页岩油气套管变形预警方法和装置

专利权人：中国石油天然气集团有限公司
中国石油集团工程技术研究院有限公司

-接续页-

地　　址：100007 北京市东城区东直门北大街9号

发明人：陈朝伟;赵庆;项德贵;谭鹏;曾波;罗晨峰;宋毅;周小金
黄浩勇;翟文宝;王倩;孟少辉;任乐佳

专利号：ZL 2023 1 0468198.5　　授权公告号：CN 116575909 B

专利申请日：2023年04月26日　　授权公告日：2026年02月17日

申请日时申请人：中国石油天然气集团有限公司
中国石油集团工程技术研究院有限公司

-接续页-

申请日时发明人：陈朝伟;赵庆;项德贵;谭鹏;曾波;罗晨峰;宋毅;周小金
黄浩勇;翟文宝;王倩;孟少辉;任乐佳

国家知识产权局依照中华人民共和国专利法进行审查，决定授予专利权，并予以公告。

专利权自授权公告之日起生效。专利权有效性及专利权人变更等法律信息以专利登记簿记载为准。

局长
申长雨

国家知识产权局
2026年02月17日

证书号第8720688号

发明专利证书

专　利　权　人：北京石油机械有限公司
申请日时申请人：北京石油机械有限公司

证书号第5757208号

发明专利证书

发明名称：一种断层激活控制方法和装置

发　明　人：陈朝伟;范宇;项德贵;宋毅;曾波;黄锐;周浪;王倩;王思敏
房超

专　利　号：ZL 2019 1 0674863.X

专利申请日：2019年07月25日

专利权人：中国石油天然气集团有限公司
中国石油集团工程技术研究院有限公司

地　　址：100007 北京市东城区东直门北大街9号

授权公告日：2023年02月28日　　授权公告号：CN 112302601 B

国家知识产权局依照中华人民共和国专利法进行审查，决定授予专利权，颁发发明专利证书并在专利登记簿上予以登记。专利权自授权公告之日起生效。专利权期限为二十年，自申请日起算。

专利证书记载专利权登记时的法律状况。专利权的转移、质押、无效、终止、恢复和专利权人的姓名或名称、国籍、地址变更等事项记载在专利登记簿上。

201910674863X

局长
申长雨

国家知识产权局
2023年02月28日

其他事项参见续页

证书号第5757208号

专利权人应当依照专利法及其实施细则规定缴纳年费。本专利的年费应当在每年07月25日前缴纳。未按照规定缴纳年费的，专利权自应当缴纳年费期满之日起终止。

申请日时本专利记载的申请人、发明人信息如下：

申请人：

中国石油天然气集团有限公司;中国石油集团工程技术研究院有限公司

发明人：

陈朝伟;范宇;项德贵;宋毅;曾波;黄锐;周浪;王倩;王思敏;房超

证书号第5757208号

发　明　专　利　证　书

专 利 权 人：　北京石油机械有限公司

2023年02月28日

中国石油天然气集团有限公司基础研究奖

CNPC Basic Research Award Certificate

证 书

为表彰中国石油天然气集团有限公司基础研究奖获得者，特颁发此证书。

获奖项目： 四川页岩气套管变形机理和防控方法

获 奖 者： 陈朝伟

奖励等级： 二等奖

证 书 号： 2021-JC-2-01-R01

中国石油天然气集团有限公司

2022年1月13日

奖励证书

为表彰在促进石油和化学工业科学技术进步中做出突出贡献者，特颁发此证书。

奖　　种： 科技进步奖

获奖项目： 页岩气井筒完整性失效机理与控制关键技术及规模应用

获 奖 者： 陈朝伟

奖励等级： 一等奖

奖励年度： 2021 年度

中国石油和化工自动化应用协会

证书编号：2021KXJSJ-JB022-1-R06

国家科技部批准登记号：国科奖社证字第 0109 号

编号：2024DJ100

中国石油天然气集团有限公司
科技项目

计划任务书

项 目 名 称 ：复杂油气钻完井基础理论与新技术新方法研究

组 织 单 位 ：中国石油天然气集团有限公司科技管理部

承 担 单 位 ：中国石油集团工程技术研究院有限公司;北京华美世纪国际技术有限公司;辽河油田分公司 ；西南油气田分公司;塔里木油田分公司

项 目 经 理 ： 袁光杰

起 止 年 限 ： 2024 年 8 月至 2027 年 12 月

2024 年 8 月

项目编号：2025ZD1401400 密 级：公开

国家科技重大专项
项目任务书

项目名称：	油气田地质力学与储层改造新技术
所属重大专项：	新型油气勘探开发国家科技重大专项
推荐单位：	中国石油天然气集团有限公司
重大专项管理机构：	新型油气勘探开发国家科技重大专项专项办公室
项目牵头承担单位：	中国石油集团工程技术研究院有限公司(公章)
项目负责人：	陈朝伟
执行期限：	2025年05月至2030年12月

中华人民共和国科学技术部制

2025 年 8 月 22 日

任务书签署

甲乙双方根据《国务院印发关于深化中央财政科技计划 （专项、基金）管理改革方案的通知》（国发〔2014〕64号）、 《国务院关于优化科研管理提升科研绩效若干措施的通知》（国发〔2018〕25 号）、 《国务院办公厅关于改革完善中央财政科研经费管理的若干意见》（国办发〔2021〕32 号）、 《科学技术活动违规行为处理暂行规定》（科学技术部令第 19 号）、《科技部 财政部关于印发〈中央财政科技计划（专项、基金等）监督工作暂行规定〉的通知》（国科发政〔2015〕471 号）、 《科技部 自然科学基金委关于进一步压实国家科技计划（专项、基金等）任务承担单位科研作风学风和 科研诚信主体责任的通知》(国科发监〔2020〕203 号)等有关文件规定，以及有关法律、政策和管理要求，依据 项目立项通知，签署本任务书。 同时，本单位和项目负责人郑重承诺：对本项目所有成果产出（包括但不限于新产品、新技术、标准、论文、专利等）的真实性、 与项目的关联性等负责，将按要求落实科研作风学风和科研诚信主体责任；项目经费全部用于与本项目研究工作相关的支出， 不截留、挪用、侵占，不用于与科学研究无关的支出；接受并积极配合相关部门的监督检查。如有违反， 本单位和项目负责人以及相关成果产出者愿接受项目管理专业机构和相关部门做出的各项处理决定，包括但不限于终止项目执行、 追回项目（课题）经费，取消一定期限国家科技计划项目申报资格，记入科研诚信严重失信行为数据库以及主要负责人接受相应党纪政纪处理等。

重大专项管理机构（甲方）：
法定代表人签字（签章）：

（公章）
2025年9月2日

项目牵头承担单位（乙方）：
法定代表人签字（签章）：

（公章）
2025年8月22日

项目负责人签字（签章）：

2025年8月22日

推荐单位（盖章）

2025年9月2日

《油气田地质力学与储层改造新技术》

项目任务书审查意见

新型油气勘探开发国家科技重大专项专项办会同总师办，于 2025 年 8 月 2 日在北京组织召开会议，对《油气田地质力学与储层改造新技术》(编号：2025ZD1401400)项目任务书进行审查，专家组在听取项目负责人汇报的基础上，经充分质询讨论，形成审查意见如下：

1、项目攻关目标清晰，重点研究适应我国复杂地质特征的油气田地质力学方法和技术体系，形成原位地应力精细测试与预测技术和强应力储层深度诱导无水改造新技术等 6 项技术。攻关目标与申报指南一致。

2、研究内容重点突出，设置深层原位地应力测试解释技术及装备等 7 项研究内容，涵盖了指南方向要求的全部内容和指标；技术路线采用理论-试验-现场闭环迭代，最终示范应用，研究方法合理可行，创新性强。项目共设置 7 个课题，课题分解科学合理，逻辑关系严密，界面清晰。

3、考核指标覆盖指南要求，设置了包括现场应用、第三方测试等考核方式，具体可行。裸眼分层原位地应力测试工具耐压差 70MPa，耐温 175℃。申报发明专利 75 件，登记软件著作权 13 项，发表论文 60 篇，知识产权指标明确。项目打造 1 套油气田地质力学方法和技术体系，形成四维地质力学模拟及甜点产能评价软件、地质体活动性评价与套变

高风险区预测预警技术、强应力储层深度诱导成缝无水改造新技术 3 项标志性成果。自主可控率超过 90%。标志性成果有显示度，具有可交付性、可考核性，符合指南要求。

4、项目预算编制紧扣目标导向，根据研究内容预算配置经费，预算编制科学合理。

5、项目由中国石油集团工程技术研究院有限公司牵头，联合 19 家单位，组建了“产学研用”一体化攻关团队。组织管理方式与协调机制明确，牵头单位、参与单位职责清晰，构建了多部门协同机制，能有力保证项目研究顺利实施。

专家组一致认为，该项目任务、目标、成果及考核指标明确，与指南一致，技术路线合理可行，组织实施措施得当，对专项目标的完成具有重要支撑作用，同意通过审查。

专家组组长：

2025 年 8 月 2 日